COMBINED ATOMIC FORCE MICROSCOPY AND LIGHT SHEET MICROSCOPY CHARACTERIZE THE MECHANOBIOLOGY OF PHAGOCYTOSIS

Megan Elizabeth Kern

A dissertation submitted to the faculty at the University of North Carolina at Chapel Hill in partial fulfillment of the requirements for the degree of Doctor of Philosophy in the Department of Physics and Astronomy.

Chapel Hill
2023

Approved by:

Richard Superfine

Michael Falvo

Klaus Hahn

Amy Oldenburg

Timothy Elston

Sheila Kannappan

ABSTRACT

Megan Elizabeth Kern: Combined Atomic Force Microscopy and Light Sheet Microscopy Characterize the Mechanobiology of Phagocytosis
(Under the direction of Richard Superfine)

Phagocytosis is a fundamental biological function which allows immune cells, such as macrophages, to internalize and eliminate harmful particles such as pathogens, bacteria, and cell debris. These phagocytic targets vary widely in their size, shape, and stiffness requiring unique and complementary modes of clearance. Macrophage cells are able to exert forces to probe for the target's mechanical properties and respond with changes in their cellular structures allowing for internalization. This force-driven mechanism of sensing a target's composition has been shown to be an important factor influencing how phagocytosis proceeds. In order to better understand the forces directing cell decision-making before and during phagocytosis, it is imperative to measure the forces exerted on the target by the cell as well as capture high spatiotemporal resolution of the underlying actin cytoskeleton providing the scaffolding for dynamic cell structure changes. In this dissertation, I measure and observe the mechanical activity of the cell by using an Atomic Force Microscope (AFM) combined with Line Bessel Light sheet microscopy to simultaneously measure the force required to pull a target off the AFM cantilever and image the filamentous action (f-actin) location and intensity over the course of engulfment.

To my parents, for three decades of love and support.

ACKNOWLEDGEMENTS

I truly believe a PhD is not an accomplishment made by one person but a reflection of the support and assistance one person gains from those around them. My decision to go to graduate school has affected virtually everyone in my life, and I have been so fortunate to be surrounded by so much encouragement during this challenging period.

I am forever indebted to Richard Superfine and Michael Falvo, who have given me so much of their time and attention over the past six years. No one has more fun discussing all the experiments that I *could* do and where that science would take us than Rich. His excitement for my project is inspiring and infectious. To Mike, thank you for teaching me to see the essential pieces of an overwhelming problem in order to "get things done." I feel so fortunate to have had not one but two amazing advisors during my time at UNC. I am so thankful for their leadership, support, and encouragement to persevere when the experiments felt impossible.

I extend my deepest thanks to Klaus Hahn and Tim Elston, my committee members, rotation advisors, and collaborators, both of whom have been very supportive of this project and very generous with their time and resources over the years. Thank you to my committee member Amy Oldenburg for empowering my confidence in optics through her exceptional optics class and for helping to push my project forward. Finally, I am grateful to Sheila Kannappan for being a mentor and role model in how to make positive change in our department and our greater communities. I am thankful for her tremendous efforts to establish

and maintain the Grad- to-Undergrad (G2U) mentorship program as well as so many other DEI initiatives in our department. I admire all six of my committee members as scholars and teachers. It has been a true privilege to learn from them and to share my work with them. Special thanks to Jen Weinberg-Wolf for her mentorship as well as her huge contribution to the G2U program. I give my sincerest thanks to Cassandra Houston, Maggie Jensen, Jean Baldwin, Jhon Cimmino, for their indispensable service to me and to the department.

To Jeremy Cribb, my Matlab guru and cherished friend in the lab, thank you for always lending me an ear to talk through problems, both scientific and personal. To Tim O'Brien, my cell culture, microscopy, and fabrication mentor, thank you for setting such a good example of what a true love of science looks like and for serving as an encyclopedia of knowledge. Thank you to Evan Nelsen, Jake Brooks, and Chad Hobson for your friendship, mentorship, and scientific expertise. Thank you to the wonderful undergraduate collaborators I have had the pleasure of working with: Oheneba Boateng, Luca Menozzi, Danielle Rice, Shriya Haravu, Simone Josey, Max Hockenberry, Melissa Kissling, Will McClain, Greg Robert, Julius King, and Anna Cresenzi. Thank you for filling the lab with energy and laughs. I also want to thank the lab members from the McNeil lab, Oldenburg lab, and Freeman lab and the users of CHANL for making the basement of Chapman feel less lonely.

Thank you to Sandy Hahn, Joe Szulczewski, Dan Marston, Bei Liu, Shiqiong Hu, Ana Nogueira, Mingyu Choi, and all the amazing members of the Hahn lab, past and present, for making me feel so welcome during (and well past) my rotation. I want to especially thank Takashi Watanabe for answering every question I had with detail, insight, and humor. I am sure it was not easy teaching a physicist molecular biology but I am eternally grateful for your

contribution to my growth as a well-rounded scientist. Once again, I have Klaus to thank. Thank you for cultivating such a great group of people. I am going to miss your bonfires.

To Zack Hall, Michele Kelley, Pa Chia Thao, Laramy Head, and Jo Moscoso, building the G2U program with you all has been one of my most rewarding experiences at graduate school. I feel so lucky have had such hard-working teammates-turned-friends. I also want to thank the G2U mentees from cohorts 2021–2023 and 2022–2023. You are what made the program so special, and I can't wait to see where your futures take you.

To my Physics and Astronomy cohort, I thought this our first year and I still believe it now: we are an extraordinary class. I would not have gotten through first year without you all. Thank you to the MCBP program for research funding and the opportunity to work in exceptional labs. I must also thank the members of the Physics Department at Loyola University Maryland for providing me with my foundation in physics and Dr. Gregory Derry for my first exposure to research. I feel blessed to have had such a nurturing start in Physics.

To my "Durham Friends," Kevin Gallin, Rachel Gevlin, Max Holle, Claire Ravenscroft, Casey Williams, Myles Oldershaw, Sarah Smith, Chris Huebner, Zoë Eckman, James Draney, Lorenza Starace, Carolin Benack, Hannah Rogers, Josh Stroud, and Catherine Lee: Thank you for welcoming me into the Duke English circle and making Durham feel like home.

To my "Baltimore Friends," Amanda Nolan, Molly Dressel, Chris Sweeney, Patrick Diamond, Mitch Corwin, Dennis Mizzoni, Sara Stanton, Maria Dontas, Casey Miller, Phil Bolton, Julianne Bolton, James Rappazzo, Lauren Cosgriff, Aaron Perseghin, Madelyn Kirsch, Ryan Zadera, Amy Tarleton, Taylor DeBoer, Brittany Thomas, Anthony and Marci Medina, Aaron Pinto, Jeff Koplovitz, and Pat Taylor: Thank you for making the pandemic tolerable and

welcoming me back into your lives no matter how much time or distance has passed. I miss you all all the time.

To Brian Kaczar, Becky Oberhauser, Amber Maag, Stephen Veith, Mary Montgomery, Marshall Forte, Deanna Ortiz, and Christine Kwak: Our lasting friendships mean the world to me, and I am so thankful to have met each every one of you.

To my mother, Heidi Kern: thank you for instilling in me a sense of curiosity, nurturing both my left and my right brain, and always correcting my spelling mistakes. Your contributions to my success cannot be measured. To John and Lynne Kern: I am so thankful for your support and encouragement throughout this journey. Our phone calls always left me feeling revitalized and focused for the path ahead. To all my parents, thank you for making me the person I am today. To the McGurk family: thank you for being so welcoming and invested in my life. I look forward to what the future holds for our two families. To Alex Kern, Max Vitas, Miles Eddy, Katelyn, Justine, and Chase DeAlmeida: thank you for always sharing the excitement of my milestones. To Kelsey and Mads Kern: I don't know how I would have stayed sane without our (almost) daily phone calls. Despite the risk of my phone dying, thank you for always picking up, even when I could not return the same courtesy. Thank you to Molly the dog for uprooting her life in Algonquin, Illinois, to come live with me in Durham only to have us move back to Chicago five years later. You're my little buddy.

Finally, I am so lucky to have Michael McGurk by my side. You are my constant source of joy, you fill in where I fail, and you make my life virtually seamless. I appreciate how hard you work to enrich our lives with travel and new experiences that make me feel like a real person again. Thank you for bringing out the best in me. I'm excited for what lies ahead of us together.

TABLE OF CONTENTS

LIST OF TABLES

LIST OF FIGURES

LIST OF ABBREVIATIONS AND SYMBOLS

AFM	Atomic Force Microscope/Microscopy
ARP2/3	Actin related protein
ATat1/*dTat*	α-tubulin acetylase, a *gene*
CDC42	Rho family GTPase
CR3	Complement Receptor
FcR	Fcγ(gamma) Receptor
F-actin	Filamentous actin, made of monomeric globular (g)-actin
IgG	Immunoglobulin G antibody
GAP	GTPase-activating protein
GDP	Guanosine diphosphate
GEF	Guanine nucleotide Exchange Factor
GEF-H1	Also knowns as ARHGEF2, is a GEF specific to RhoA
GTP	Guanosine triphosphate
GTPases	Guanosine Triphosphatases
K40	Lysine 40, the 40^{th} lysine in the amino acid sequence for α-tubulin, an amino acid
LS	Light Sheet (Microscopy)
mDia1	Mouse Diaphanous-related formin-1
MEC-17/dTAT	K40-specific α-tubulin acetyltransferase, a protein
PNS	Peripheral Nervous System
PTM	Post Translational Modifications

Rac1	Rho family GTPase
Rho	Ras homologous, subfamily of the Ras (Rat sarcoma virus) superfamily of small GTPases
RhoA	Rho family GTPase
RNAi	RNA interference or Post-Transcriptional Gene Silencing, block protein translation
ROCK	Rho-associated protein kinase
S2	Schneider 2 cells, derived from Drosophila embryos
TRP	Transient receptor potential channel, a protein
TRPN/NOMPC	No mechanoreceptor potential C, a *gene*

Chapter 1: An Introduction to the Cell Biology of Phagocytosis

1.1 Phagocytosis: A Critical Macrophage Function

Phagocytosis is a fundamental process where particles larger than 0.5um in diameter are internalized by various types of phagocytic cells. [1] This mechanism is utilized by some unicellular organisms to collect nutrients as well as aid in antimicrobial defense [2]. In multicellular organisms, tissue-resident macrophages undergo phagocytosis to aid in immune defense [3], homeostasis [4], tissue development [5], and repair [6]. As part of the innate immunity, phagocytosis acts as an early response to internalize and dispose of pathogenic bacteria, fungal cells, and cancerous cells. The innate and adaptive immunity work in harmony thanks to a host of unique receptors decorating the plasma membrane of immune cells which recognize an assortment of foreign and endogenous ligands on the surface of their targets. [3] In order to maintain homeostasis, the human body turns over billions of cells daily. This routine clearance of dying cells requires recognition and elimination by phagocytes. [4] Apoptosis, a form of programmed cell death, is vital for tissue morphogenesis in a developing multicellular organism. Proper ingestion and degradation of apoptotic cells is performed by professional, nonprofessional, and specialized phagocytes through phagocytosis. [5] If not efficiently engulfed, apoptotic cells undergo autonomous degradation and release potentially harmful cell components which may lead to autoimmune diseases. [7] However, cell death is not always deliberate and cell debris resulting from damage still poses a risk to the body requiring removal.

Clearance of necrotic cell debris is necessary to initiate the regeneration of tissue required after injury and to prevent damage from sustained inflammation. [6] Upsetting this careful balance of cell death and survival can lead to cancer cell metastasis, malignancies, and drug resistance. [8] Phagocytosis is therefore an important first line of defense for protecting our bodies from invading external threats and internal systemic and inflammatory diseases.

1.2 The Role of the Actin Cytoskeleton in Phagocytosis

The actin cytoskeleton allows for dynamic cell shape changes that drive many fundamental processes such as cell motility, cell division, and of course, phagocytosis. Actin structures are composed of monomeric actin (globular or G-actin) units which bind in long helical chains to form filaments (filamentous or f-actin). These actin filaments can bind to neighboring actin filaments to form distinct superstructures in cells such as branched actin sheets, cross-linked cortical actin meshworks, cross-linked bundles of parallel actin filaments, and contractile actomyosin bundles. [9] The utility of the actin cytoskeleton comes from its ability to quickly assemble and disassemble these complex structures to respond in accordance to environmental or internal stimuli. The specific structural forms of the actin cytoskeleton are dictated by actin associated proteins and signaling proteins. For example, the branched actin underlying lamellipodia (**Fig. 1.1**) are assembled with the aid of the Arp2/3 complex, an actin nucleating protein which binds to the side of an existing actin filament and seeds a new actin filament to form from it. [10] Similarly, finger-like protrusions of the membrane are supported by subjacent actin filament bundles mediated by formins, fascin and other crosslinking proteins, as well as the Arp2/3 complex. [11] These actin structures may be stimulated by cytokines in

the extracellular surroundings or constitutively activated. Prior to phagocytosis, macrophage cells use lamellipodial ruffles and filopodial protrusions to survey their local environment for prey as well as a form of actin-dependent target capture.

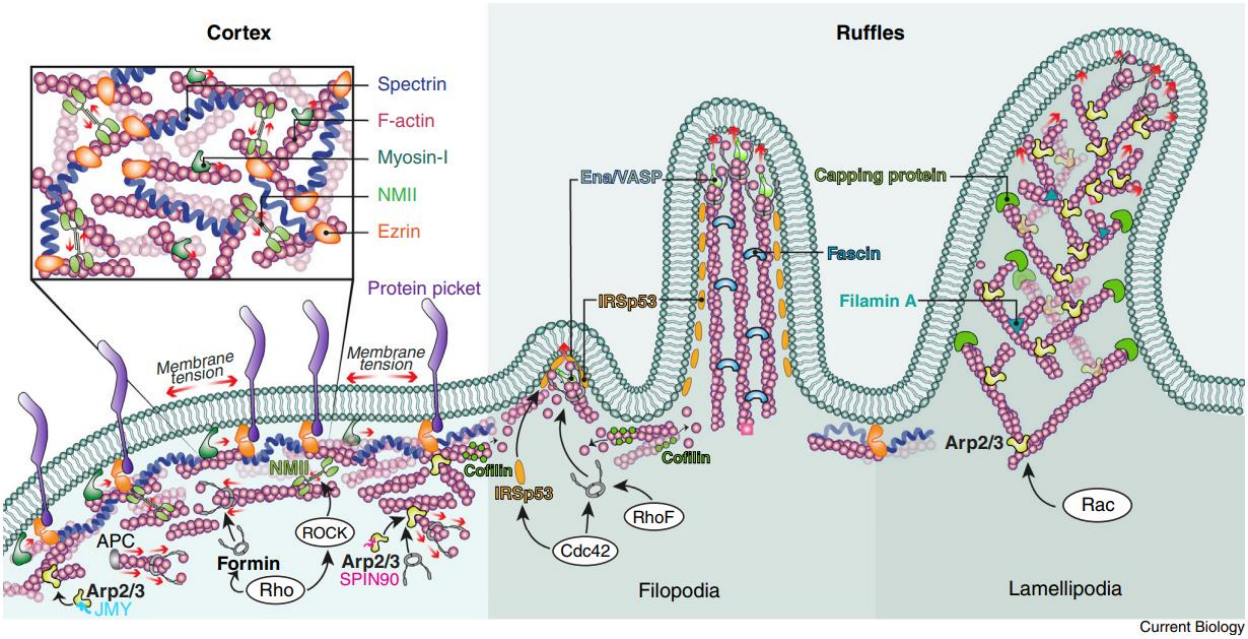

Figure 1.1. Schmatic of the Actin Cytoskeleton and Actin-related Protein Near the Cell Edge. Taken from S. Mylvaganam, S. A. Freeman and S. Grinstein, "The cytoskeleton in phagocytosis and macropinocytosis," *Current Biology,* vol. 31, pp. R619-R632, 2021. [16]. This schematic depicts the various cytoskeletal structures and actin regulators found beneath the plasma membrane, whether the membrane is at rest (left) or ruffling (right). The actin cortex represented on the left is a dense meshwork of filamentous actin, myosins, formins, and other cytoskeletal regulators such as Rho GTPases and kinases. This clustering of transmembrane receptors create 'picket fences' which limit transmembrane protein motility within the membrane but also physics constrain which proteins can experience inside-out activation [31] [17]. On the right, we can see the different actin architecture resulting in filopodia (linear, parallel actin filamments crosslinked by fascin) and lamellipodia (branched actin networks nucelated by Arp2/3 via the Rac signaling pathway).

1.3 Distinct Receptor-Ligand Pathways to Initiate Phagocytosis

Phagocytosis is initiated by binding of receptors on the cell surface to proteins natively present on the surface of the phagocytic targets or to antibodies or other serum components

that have coated or opsonized the target surface. [1] Phagocytes express a broad spectrum of surface receptors, each targeting a corresponding ligand, including Fcγ-Receptors (antibody IgG), complement receptors (complement fragments C3b and iC3b [12]), scavenger receptors (Bacterial lipopolysaccharide or LPS), lectins like dectin-1 (fungal β-glucans like zymosan), and other integrins (fibronectin or vitronectin) [13]. These receptors work alone or in combination with other surface receptors to aid in binding, increase uptake efficiency, or even trigger signaling cascades inside the cell which induce phagocytosis [14]. A well-studied example of this is the case of FcR-mediated phagocytosis. Activation of the FcR-mediated signaling cascade requires the target to present a dense coating of surface-bound ligands for the Fc receptor to bind. After engagement, the tethered receptor-ligand interaction promotes the binding of neighboring receptors in the Fc family as well as integrins. This clustering of several different receptors results in phosphorylation of the intracellular domains of the receptors leading to inside-out signaling and actin reorganization into the phagocytic cup. [15] [16] Once this adhesion to the target is successfully made, the actin cytoskeleton beneath the membrane undergoes a considerable rearrangement to create an enveloping mouth (or phagocytic cup, see **Fig 2**) which advances around the object and eventually closes, completing the engulfment. [17] This orderly process is made possible by the tightly regulated spatial and temporal organization of the actin cytoskeleton.

1.4 Regulators of the Actin Cytoskeleton During Phagocytosis

This broad range of unique and specific receptor-ligand interactions led to the popular theory of receptor-dependent phagocytic cup morphology and internalization mechanisms.

Early studies of particle internalization revealed seemingly distinct modes of engulfment for FcR-mediated versus complement mediated phagocytosis. The hallmarks of FcR-mediated phagocytosis included membrane ruffling and the extension of pseudopodia (an arm-like protrusion) around the target, binding to the surface ligands like a zipper. In contrast, complement mediated phagocytosis appeared to show no signs of membrane activity and the particle simply 'sunk' into the cell. [18] [19] In 1998, these distinct mechanisms were further differentiated in terms of their Guanine nucleotide-binding proteins (GTPases) signaling pathways, suggesting that there were unique actin-regulatory mechanisms depending on the ligand presented to the phagocyte. Rho-family GTPases and their associated factors are a large part of the fundamental signaling pathways which bring about the reorganization and polymerization of specific actin structures at the plasma membrane. [20] These early studies revealed that Rac1 (typically associated with lamellipodia formation) and Cdc42 (ubiquitously important for cell motility) were required for FcR-mediated phagocytosis [21] [22], while complement mediated phagocytosis depended on RhoA (actin stress fibers formation, focal adhesions, and actomyosin contractility) [21]. Because Rac1 and Cdc42 are known to activate Arp2/3 [20], FcR-mediated phagocytosis was seen as a process driven by branched actin networks, consistent with the observed lamellipodial ruffling. In contrast, RhoA's role in actomyosin contractility along linear actin filaments fit the hypothesis for the 'sinking' perceived in complement mediated phagocytosis [23]. However, recent developments in fluorescent imaging have debunked the theory and revealed that these two processes have much in common. Lamellipodial ruffling was seen in both FcR-mediated phagocytosis and complement-mediated phagocytosis [24], the pseudopodia previously related to only FcR-

mediated phagocytic cups was observed in both cases [25] [26], and finally, removing active Arp2/3 from the phagocytes decreased particle uptake for both types of phagocytosis [27] [28], implying that the Arp2/3 signaling pathway is required for both FcR and complement mediated particle uptake. Furthermore, it has been shown that FcR-mediated phagocytosis employs the use of integrins for efficient phagocytosis [25], opening the door for RhoA's role in both the FcR and complement pathways.

Walbaum et al. found that macrophage cells lacking the complement receptor type 3 (CR3), also known as $\alpha_M\beta_2$ integrin, had an elongated pseudopodal cup and incomplete engulfment when challenged with IgG-opsonized red blood cells [25][1].This implies that Fc receptors work in coordination with CR3s for late-stage cup squeezing and closure to complete engulfment. Like other integrins, $\alpha_M\beta_2$ has a closed, inactive conformation and an open, active conformation. LPS and other extracellular signals can prime integrins to their active conformations [29] allowing ligand binding the $\alpha_M\beta_2$ integrin and initiating complement mediated phagocytosis. However, this priming can also come from interactions with other phagocytic receptors such as Fcγ receptors [30]. In situations where the specific ligand (like IgG) density of the target is sparse, secondary activation of the abundant $\alpha_M\beta_2$ integrins by nearby Fcγ receptors may help establish the otherwise weak interaction between macrophage and target [31]. Furthermore, there is no physical link between Fcγ receptors and the actin

[1] This is reminiscent of one of the failure modes for a phagocytosis simulation ran by Herant et al. in 2011. To replicate the protrusive push observed in zymosan particle uptake, the authors had to tune their parameters such that the protrusive force was at 75% of the maximum for antibody phagocytosis and the attractive force between the membrane and the cytoskeleton was zero. However, at a full-strength protrusive push, there was an elongated 'neck' to the phagocytic cup which never closed around the particle. Though the pathways studied are different, removing the complement receptor from phagocytes, as done in Walbaum et al., may have led to rampant actin polymerization which generated a large protrusive force which overpowered the adhesive forces on the periphery of the cup.

cytoskeleton. However, adhesion proteins commonly associated with integrins do get recruited to the phagocytic cup during Fc-mediated phagocytosis [19]. Therefore, secondary activation of integrins by these specific receptors is crucial to establish contacts with the target and form the actin machinery necessary to rebuild the cytoskeleton from cup to closure. These recent insights suggest that phagocytes engage a variety of receptors, follow several regulatory pathways, and use multiple strategies of actin assemblies to accomplish robust clearance of harmful particles resulting in a healthy and productive immune system.

1.5 The Molecular Clutch Model and Phagocytosis

In 2020, Jaumouille et al. used high-resolution microscopy to confirm that branched and linear actin networks work together in order to generate the forces necessary to drive complement-integrin-mediated phagocytosis [26]. In their study, the Arp2/3 complex and mDia1, a formin, cooperate to form the dynamic actin networks necessary for complement-mediated phagocytosis. This is explained in the framework of the molecular clutch model. First proposed by Mitchison and Kirscher in 1988 [32], this model for cell mechanotransduction explains how the mechanical link between transmembrane integrins and intercellular actin polymers leads to a force feedback loop that allows cells to mechanically sense their surroundings. Myosin contractility drives retrograde actin flow, a continuous flow of actin from the leading edge of the cell towards the center of the cell [33]. Since the molecular clutch is coupled to the rate of retrograde actin flow, as the waves of actin reach a point of contact, myosin contractility is counteracted by the elasticity of the substrate and the flow is decreased.

With stiffer environments, the loading rate increases and actin polymerization pushes the leading edge forward, while producing a rearward traction force on the substrate. At lower stiffness, lower loading rates and higher retrograde actin flow lead to higher turnover at the leading edge, discouraging protrusions. The molecular clutch is well studied in the context of

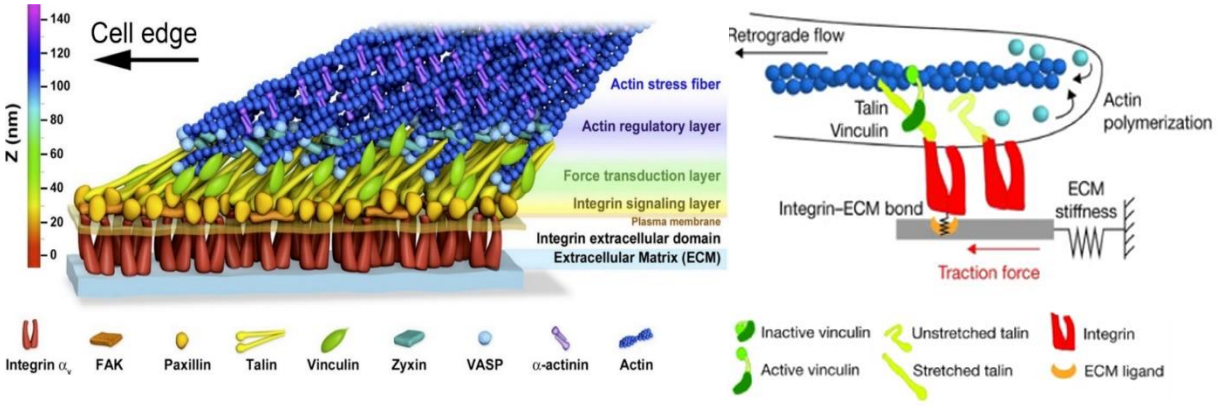

Figure 1.2. Molecular Clutch Model. Taken from Swaminathan, V., Waterman, C. The molecular clutch model for mechanotransduction evolves. Nat Cell Biol 18, 459–461 (2016) [163] and Kanchanawong P, Shtengel G, Pasapera AM, Ramko EB, Davidson MW, Hess HF & Waterman CM (2010) Nanoscale architecture of integrin-based cell adhesions. Nature 468, 580–584 [34]. The top figure illustrates the complex packing of adhesion proteins which make up the focal adhesion. Integrins transverse the plasma membrane and make contacts with the extracellular matrix. The cytosolic tails of integrins are physically coupled to focal adhesion kinases (FAK), paxillin, and talin. Talin unfolds under tension to reveal binding sites for vinculin. Talin and vinculin both bind to filamentous actin aided by VASP. Crosslinking proteins like α-actinin bundle actin filaments together to create thick, load bearing actin stress fibers which aid the cell in mobility. It's important to familiarize oneself with the well-studied focal adhesion and adhesion protein binding partner because many of the adhesion proteins found here are also reused for binding of the macrophage to the target during phagocytosis. The bottom figure is a simplified schematic for the molecular clutch model. Shown outlined in black is the leading edge of a cell filled with polymerizing actin and connected to the extracellular matrix via integrins. The left side if the blue actin filament is experiencing retrograde actin flow and moving towards the cell center while the right side of the actin filament is polymerizing new monomeric g-actin into the actin filament, pushing the membrane to the right. Talin is shown in the stretched and unstretched form, where in the stretched form, vinculin has become bound to reinforce the connection between actin and talin. The integrin is bound to the extracellular matrix via a ligand. This interaction has its own binding strength that must overcome the stiffness of the extracellular matrix to prevent slipping. If the extracellular matrix is stiff enough, the molecular clutch will engage, slowing

focal adhesions: large, multi-protein complexes that form mechanical linkages between the cytoskeleton and the extracellular matrix via integrins and integrin associated adhesion proteins. These focal adhesions are composed of over 100 different adhesion proteins which may include talin, vinculin, paxillin, focal adhesion kinase (FAK), α-actinin, and more (**Fig. 1.2**) [34]. Talin binds to the cytosolic tail of β integrins and undergoes conformational changes under tension (**Fig. 1.2**). For high loading rates, force transducing proteins such as talin unfold, revealing binding sites for other adhesion proteins like vinculin which fortify and enlarge the adhesion contact area [35] [36] [37]. The more talin is stretched, the more binding sites are revealed to recruit vinculin [38]. Talin can bind to actin directly but vinculin stabilizes the interaction between talin and actin by also binding to actin and other proteins in the focal adhesion like the Arp2/3 complex [39] [40]. In this way, the connection to the extracellular matrix is reinforced under high tension instead of severing and the density and arrangement of the adhesion proteins provide the cell with a way to 'sense' the stiffness of their environment.

In the context of phagocytosis, the vinculin bound to talin as a result of mechanical unfolding act as a stabilized molecular clutch to resist retrograde actin flow. Similar to focal adhesions, the slowed retrograde actin flow due to the molecular clutch drives Arp2/3-mediated actin polymerization at the leading edge. This in turn reinforces the connection between the actin cytoskeleton and the phagocytic target, propelling the phagocytic cup rapidly around the target, as well as grants phagocytes the capacity to sense the target stiffness. The molecular clutch model predicts that rigid targets, and therefore high loading rates, would be engulfed more efficiently than soft targets. In good agreement with this hypothesis, the mechanical properties of the target have previously been shown to affect phagocytic efficiency

for FcR-mediated phagocytosis [41]. Furthermore, the speed of the phagocytic cup was also found to be proportional to the stiffness of the target in complement mediated phagocytosis [26]. Macrophages encounter a broad range of target rigidities; from soft cell debris or apoptotic cells in the 0.01-10kPa range to gram-positive bacteria in the hundreds of MPa range [42]. The lack of molecular clutch engagement could explain why the internalization of softer targets (like damaged or effete cells [6]) is relatively slow or how macrophages employ different ingestion strategies such as trogocytosis on deformable targets [43].

Chapter 2: The Biophysics of Phagocytosis

2.1 Models for Force Generation in the Phagocytic Cup

Phagocytosis is a multistage process which requires several key force generation mechanisms to accomplish a successful engulfment (**Fig 2**). As we have seen, the receptors on the phagocyte binding to the ligands of the target are necessary for recognition and initiation of the signaling pathways stimulating the phagocytic response. However, it has been reported that before reaching the receptor reaches the ligand, it must first bypass the glycocalyx, the outer surface of the membrane composed of tall, highly glycosylated membrane proteins which can block receptors from binding. This obstacle requires a fraction of a pN of force to navigate and allow for binding [44]. Receptor-ligand binding leads to biochemical signaling that can initiate phagocytosis alone, however, it has been shown that engulfment can still be achieved with the

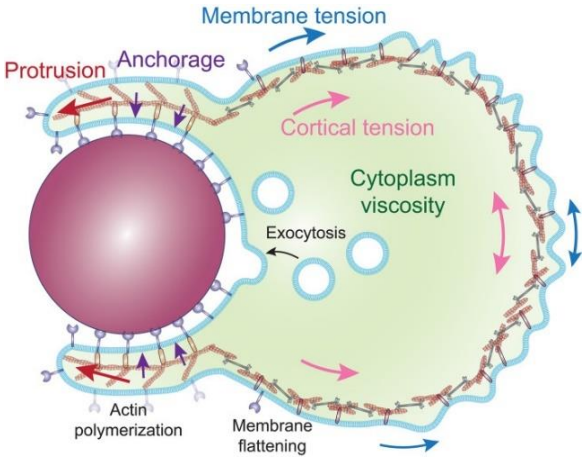

Figure 2. Key Players in Force Generation During Phagocytosis. Taken from V. Jaumouillé and C. M. Waterman, "Physical Constraints and Forces Involved in Phagocytosis," Frontiers in Immunology, vol. 11, p. 1097, 2020. *[164]* Simplified representation of the major sources of force in the engulfing phagocyte Actin polymerization (red arrows), adhesive forces (purple arrows), cortical actin tension (pink arrows), membrane tension (blue arrows). Excess membrane reserves are added to the cup via a process called exocytosis. Copyright © 2020 Jaumouillé and Waterman

advent of cell surface deformations [45]. Other models for phagocytosis have suggested a protrusive force from the cell is necessary in order to cause the unique cup geometry surrounding the target [46] [47] [48]. The origin of this force is commonly attributed to the actin cytoskeleton and actin polymerization. In studies where actin polymerization is inhibited with cytochalasin B, phagocytosis is blocked [49] [50]. As we have seen, actin-based protrusions are a general feature of phagocytosis regardless of the receptor pathway [19] [26] [25]. Mechanical models for cell shape changes often incorporate the energy cost of forming protrusions around the target and deforming the membrane [45] [51]. Herant et al. proposed a model for internalization which involved a protrusive force generated by actin polymerization at the leading edge of the phagocytic cup. This force remained close to the target via an attractive force, directing the protrusion, and adhesive forces from protein-ligand interactions. These combined engulfment forces must overcome the membrane tension and cortical actin tension (tension within the actin network beneath the surface of the membrane) to achieve engulfment [46] [48]. Their results show that the cortical tension is directly related to the surface area of the particle and this tension balances the protrusive force to propel the target inward without a 'pulling' force at the base of the cup. The combined surface tension and cytoplasmic viscosity determine the rate of cell deformation, and the total time for engulfment is therefore dependent on target size and geometry [41]. However, before the target's widest cross section, this balance can reach a 'bottleneck' that stalls phagocytosis [47]. Tension in the membrane can then be relived by flattening the surface folds of the membrane and vesicle delivery of excess membrane. Furthermore, disassembly of the actin network at the base of the cup was shown to be required for proper a complete engulfment [52], which may explain a

local decrease in cortical tension reliving the bottleneck. The bending resistance of the cell membrane is unlikely to play a significant role in the uptake of particles in the regime under study. For a moderate sized particle, phagocytes can expend upwards of 10^-14 J of energy to combat the cortical actin tension during phagocytosis. In comparison, bending the plasma membrane the same amount results in a 10^-18 J energy cost [53]. Though occasionally included in models for engulfment [54], cortical actin tension dominates the forces resisting internalization of targets [51]. In summary, the current model for the forces at play during phagocytosis includes actin polymerization at the leading edge of the cup overpowering the cortical actin tension to cause a protrusive cup surrounding the target.

Chapter 3: The Atomic Force Microscopy and Light Sheet (AFM-LS) Microscopy System

The central goals of mechanobiology are to understand how cells generate force and how they respond to environmental mechanical stimuli. A full picture of these processes requires high-resolution, volumetric imaging with time correlated force measurements. We have combined a vertical light sheet, single objective system that provides fast side-view volumetric imaging simultaneous with AFM for mechanobiology applications. The implementation of a reflecting prism provides sufficient light collection and convenient access for functionalized force probes. The employment of fast steering mirrors and a high aspect ratio, low phototoxic Line Bessel light sheet uniquely poises our system to capture both sub-second and long-term cellular processes. The ability to couple force measurements with high-resolution, volumetric optical imaging is a powerful tool for studying the mechanobiology and regulation of the actin cytoskeleton and as well as other cytoskeletal structures.

We have applied this tool to image both interactive and reactive force studies. For interactive, I share a volumetric timelapse of a new stable SKOV-3 cell line expressing Halo-H2B and SNAP-KRas during nuclear compression. For the reactive cases, I share a volumetric timelapse of a new stable RAW 264.7 cell line expressing Ftractin-Halo. This unique instrument allows for a myriad of novel studies investigating the coupling of cellular dynamics and mechanical forces.

3.1 Results

The AFM-LS system was designed by Dr. Richard Superfine with the help of many past lab members. Most recently, Dr. Kellie Beicker implemented the PRISM system [55], Dr. Evan Nelsen made improvements to the system for live cell mechanobiology studies [56], Dr. Joe Hsiao wrote the Labview scripts for image acquisition [57], and Dr. Chad Hobson added the Line-Bessel Light Sheet path for improved resolution. [58] With so many improvements made to the system, my role in the history of the AFM-LS has been as an expert user. I have improved existing assays, developed new ones, written extensive user protocols, and captured the first complete engulfment of a phagocytic target (Chapter 4) and the first FRET imaging in side view (Chapter 6). I have pushed the system to the limits of its abilities and showcased its true potential. Therefore, before jumping into chapters about mechanobiology results, I would like to explain the exceptional system the data was taken on.

3.1.1 A Tour of the AFM-LS System

Combining AFM with light sheet imaging has two challenges. 1. Mechanical noise shielding 2. Physical space constraint. The genius behind the success of this system for overcoming 1. Lies within the electrically controlled steering mirrors and ETLs (electronically tunable lenses). AFM is a sensitive force spectroscopy technique that picks up even the smallest vibrations, including any mechanical noise from controllers or moving elements. Neatly packed into an AFM isolation hood are a set of two ETLs, one on the laser excitation path (ETLa; **Fig 3.1A&E**) and one on the emission path (ETLb; **Fig 3.1B&E**). Both ETLs are position conjugate to the back focal plane of the objective. Effectively, adjustments to ETLa control the light sheet

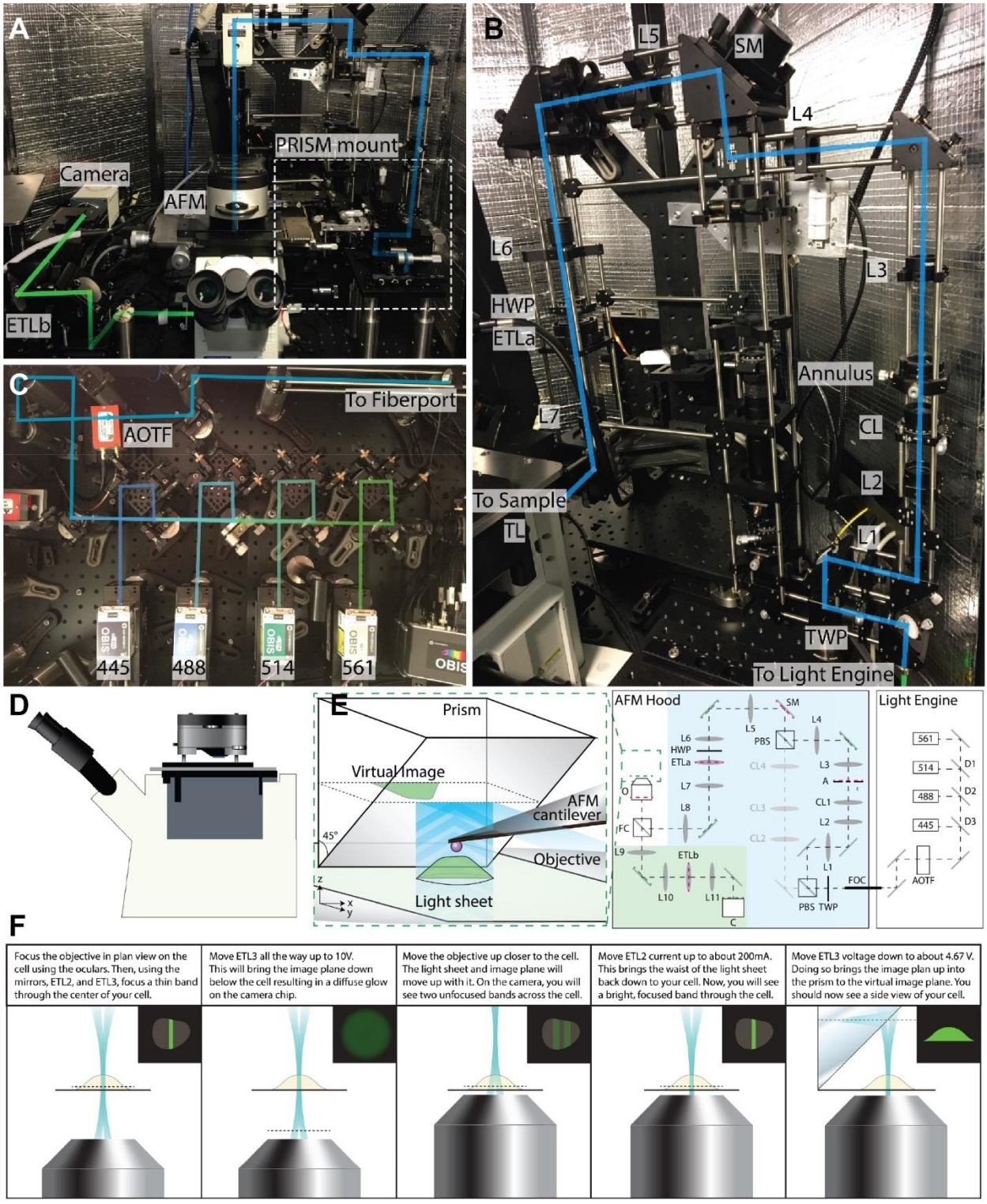

Figure 3.1. Optics Diagram of the Combined AFM and LSFM system. **A** View from the front of the AFM hood. **B** Close up of the Light sheet forming optics. **C** "Light Engine" Four single mode coherent lasers are focused into a fiber port and brought into the AFM hood. **D** Diagram of the AFM head on the microscope body obscuring the space above the objective. **Ei** Close up od the same space with the PRISM. **Eii** Optic Diagram. **F** Alignment Procedure. © Nelsen, et al. 2020

beam waist coming out of the objective (z) and adjustments to ETLb control the focus of the image on the camera chip. A fast-steering mirror also lies conjugate to the back focal plane of the objective allowing for positioning of the light sheet in y (orthogonal to the cantilever, **Fig 3.1E**). The full alignment procedure is described in **Figure 3.1F**.

To overcome the physical constraints imposed by the AFM head, the LS system was designed to be a single objective, open top configuration allows AFM-PRISM integration into the sample space (**Fig 3.1D-E**). Laser lines pass into the AFM hood through a single mode fiber (FOC) (**Fig 3.1C**). A cylindrical lens focuses a sheet of light onto an annulus which is re-imaged to

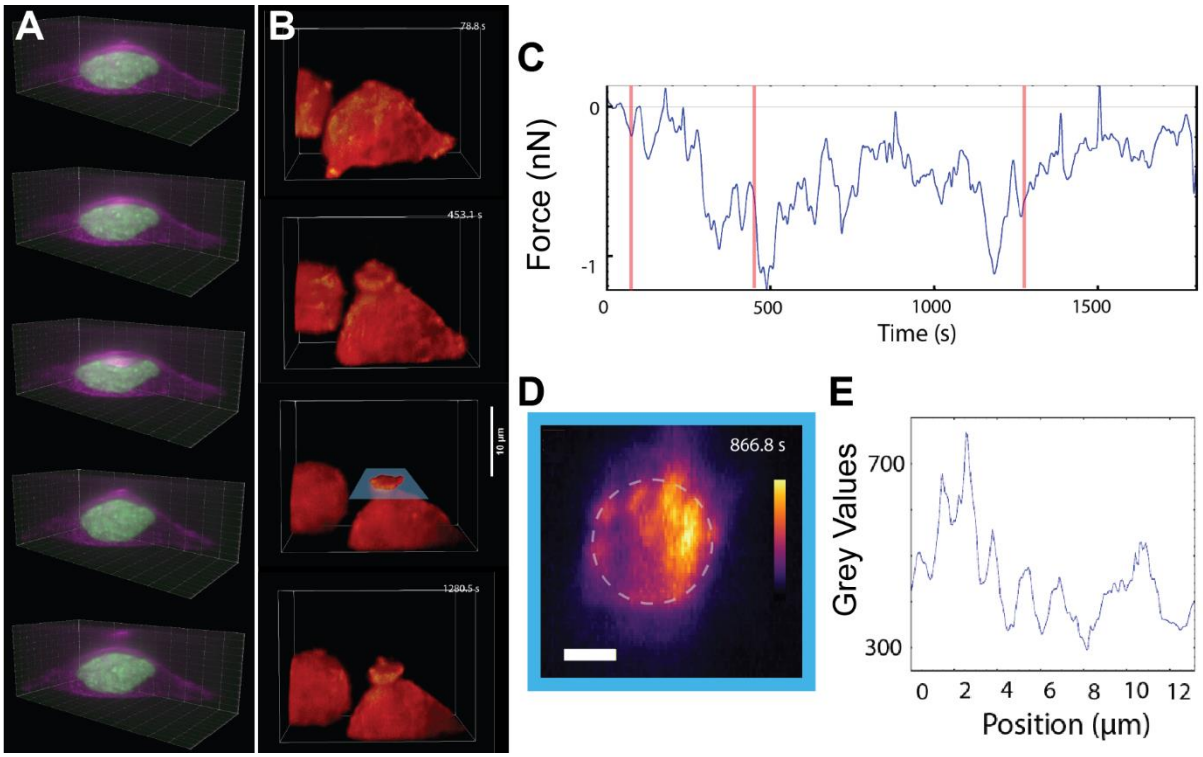

Figure 3.2. Interactive and Reactive Mechanobiology Applications. **A** Volumetric imaging of a SKOV3 cell expressing H2B-Halo and SNAP-KRastail being compressed by the bead on the AFM cantilever. Courtesy of Chad Hobson. © Hobson, 2021. **B** Volumetric Imaging of a RAW 264.7 cell expressing Ftractin-Halo and engulfing the bead on the AFM cantilever. Scale 28.080 µm x 21.708 µm x 19.000 µm. Each slice was imaged for 10ms with 5ms alloted readout time. Each two-color volume is 2.85 s in total with 7 s delay in between. **C** Force data synchronized to the imaging in **B**. A lowpass filter with cut off frequency of 0.064 Hertz was applied to the data for visualization purposes. **D** A maximal image projection of the XY slice through **Biii**. **E** Intensity profile through **D**. © Nelsen, et al. 2020

the back focal plane (red) of the objective to generate a Line Bessel Sheet. Electrically tunable lenses (ETL) control the axial position of the light sheet and image plane (green), while the fast-steering mirror (SM) controls the position of the light sheet at the sample plane. The illumination path and excitation paths are shaded blue and green, respectively (**Fig 3.1E**).

3.1.2 Applications of the AFM-LS System

Here I will highlight two types of force experiments that benefit from volumetric imaging. **Figure 3.2A** shows a volumetric timeseries of an ovarian breast cancer cell (SKOV3) dual labeled with Halo-H2B (nucleus/green) and SNAPtag-Krastail (membrane/magenta). In this experiment, the cell was pressed into with the AFM cantilever to look for any changes to the condensation of chromatin. **Figure 3.2B** shows 3D Light sheet imaging of a RAW 264.7 macrophage cell labeled with Ftractin-Halo (actin/Red). In this experiment, phagocytosis was an initiated with an IgG bead nearby but no force was applied to the cell. Instead the AFM cantilever simply measured the forces exerted on it instead of generating them itself A maximal image projection in the xy plane revealed punctate actin structures surrounding the target during phagocytosis, a finding previously only speculated. The accompanying intensity plot shows bright, punctate actin structures with regular separation of ~1.5µm around and underneath the bead tip.

3.2 Final Thoughts

The ability of the AFM to act as a interactive and reactive force probe allows for creative problem solving when designing mechanobiology studies. “Contact Mode” used here in both

experiments, is just one of the many built-in modalities of the AFM itself. Partnering the AFM with a LS further increases its applications and some one-of-a-kind experiments exploiting both have already been designed. [59]

Chapter 4: Forces of Phagocytosis and Particle Detachment

Phagocytosis is a force-driven cellular process that requires fine spatial and temporal control of the actin cytoskeleton to effectively ingest targets of engulfment. To dislodge disease-causing pathogens embedded in tissues or attached to surfaces, macrophages must overcome the adhesive force and disrupt the contact between the target and the surface. The majority of phagocytosis assays are limited to observing the internalization of freely diffusing targets, ignoring the obstacles immune cells face in native tissue. Here, I present a method to challenge individual macrophage cells to engulf and detach opsonized polystyrene beads from atomic force microscope (AFM) cantilevers. With the aid of line-Bessel light sheet microscopy (LS), our system allows for high resolution sideview imaging of the events leading up to the bead detachment event simultaneous with sub-nanonewton level force sensitivity to quantify the boundaries of the progressing, actin-filled phagocytic cup as well as quantify the engulfment force. To better understand the force generating mechanisms leading up to engulfment, I have considered several models for how phagocytic cup height implicitly scales with force and test their validity by fitting them to the experimental data. I have found that the observed force behavior can be broadly categorized into three categories: cells which exert an upward push before downward engulfment forces, only downward forces, or only upward forces. In every case, there are positive forces on the bead immediately before engulfment. This is consistent with a model for engulfment in which the dominating contributions to the

engulfment force originate from a contractile ring exerting inward and tangential forces on target. Other contributions may be from a force proportional to the cell-target contact area. To further analyze the causal relationship between the force generated on the target and the phagocytic cup, I have also cross-correlated the AFM force data with the cup height. Finally, I report the maximum engulfment force exerted by the cell on the target and argue that bead detachment is achieved via a peeling mechanism. With this, I have provided new insight into the mechanistic engulfment strategies macrophage cells use to navigate host tissues.

4.1 Phagocytosis Requires Particle Detachment in Native Tissues

Macrophages are present in virtually every tissue and have a diverse set of activation states induced by the local microenvironment. [60]. The microenvironment of these tissues can range in stiffness from 17 Pa in adipose tissue to 310 mPa in tendons [61] and macrophages have been shown to tune their phagocytic function in response to the rigidity of their substrate. [62] [63] For example, monocytes [64] and neutrophils [65] [66] placed under high fluid shear stress had increased adhesions, phagocytosis, and cytokine secretion. Macrophages have also been shown to have enhanced phagocytosis on stiff matrices. [67] [26] Therefore, macrophages routinely respond to mechanical ques in their environment to perform target clearance.

The hallmark structure of phagocytosis is the phagocytic cup. As its name suggests, this actin-filled membrane structure is a curved, concave protrusion which grows parallel to the target surface eventually sealing in the ‘cup-closure’ event, thus producing a membrane-wrapped vessel called a phagosome. This process has been well-studied in vitro using unconstrained targets which randomly drop on the phagocytes [25] [68] [69]; however, the

environment that macrophage cells are commonly hunting are tissues and surfaces where the targets are anchored to their surroundings. The strategies phagocytes utilize to navigate these obstacles and form suitable actin structures remain largely unknown. Though Moller et al. made significant progress in describing a process by which macrophages first 'lift-off' bacteria from their substrate via a lamellipodial 'hook and shovel' method and then proceed with engulfment [70], no one has studied how the leading edge of the cup itself acts as a structure to separate the target from its bound surface. Furthermore, the forces required to dislodge a target from a surface prior to engulfment have yet to be measured.

In this chapter, I present a novel technique to measure the engulfment force of adhered targets. The dynamics between phagocytic cup height and force prior to and leading up to engulfment are also characterized by dynamic time warping and cross correlation analysis to identify a universal sequence of events unique to phagocytosis despite the innately heterogenous nature of individual cells. I also compare the differences in f-actin recruitment to the base of the cup in engulfing and non-engulfing cells to identify trends that forecast engulfment. Finally, I report the maximum force the cell exerts on the target before engulfment and contextualize it in terms of the adhesion force of the bead to the cantilever, resulting in a proposed 'peeling' method for particle detachment.

4.2 Results

4.2.1 A Side View Phagocytosis Assay to Measure Cup Geometry and Engulfment Forces

We have designed a phagocytic assay to image the phagocytic cup during phagocytosis while simultaneously measuring the forces generated by the cell as it engulfs and dislodges the

target from its bound surface. Sideview imaging in the XZ plane of force actuation was achieved using a single objective light sheet system combined with an atomic force microscope (AFM) as described previously [55] [57]. To visualize the filamentous actin cytoskeleton comprising the cup, we used Raw 264.7 macrophage cells stably expressing Ftractin-Halo. Polystyrene beads labeled with fluorescent IgG were attached to the AFM cantilever and introduced to the macrophage cell to initiate phagocytosis studies. **Figure 4.1A-B** depict the sequence of events leading to engulfment of the target including cell probing, introduction of the target by the cantilever, early-stage cup formation, late-stage cup formation, and separation of the target from the cantilever surface. To extract cup geometrical parameters from these images, the position and diameter of the bead was tracked using custom segmentation scripts written in ImageJ and Matlab. **Figure 4.1D-E** shows the bead height above the surface versus time and a subset of the tracked center (white) and outline (hot colormap) of the bead over time, respectively. From this, you can see that the bead-cantilever system begins approximately 10um above the cell surface, quickly moves down towards the cell to a certain set point, as predetermined by the AFM user, and then slowly moves downward as the bead is internalized by the cell and separates from the cantilever. Using the bead center and diameter at each frame as a reference, the phagocytic cup was defined as the thin area outside of the bead in the actin channel (the inner and outer radius of this area is outlined in white in **Figure 4.1E-F**). This region of interest was collected from the actin channel and plotted linearly as a function of time in a 'circular kymograph' [56] (**Fig 4.1H**). Briefly, we collected an intensity profile of the actin channel centered on the bead location and rotated around the outside of the bead (**Fig 4.1F-G**). With this data visualization method, cellular features such as individual filopodia and

lamellipodia in close proximity to the bead are clearly visible in the early stages of phagocytosis. **Figure 4.1H-J** show the imaging from the first few minutes of the experiment. **Figure 4.1I&J** show a detailed view of the first few minutes of the experiment where the cell is probing the bead. The microscopy images (**Fig 4.1I**) show a single filopodia moves to the left between 38.2 and 67.2 seconds. This is followed by a ruffle on the right side of the bead at 132.8 seconds,

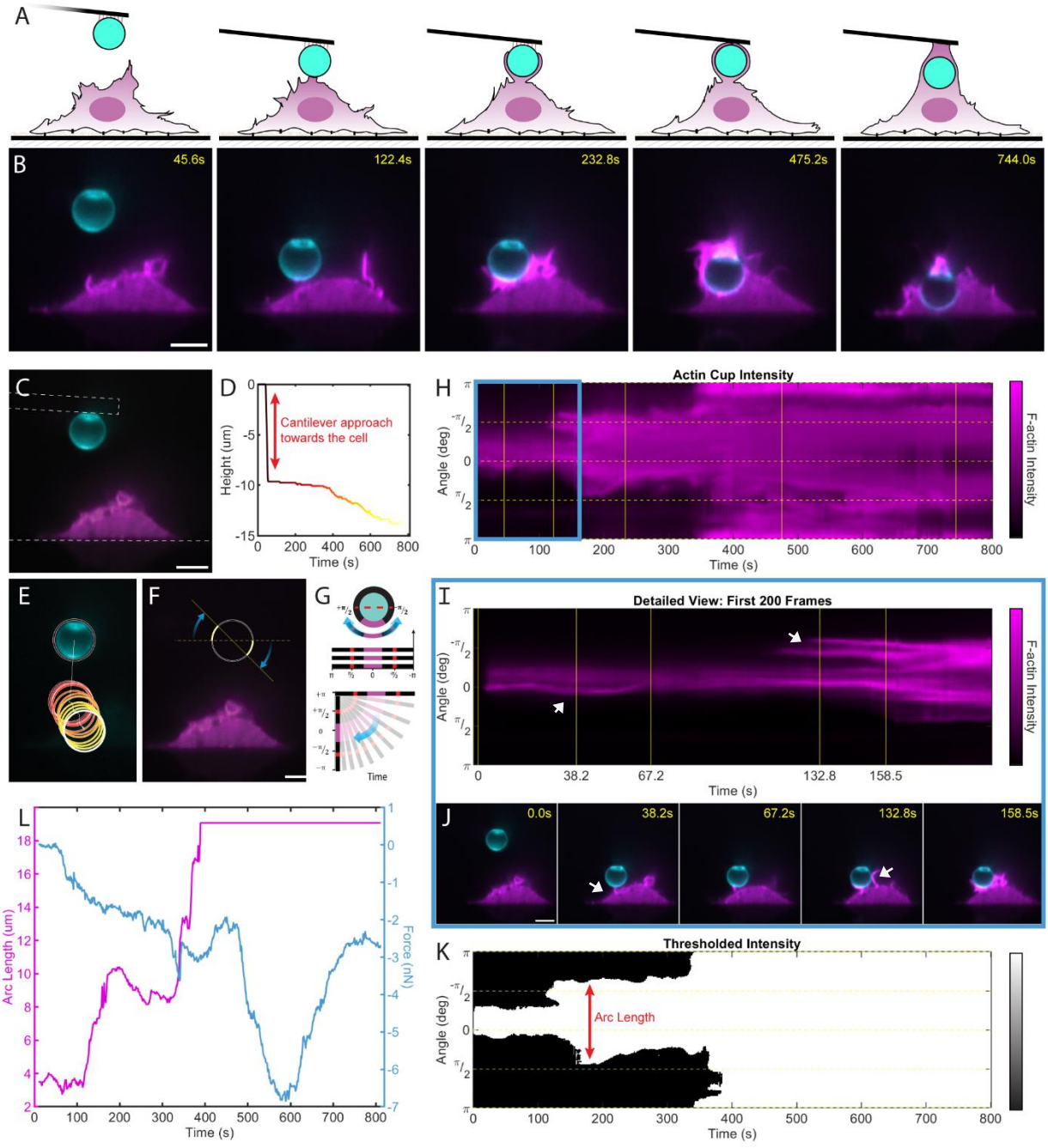

Figure 4.1 Design of the Phagocytosis-Force Assay. A Representation of the phagocytosis experiment. The cross section of the cantilever (black), bead (cyan), and cell (purple) are shown from the beginning of the experiment and prior to bead introduction to the end of the experiment and bead pull off. B Side view (xz) microscopy images of the bead labeled with AF488 IgG and the cell labeled with F-tractin-Halo (JF549) corresponding to the events portrayed in A. C Dotted white lines overlaid on microscopy image delineate the AFM cantilever (above the bead) and coverslip (beneath the cell). D Height of the bead over time derived from the bead tracking shown in E. E Bead microscopy image overlayed with the projection of the bead tracking over time. The center of the bead at each time point is shown as a white line tracing the bead's trajectory and the region of interest where the actin filled cup is considered is shown as two white circles with an inner (diameter of the bead, d) and outer (d + 5pixels) diameter. The color map (hot) denotes the time of each outline where black is the first frame and white is the final frame. The outlines have been downsampled by 65 to aid the visualization. F The corresponding microscopy image of the actin channel. Overlayed onto the image is the bead location (derived from the bead channel) and one representative line profile. For each frame, the line profile was rotated about the bead center in increments of 2 degrees to prevent double counting pixels around the bead. Only the pixels immediately outside of the bead (the white outlined area shown in E) were used in the circular kymograph. G Schematic explanation of how the circular kymograph is constructed. The area around bead is averaged radially across the inner and outer dimeters and 'unwrapped' into a straight line and plotted against time as shown in H. The red dashed line at -pi/2 to pi-2 marks the 'equator' of the bead. H The resulting circular kymograph of the actin-filled cup from cell shown in B. The yellow vertical lines correspond to the timestamps in B. I Zoom-in of H showing the first few minutes of the kymograph. The yellow vertical lines correspond to the timestamps in J. J Merged microscopy images of the actin (magenta) and bead (cyan) at 5 time points in the experiment. K Kymograph shown in H after thresholding. The vertical distance at each time point is the arc length of the phagocytic cup. L Plot of Arc length (magenta) and AFM force (blue) versus time for cell shown in B. All scale bars are 10um. All time is in seconds.

both eventually fusing into the beginning of the cup at 158.5 seconds. These features are also observed in the kymograph (**Fig 4.1J**) as noted by the white arrows. Thresholding the circular kymograph (**Fig 4.1H**) results in a binary kymograph (**Fig 4.1K**) from which the edges of the phagocytic cup can be detected. The distance from one end of the cup to other is the arc length. Finally, **Figure 4.1L** shows the resulting arc length and measured force from the AFM synchronized in time.

With this capability, I have studied the relationship between the engulfment force and the phagocytic cup height, an accessible geometrical parameter which easily translates to the

fraction of the target engulfed and thus references critical milestones in the engulfment process. I have looked at this relationship in time and abstracted from time in order to elucidate the sequence of mechanical checkpoints in phagocytosis despite cell-to-cell variability.

4.2.2 Implicit Force Scaling Laws of Phagocytic Cup Height

A handful of studies have reported the forces associated with engulfment, but never directly measuring the force the cell exerts on the target for internalization. The membrane tension during engulfment was measured using micropipette aspiration resulting in a model that is suggestive of an engulfment force [47] [49] [51]. However, other studies have reported that while engaging the cortical actin skeleton can result in long-range tension propagation along the cell [71], locally altering the cell membrane tension does not affect the tension in other parts of the cell. [72] [71] Furthermore, the propagation speed of this tension spans orders of magnitude depending on the cell type. [73] This obscures the relationship between the tension measured on other areas of the cell during phagocytosis and the actual tension within the leading edge of the cup. Taken together, the forces necessary to internalize a target during phagocytosis still require reliable measurement. Additionally, the field would benefit from an analysis technique that controls for cell-to-cell variations in order to come to a conclusive mechanistic understanding of phagocytosis.

To begin to understand the trends in the force during phagocytosis and the cup height (as measured from the bottom to the top of the target), I have compared a dataset of 22 engulfing cells (**Fig 4.2A**) with 23 non-engulfing cells (**Fig 4.2B**). In the first two leftmost plots we

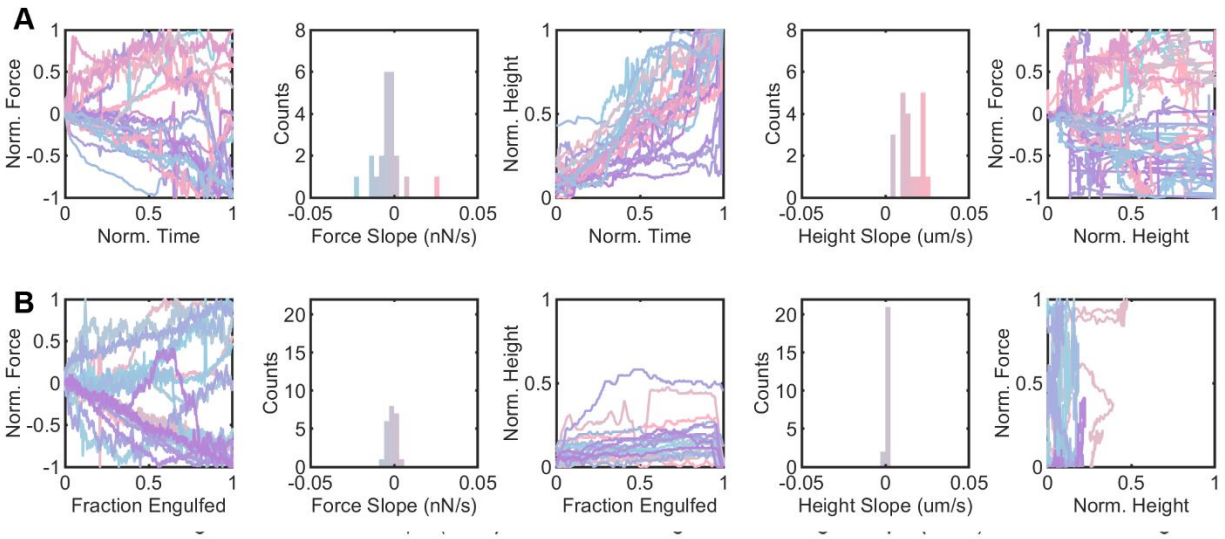

C

	Force Generation Mechanism	Implicit Scaling Law
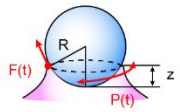	**PCLE-1**: Perimeter of the Cup or Leading Edge of the cup pulling tangentially downward	$F_z \propto z(2-\frac{z}{R})$
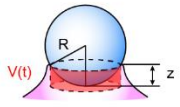	**CV**: Cup Volume i.e. Actin Network beneath the cup pulling downward	$F_z \propto V = \pi(Rz^2 - \frac{2}{3}z^3)$
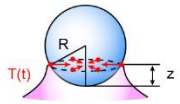	**PCLE-2**: Perimeter/Leading Edge of the cup exerting a contractile ring or 'Purse String' squeezing	$F_z \propto \sqrt{2\frac{z}{R} - (\frac{z}{R})^2}\left(T(1-\frac{z}{R}) - f\right)$
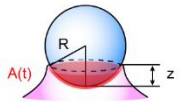	**CTA**: Cup-Target contact Area dependent 'Flattening Force'	$F \propto 2\pi Rz, F \propto z$

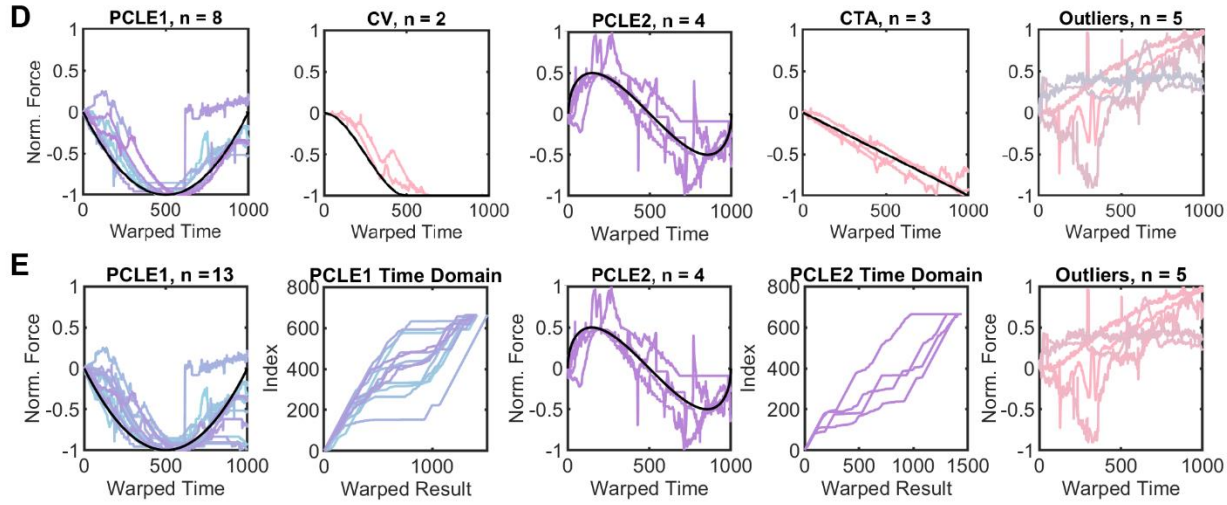

Figure 4.2. The Engulfment Force and Cup Height Follow Three Distinct Scaling Behaviors. **Ai** Plots of AFM force data for each engulfment experiment as a function of fraction engulfed. Each force curve has been normalized to its maximum value. **Aii** Histogram of the overall slope of each force curve. **Aiii** Plots of the phagocytic cup height for each engulfment experiment as a function of fraction engulfed. Each height curve has been normalized to its maximum value, equivalent to the bead diameter. **Aiv** Histogram of the overall slope of each height curve. **Av** Parametric plot of the Normalized Force versus Normalized Height. Colors of the curves correspond to individual experiments across all plots. **B** Same plots as **A** but for the experiments in which the cells did not engulf. **Ci-iii** Table of biophysical force models for engulfment. **Ci** Cartoon representations of the relevant geometrical features and forces in each model. **Cii** Explanation of each force generating mechanism. **Ciii** Equations for the implicit scaling laws for force in terms of cup height, z. PCLE2 *[75] [17]*and CTA *[47]* are derived from previously proposed models for engulfment. **Di-v** Dynamic time warping of each force curve to each force model grouped by the model which minimized the square of the Euclidean distance between the newly warped force curve and the model. **Dv** shows outlier force curves which had no distinguishable preference for any of the four models. The number, n, of experiments which fit into each category are referenced in the plot titles. **Ei-v** Results of reducing the considered models to only PCLE1 and PCLE2. **Eii** & **Eiv** Plots of the time domain warping for each corresponding force curve in **Ei** & **Eiii**. **Ev** The force curves which fell into the outlier category remained unchanged.

see the force curves and their associated slopes. Positive force indicates the cell is pushing up on the cantilever and negative force indicated the cell is pulling down on the cantilever, relative to its initial position. The force curves have all been aligned by normalizing each to its max value and plotting against fraction engulfed instead of time due to differences in engulfment times. However, since the non-engulfing cells never reach engulfment, they have been plotted against normalized time, where “1” denotes the end of the 800 second experiment. In comparison, engulfment times ranged from 76 to 664 seconds. The histogram of their overall slopes was calculated on the unnormalized data. Immediately, we can see that both the engulfing and non-engulfing datasets have slopes centered around zero, implying both positive and negative trends in the force data are present. However, while the force curves from the non-engulfing cells are relatively linearly, the engulfing cells have more fluctuations in the force and a few distinct populations of curves begin to become visible.

In the center plots of **Figure 4.2A-B**, I have plotted the cup height for all datasets versus fraction engulfed. The y-axis has been normalized to each experiment's bead diameter due to variations in the bead size (6.2 ± 0.35 um). While the cup height for the engulfing cells trend upwards, the non-engulfing cells exhibit a relatively constant cup height for the duration of the experiment which never reaches 1. As excepted, the cup height slopes for the engulfing cells are all positive and the cup height slopes for the non-engulfing are very close to zero.

The final two plots for **Figure 4.2A-B** show the parametric plot of normalized force versus normalized cup height. For the engulfing cells, the trends in this plot are very similar to the normalized force versus fraction engulfed. This is because the normalized cup height is increasing and roughly linear, though there are significant deviations. The same plot for the non-engulfing cells looks drastically different. Because the normalized cup height for the non-engulfing cells is relatively constant, the force values are constrained to a limited range on the x axis and therefore exhibit little to no scaling relationship between force and cup height. From this, the distinction between cells that engulf and cells that do not engulf is clear.

I have considered several geometrical models informed by the biophysical understanding of the phagocytic cup. I have tested these models against my experiment data to examine the geometry of the cup relates to the forces exerted on the target in different stages of phagocytosis. Previously proposed models describing phagocytic engulfment each have an implicit scaling relationship between geometric markers of the cup and the forces on the target. For example, arguments considering actomyosin contractility have proposed 'squeezing' present in the leading edge of the cup followed by a trailing disassembly of actin at the base of the cup, attributing the closure of the cup to a 'purse-string' model [74] [69] [75] [17] [49]. As

shown in **Figure 4.2C**, the Perimeter Cup Leading Edge 2 or 'purse-string' model (PCLE-2) predicts an inward pointing force of the 'purse string' that decomposes into a central force and a tangential force. Therefore, below the equator of the bead, the net forces on the target would be upward and passed the equator of the bead, the net forces on the target would be downward. Herant et al. proposed a "flattening force" present in the interface between the leading edge of the cup and the target thereby implying that the engulfment force should scale with the contact area, as shown in **Figure 4.2C** as the 'Target Contact Flattening' model (CTA). [47] In this model, the scaling law is be dominated by a linear relationship between force and surface area, where the largest downward force would increase in magnitude until reaching a maximum at the end of the engulfment process.

Furthermore, we hypothesized that protrusions advancing the leading edge of the phagocytic cup would generate net downward forces on the bead consistent with retrograde actin flow present in the leading edge of the cup and stabilized by a molecular clutch at the cup-target interface. For this to be true, we consider the arrangement of available contacts (or sites of molecular clutch engagement) the leading edge of the cell can make on the target in two additional models. The Perimeter/Cup Leading Edge model 1 (PCLE-1) proposes that force is proportional to the perimeter of the leading edge of the cup but acts tangentially to the target. This implies that force is at a maximum at the equator but at a minimum at the bottom and top of the target. The Cup Volume (CV) model assumes that the force bearing contacts are found at the base of the cup where the contacts on the cup interface connect to the larger cellular cytoskeleton. The force is therefore proportional to the volume of actin beneath the target, reaching a maximum at the equator and then plateauing.

Each of these models assumes a monotonically increasing cup height, however, from observations of the engulfment process in my own data, as well as the literature, we know that this is not often the case. Macrophages have been reported to undergo a slow initial wrapping of the target followed by a quick internalization. [76] [77] The duration of stalling before completing engulfment and the time of transition to the second stage varies. Also, it is not necessarily coincident with the halfway point of the target. [76] This could be due to a number of different internal and environmental factors but this behavior is ultimately different for each cell. Therefore, I have incorporated 'Dynamic Time Warping' (DTW) of the force curves in my analysis pipeline before categorizing the scaling behavior. **Figure 4.2D** shows the initial grouping of all the force curves when considering all four potential scaling laws. Each curve was paired with each of the four models and passed through a DTW Matlab script to minimize the sum of the square Euclidean distances (ssed) between the resulting warped curves. Curves were grouped (and plotted) based on the model with the minimum ssed. Without DTW, the ssed between each pair of the models was calculated to determine the maximum cutoff ssed. Force curves with a ssed above 194.42 for each model were considered outliers. Passing this DTW script through the models themselves resulted in an interesting finding. The CV and CTA model had an ssed 0.61, essentially zero after DTW while every other DTW pair had an ssed greater than the minimum ssed from the dataset. Therefore, I fit the curves again, this time only considering the PCLE1 and PCLE2 models (**Fig 4.2E**). Surprisingly, each curve previously categorized as CV was placed into the PCLE1 category, each curve previously categorized as CTA was place into the PCLE2 category, and the outliers were unchanged. Furthermore, next to both the PCLE1 and PCLE2 plots I show the result of warping on the "time" domain. Here we can

clearly see a ‘plateau’ in each curve. In terms of the cup height, this would be equivalent to the rim of the phagocytic cup staying at one position, consistent with experimental observations [76] [77].

Overall, these results support the alignment of the engulfment force to the PCLE1 model, PCLE2 model, and an outlier category with predominantly positive force throughout engulfment. The PCLE2 model is constructed such that force applied to the target originates from a contractile actomyosin ring in the leading edge of the phagocytic cup; observed [75] [69] and measured [68]. Though previously unproposed, the PCLE1 model borrows from the work on describing the molecular clutch in cell migration [26], where adhesions to the target serve as contact points from which actin polymerization pushes the membrane forward. In our model for PCLE1, we assume this careful force balance results in a net downward force below the halfway point of the bead, assuming the force of the cell on the contacts dominates over the actin polymerization force. However, it could easily be the other way around, where actin polymerization at the leading edge of the cup dominates resulting in an upward pushing on the target. The second case would be consistent with the outlier category where the forces on the bead are largely positive throughout engulfment. Altogether, I have identified three distinct scaling relationships for the forces on the bead during phagocytosis.

4.2.3a 3D Cross Correlation Analysis of Two Time Series

As a quick intermission, I would like to explain how to interpret the 3D cross correlation plots provided in this chapter. **Figure 4.3** shows an example cross correlation of two sinusoidal curves standing in for “Force” and “Cup Height.” **Figure 4.3A** shows the raw signals. From this

we can see that they each have a period of 380 seconds and are phase shifted by 80 seconds. **Figure 4.3B** is the cross-correlation strength at zero timelag. In other words, this represents the overlap (Force*Cup Height) as plotted in **Figure 4.3A**. The maximum overlap occurs at 238 seconds and the minimum overlap occurs at 143 and 332 seconds. You'll notice that the curve in the Zerolag correlation plot (**Fig 4.3B**) has the same color map as the bottom 3D plot (**Fig**

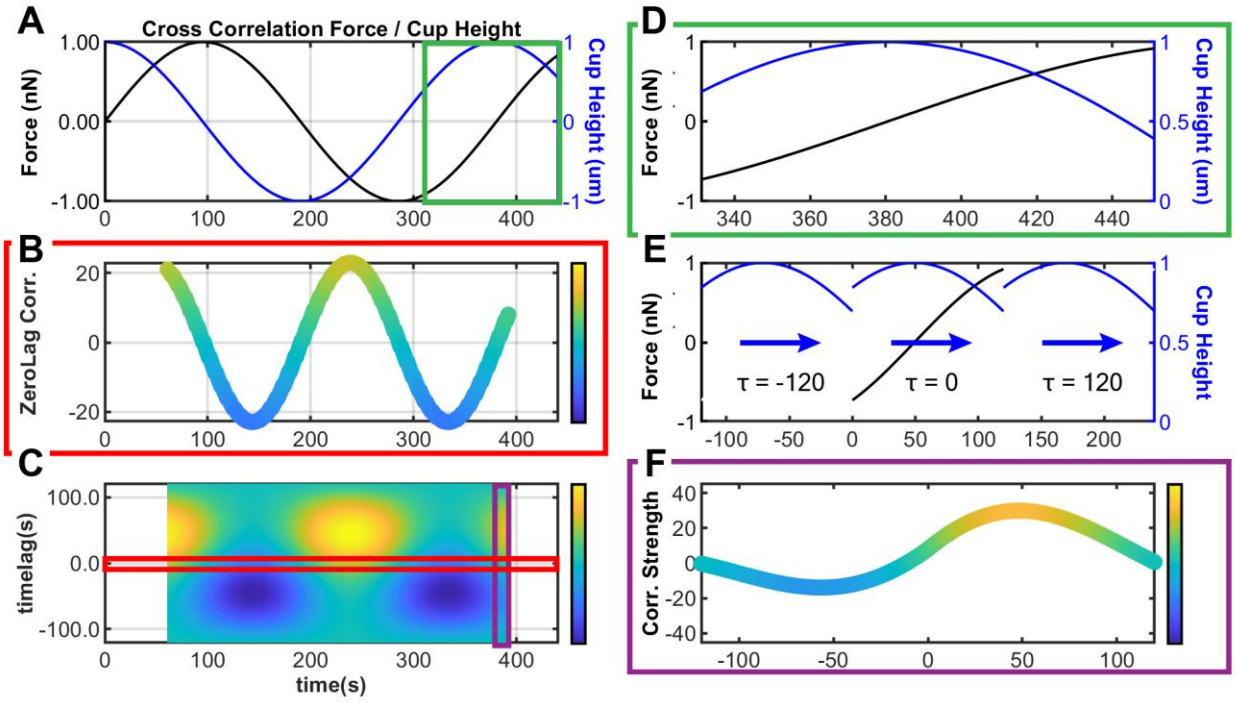

Figure 4.3. Guide to 3D Cross Correlation Plots. **A** Plot of two example time series. The green inset is equivalent to **D**. **B** Zerolag cross correlation plot of the curves in **A**. **C** 3D cross correlation plot of the curves in **A**. The red inset is equivalent to **B** and the purple inset is equivalent to **F**. **A-D** share the same x axis, the time according to the force curve. **D** shows a zoom in of **A** representing the window of data used in the last step in the correlation. **E** is a visual aid demonstrating cross correlation as a "sliding dot product." The two curves are the same ones referenced in **D**. **F** shows a zoom in of **C** along the zero axis. **E-F** share the same x axis, the timelag (y axis of **C**).

4.3C). That is no coincidence, as the Zerolag Correlation plot is simply the plot of the values from the 3D plot along the zero axis (red box). Finally, the 3D Correlation plot represents correlation strengths allowing for timelag of up to 120 seconds. The cross correlation was

performed on subsets of the data in lieu of the full sequence to find local regions of correlation. The green inset on the top plot (**Fig 4.3D**) shows an example of the final subset used to create the purple inset on bottom plot (**Fig 4.3F**). I used a sampling window of 120 seconds, meaning the last vertical line of the 3D plot is the result of the cross correlation between the last 120 seconds of the force with the last 120 seconds of the cup height (**Fig 4.3A & D**). The cross-correlation process is also known as a "sliding dot product" and for this example we imagine the subset of the cup height (blue) curve sliding across the subset of the force (black) curve in the green box from -120 to 120 seconds (**Fig 4.3E**). At -120 and 120 seconds timelag, there is no overlap between the two curves and therefore the correlation strength is zero at either end of the curve. See methods for more details.

4.2.3b Cross Correlation Analysis of Engulfment Force and Cup Height

Since each model presumes an underlying molecular mechanism responsible for the observed variations in force and cup geometry, I next asked whether the causal relationship between fluctuations in force and cup geometry could reveal more information about the sequence of events. To accomplish this, I used cross correlation analysis of Force, *F(t)*, relative to the Cup Height, *H(t)* (**Fig 4.4**). In this analysis, negative timelag means the force precedes the cup height, while positive timelag means the cup height precedes the force. Additionally, positive correlations (yellow) occur when the force and the cup height have the same behavior (both increasing, both decreasing) and negative correlations (blue) occur for opposite behavior. Because we expected the cell to employ different engulfment strategies at different locations

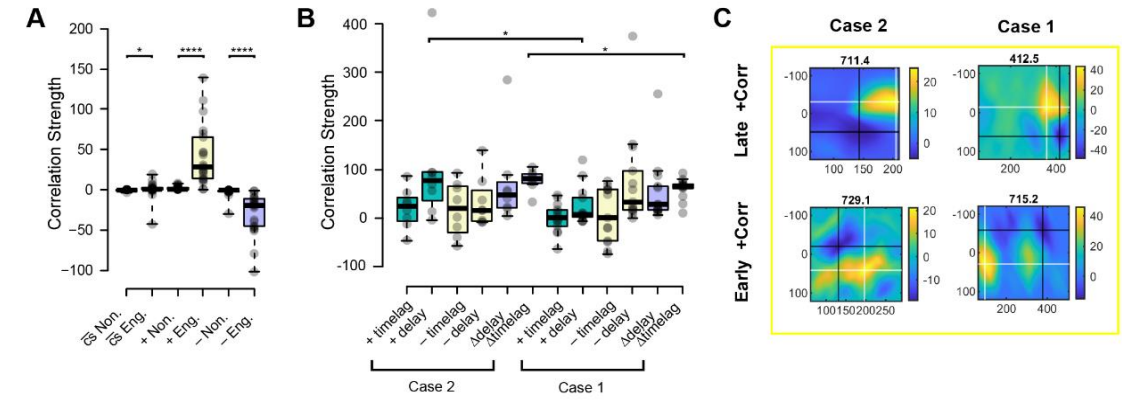
A
Correlation Strength
ES Non.
ES Eng.
+ Non.
+ Eng.
– Non.
– Eng.
B
Correlation Strength
+ timelag
+ delay
– timelag
– delay
Δdelay
Δtimelag
Case 2
Case 1
C
Case 2
Case 1
Late +Corr
Early +Corr
711.4
412.5
729.1
715.2

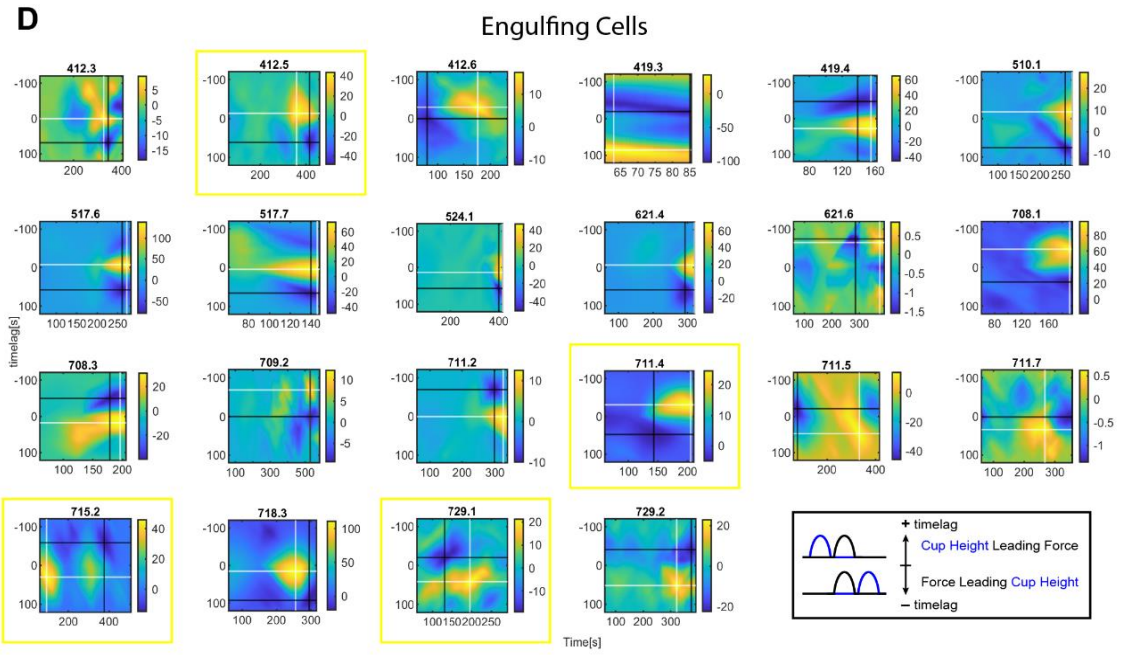
D
Engulfing Cells
412.3
412.5
412.6
419.3
419.4
510.1
517.6
517.7
524.1
621.4
621.6
708.1
708.3
709.2
711.2
711.4
711.5
711.7
715.2
718.3
729.1
729.2
timelag[s]
Time[s]
+ timelag
Cup Height Leading Force
Force Leading Cup Height
– timelag

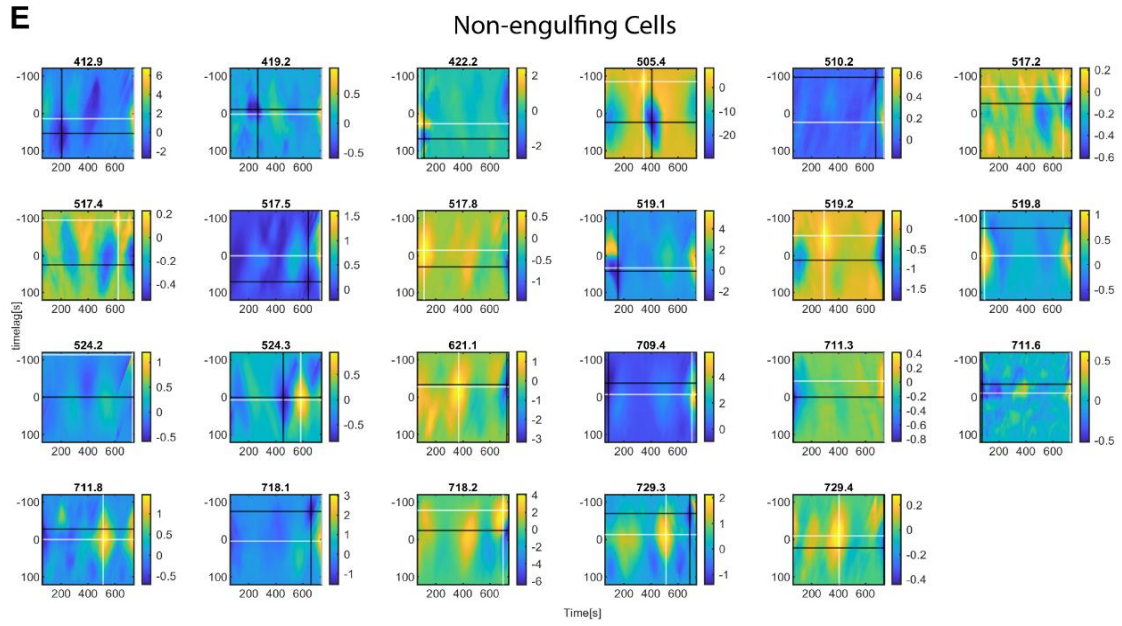
E
Non-engulfing Cells
412.9
419.2
422.2
505.4
510.2
517.2
517.4
517.5
517.8
519.1
519.2
519.8
524.2
524.3
621.1
709.4
711.3
711.6
711.8
718.1
718.2
729.3
729.4
timelag[s]
Time[s]

Figure 4.4. 3D Cross Correlation of Force and Cup Height for Engulfing and Non-engulfing cells. **A** Boxplot comparing the mean, maximum, and minimum correlation strength for between engulfing (+; n = 22) and non-engulfing (-; n = 23) cells. **B** Boxplots comparing the timelag, delay to engulfment, difference in timelag, and difference in delay between maximum and minimum correlations for curves of Case 2 (-Corr -> +Corr) and Case 1 (-Corr -> +Corr). Whiskers extend to data points that are within 1.5 times the interquartile range. Significance was tested using Wilcoxon ranksum test. $P < 0.05$ are denoted by * and $P < 0.0001$ are denoted by ****. **C** Four example 3D cross correlation plots from **D** showing each scenario between the timing of the maximum and minimum correlations. Black crosshairs identify the minima and white crosshairs denote the maxima. Timelag is on the y axis and the cross-correlation strength is now represented by the colormap. The x axis represents lab time. **D** All cross-correlation plots from the engulfment dataset. The last two tiles show a ky for interpreting sign of the timelag. If the change in force precedes the change in arc length, the timelag is negative. If the change in force follows the change in arc length, the timelag is positive. **E** All cross-correlation plots from the non-engulfment dataset. Force and Cup height curves were high pass filtered prior to correlating. Each color scale is unique and represents the range of correlation strength.

along the bead, we used a time window of 60 seconds to assess cross-correlations more locally in time.

To begin, I compared the correlation coefficients (strength) of the engulfing cells versus the non-engulfing cells (**Fig 4.4A,D,E**) after the same cross correlation analysis. Note that the colormap for each 3D cross correlation plot in **Fig 4.4D-E** is unique. Overall, the distribution of mean correlation coefficients was centered around zero for both engulfing and non-engulfing cells, however the engulfing cells had a significantly wider distribution. (**Fig 4.4A**; $\overline{cs}$ Non./$\overline{cs}$ Eng.) Therefore, I next looked at the maximum and minimum correlation strength throughout each experiment. Both the maximum and minimum correlation strengths in the engulfing category were strikingly larger in magnitude than the cases. (**Fig 4.4A**; + Non./+ Eng. and – Non./– Eng.) This strengthened the hypothesis that force and cup height are correlated in a distinctive way during phagocytosis as opposed to non-engulfing uncoordinated, low-level fluctuations of the cell membrane when phagocytosis is not initiated.

Focusing on only the engulfing cells, I further quantized each experiment into when the maximum and minimum correlations occurred with respect to timelag (measure of the difference in phase between the force and the cup height, positive timelag implies the cup height is leading the force and negative timelag implies that force is leading the cup height) and delay (the 'time until closure' i.e. the time in the lab frame when the engulfment is complete minus the time, with respect to the force curve, when correlation is maximal/minimal). In doing so, I identified two[2] types of behaviors within the engulfment dataset. 1. Maximum positive correlation comes *before* Minimal negative correlation (Case 1; 8/22 cells) and 2. Maximum positive correlation comes *after* minimum negative correlation (Case 2; 13/22 cells). (**Fig 4.4B**) What this means physically is that the cells were 1. Pushing up on the bead and increasing cup height followed by pulling down on the bead and increasing cup height or 2. Pulling down on the bead and increasing cup height followed by pushing up on the bead and increasing cup height. This is evident by a statistically significant delay time for the maximum correlation (**Fig 4.4B**; + delay/+ delay; $p = 0.0326$). While the positive correlations happening before the negative correlations showed a statistically significant difference in the delay time to engulfment, the negative correlations in these two cases did not. This suggests that there are cells that exhibit *early-stage* positive correlations (103.4 sec before engulfment) and cells that exhibit *late-stage* positive correlations (23.8 sec before engulfment) that are accompanied by negative correlations on either side of them. Representative examples of each of these four possibilities are shown in **Figure 4.4C**.

[2] One cell had the max and min correlations occur at the same time but with different timelags.

In both the positive and negative correlation cases, the timelag between force and cup height is observed to be both positive and negative. In Case 2, the difference in timelag between the maximum positive correlation and the minimum negative correlation was statically less than the same metric for Case 1 (**Fig 4.4B**; Δtimelag/Δtimelag). This means that in Case 2, the force and cup height were less out of phase than in Case 1.

Finally, I compared these categories to the grouping discovered in **Figure 4.2** to see if there were any trends between the scaling models and correlations in time. Though there were mismatched curves in each category, the majority of PCLE2 curves were in Case 2, the majority of PCLE1 and 'Misc.' curves were in Case 1. This is an exciting finding that requires further validation but I am happy to speculate on what it could imply.

First, the hallmark of the PCLE1 and 'Misc.' models are a parabolic shape (concave down for PCLE1 and concave up for 'Misc.'), and Case 1 describes situations where force and cup height first have the same behavior and later have opposite behavior. Assuming the 'stalling' found in **Figure 4.2** is ubiquitous, the PCLE2 model is consistent with two situations: an initial downward force, followed by an upward force, terminating in a downward force, while the cup height either increases linearly or when the cup height has two stalling periods. This variability may explain the diversity in the warped time domain plots in **Figure 4.2** for PCLE2. The 'Misc.' model suggests an initially upward force followed by downward force with a single stalling event in the cup height. PCLE1 model is less clear. However, it could be consistent with initially downward force followed by upward force and the cup height stalling later in engulfment, multiple stalling events or no stalling at. The importance of this stalling event in the progression

of target internalization is a something I feel is under appreciated in the field [49] [77] and it has been an enjoyable dial to turn in my thought experiments.

4.2.4 Measurement of the Pull of Force during Phagocytosis

Now that we have a detailed description of the coordination between force and cup height in the events leading up to engulfment, we are well positioned to discuss the bead "pull-off" event itself. We have established the dominating geometrical features influencing the force generation as well as the timescale over which force and cup progress influence each other during phagocytosis, but what is the magnitude of the force and what exactly does the cell do to detach it? One observation that should be brought to light is that the cell exerts force (positive or negative) on the bead for the entirety of the engulfment process. One might assume that a cell could pull the bead off by forming sufficient contacts around the equator of the bead and then pulling down. We have termed this mechanism "plucking." This is consistent with a model where the maximum force of the cell on the bead is downward and it is reached after passing the midpoint of the bead. This criterion is met with the CV and PCLE1 models. Another hypothesis that I have formed from observing the engulfment process in side view is one in which the cell wedges itself in between the surface and the bead, severing any attachments. This process would be much slower and perhaps energetically more favorable for the cell. We have termed this mechanism 'peeling.' Assuming the pressure created by the polymerizing actin within the leading edge of the cell membrane is negligible, the only requirement for this model is an upward force at the base of the cup that decreases to a downward force at the top of the cup. In order to narrow down the mechanism of pull off, we

directly measured the adhesion strength of the bead to the cantilever in “pull off” assays. We then compared the magnitude of force required to achieve “pull-off” with that method to the observed measured ‘engulfment force.’

To measure the strength of the attachment between the bead and the cantilever, we performed pull-off measurements. After “beading” the cantilever, the sample was moved to an adhesive layer and the bead was brought down to the surface for 10seconds and then the cantilever was retracted. **Figure 4.5A-B** show this process in action and **Figure 4.5D** shows a representative force curve for this measurement. The approach and retraction portions of the force curve act as a flat baseline from which to measure the force required to pull the bead off of the cantilever. Jim Fan performed 39 trials of the “control” experiments, resulting in a mean pull off force of -13.45 +/- 13.56 nN. This provides us with an upper bound on the force required to “pluck” the bead off of the surface of the cantilever.

Two other scenarios were salvaged from phagocytosis assays in which the cell did not engulf. These a noted as “Bead Pluck” and “Bead Stuck” and drawn in **Figure 4.5C**. In the “Bead Pluck” scenario, the cell did not engulf but, upon retraction, the bead came off of the cantilever and stayed on the cell. This value was measured to be in good agreement with the “control” experiments (-9.75 +/- 8.78 nN) and was shown to be not significantly different from the “control” values using a Wilcoxon ranksum test. Both experiments measure the adhesion force between the bead and the cantilever so this should not be surprising. However, the “bead stuck” cases, where the cell did not engulf but the bead did not stick to it, were also shown to be not significant when compared to the “control” and “bead stuck” cases. I understand this to mean that the cell surface as a passive material does not provide sufficient force to overcome

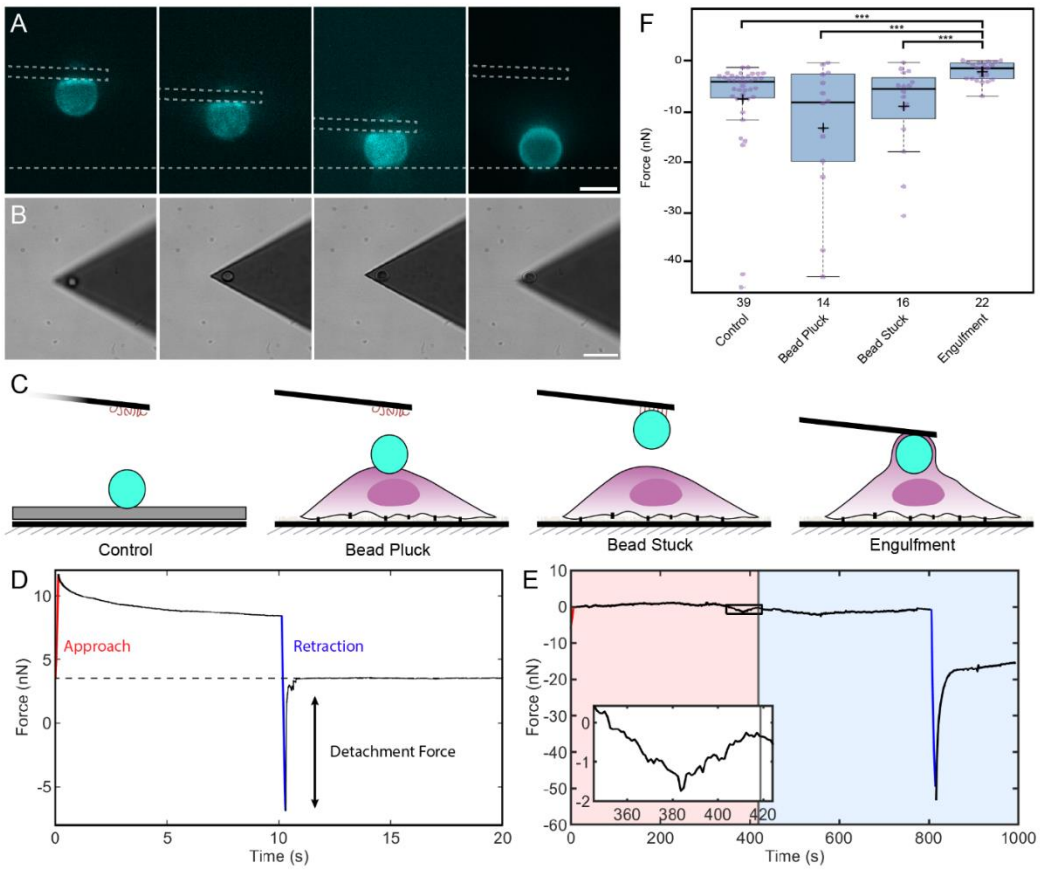

Figure 4.5 Cantilever-Bead Pull-Off Force Measurement**. A** Side view Fluorescence and **B** Brightfield microscopy images of the tip of the cantilever (dotted white line) and the 6um AF488 IgG bead (cyan) during bead attachment. **C** Cartoon representation of each of the resulting pull off experiments quantified in **F**. **Ci** shows the bead sticking to the adhesive layer after pull off, **Cii** shows the bead sticking to the cell after pull off, **Ciii** shows the bead failing to pull off the cantilever after contact with the cell, and **Civ** shows the bead being removed from the cantilever during phagocytosis. **D** Representative force curve from the bead pull off experiments. The cantilever approached the surface until it reached a set point of 10nN, maintained constant z-piezo position for 10s and then retracted from the surface, leaving behind the bead and a characteristic 'detachment' adhesion force. **E** Representative force curve from the engulfment experiments. The cantilever approached the surface until t reached a predefined z-piezo height, maintained in constant z-piezo position for 800s seconds and then retracted. The inset shows a zoom in of the region of the curve where the engulfment force was reached. The light red area of the graph is the engulfment period, the vertical line at about 420 seconds is the moment of closure and the light blue portion of the graph is after engulfment. **F** Boxplot of the pull-off force measurements from each pull-off method shown in **C**. Black horizontal line marks the median and black plus sign marks the mean. Means are the following: Control = -7.73nN; bead pluck = -13.45nN; bead stuck = -9.17nN; Engulfment = -2.19nN. Whiskers extend to data points that are within 1.5 times the interquartile range. Significance was tested using Wilcoxon ranksum test. $P < 0.05$ are denoted by * and $P < 0.001$ are denoted by ***.

the adhesion force between the cantilever surface and the bead. Hence, macrophages must employ alternative strategies to dislodge their targets from surfaces.

Finally, we defined the "engulfment" force to be the maximum downward force before engulfment. The moment of cup closure was determined using the circular kymograph and was defined as the time when the edges of the kymograph both met -180 and 180 degrees and thus both sides of the leading edge of the phagocytic cup were connected at the top of the bead. I found that the mean engulfment force was -2.19 +/- 1.89 nN. This was shown to be statistically smaller than all three of the other measurements (**Fig 4.5F**). This result refutes the "plucking" mechanism, as this force is not sufficient to overcome the adhesion between the bead and the cantilever. This event also occurs over a much longer period of time when compared to the "control" experiments (**Fig 4.5D-E**) aligning more with a "peeling" mechanism for particle detachment.

4.2.5 Actin Intensity at the Base of the Cup is Predictive of Engulfment

In engulfment cases, we have seen an overall downward engulfment force generated by the cell on the bead. However, we wanted to delineate forces actively generated by the cell from force contributions by the cell as a passive material. To do this, we analyzed the phagocytosis experiments in which the cells did not form a phagocytic cup and compared the actin accumulation in engulfing versus non-engulfing cells. The majority of this study has been on strictly the location of the leading edge of the phagocytic cup. This was achieved through segmenting the actin channel of the microscopy images. However, changes in F-actin intensity

can provide insight into the recruitment of actin or other cytoskeletal proteins to the base of the cup. Thus, I asked, is there something fundamentally different about the state of the actin beneath the bead of an engulfing versus a non-engulfing cell?

Non engulfing cells still has plenty of cytoskeletal activity and in every instance, associated with the target in some way. Therefore, both the engulfing and non-engulfing cells shared a similar region of actin beneath the bead (**Figure 4.6A**) which either remained relatively constant, or sprouted a cup. I defined an area of arc length 20 degrees by 0.5um outside of the bead surface as the base of the cup, as seen by the white lines in **Figure 4.6B-C**. Due to variations in Ftractin expression and general cell to cell variability, the time series of actin intensity was normalized to the initial value. Therefore, I chose to compare relative changes in F-actin intensity rather than absolute concentration.

Figure 4.6D-E show all experiments plotted together. For reference, I have also plotted the total cellular actin in the cell cross-section (not bleach corrected!) and the total cellular actin in the cup region over time. We can see that for both the engulfing cells and non-engulfing cells, the "whole cell" actin (assuming the distribution is similar in all planes) is constant throughout the experiment. (**Figure 4.6D-E**; pink) As a matter of fact, all three curves for the non-engulfing cells are relatively flat except the "whole cup" which slightly increases and the plateaus (**Figure 4.6E**; blue). This implies that the cell makes an initial association with the bead but does not wrap around the bead further. Perhaps the cell is still 'sensing' the bead, and potentially forming some filamentous actin in response to the IgG on the bead but still missing some essential link in order to cluster the receptors and produce the large-scale engulfment structures. Conversely, the "whole cup" curves for the engulfing cells appear to

experience a 2.5 fold increase in f-actin followed by a plateau (**Figure 4.6D**; blue). This makes sense because initially, there is only actin in the base of the cup and so we expect that the cup region will increase in actin as the cup proceeds up and around the bead. What is really interesting is the base of the cup. For non-engulfing cells, there is essentially no change in the intensity of actin. (**Figure 4.6E**; purple) For the engulfing cells, there is an initial increase followed by a decrease. (**Figure 4.6D**; purple) Furthermore, his peak in the cup base actin intensity occurs before the cup regions reaches the plateau. (**Figure 4.6D**; blue) This implies that early on in the initiation of phagocytosis, f-actin is recruited to the base of the cup.

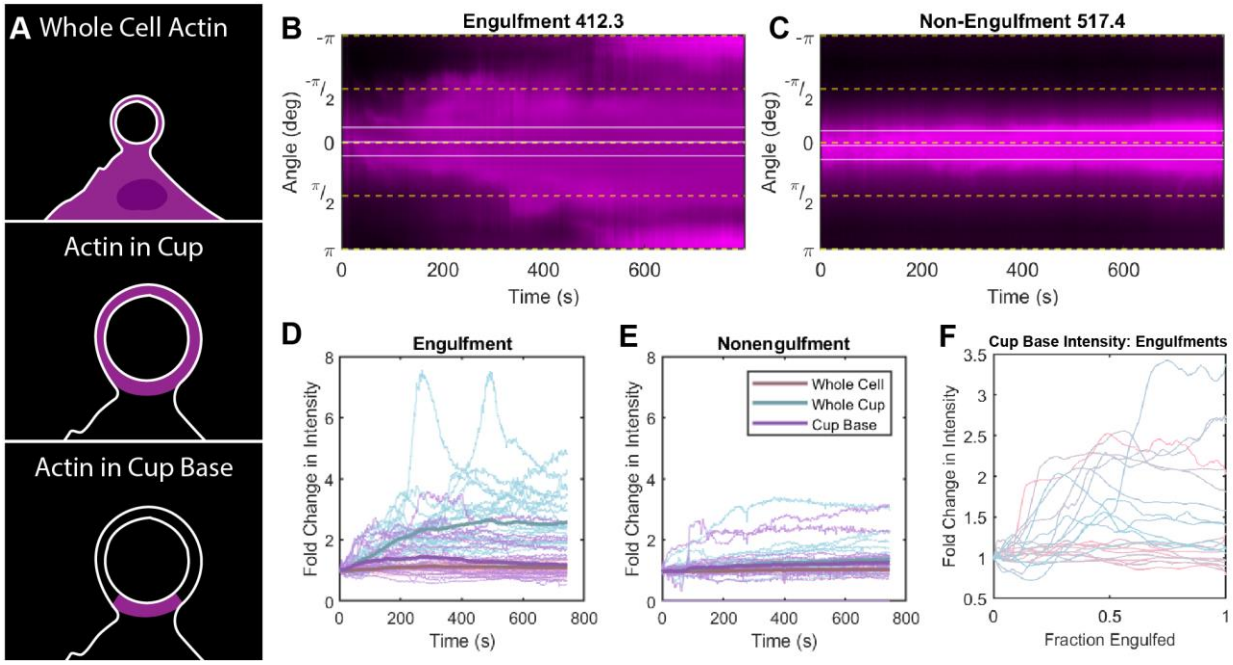

Figure 4.6. Comparing Cup Actin Intensity Between Engulfing and Non-engulfing cells. **A** Cartoon representation of the three areas of F-actin quantified; the entire 2D cross section, the area surrounding the bead (phagocytic cup), and the base of the cup. **B** and **C** Circular kymograph of an engulfing cell and non-engulfing cell, respectively. White horizontal lines mark the center of the cup and 10 degrees on either side of the center to define the "base" of the cup. Yellow dotted lines are at -pi, -pi/2, 0, pi/2, and pi for reference. **D** and **E** Fold change in F-actin intensity in the three regions defined in **A** (Pink: whole cell; Blue: whole cup; Purple: Cup Base) for engulfing and non-engulfing cells, respectively. Darker colored lines show the mean of each dataset. **F** Plot of the fold change in F-actin intensity as a function of fraction engulfed for the engulfing cells.

However, this concentration of f-actin is not maintained at the base of the cup, instead that f-actin to spread out into the leading edge of the phagocytic cup and the base of the cup returns to the original concentration. This is consistent with observations of the actin beneath the cup disassembling [44] [17] during FcR-mediated phagocytosis. Thus, we have identified actin recruitment as a in indicator of eventual internalization of the target particle.

4.3 Discussion and Conclusion

These results support three distinct models for phagocytosis, where the downward force of engulfment scales with the cup height. The implicit scaling laws of these models are derived based on previously and recently proposed mechanistic models for phagocytosis involving a contractile ring, a molecular clutch and actin polymerization [75] [69] [68] [26]. 3D cross-correlation analysis provided us with more details on the temporal order of events in the engulfment process, some of which were in good agreement with the proposed mechanical models. Furthermore, I have proposed a “peeling” mechanism for particle detachment from bound surfaces, a strategy that requires less force exertion from the cell. This could be advantages for the cell since studies have shown that cells under force respond to force, even altering gene expression. [78] To that end, we have ruled out the “plucking” mechanism in favor of the gentler “peeling” mechanism which is consistent with the measured engulfment force. Finally, I have confirmed that a “flush” of f-actin recruitment beneath the cup is a predictor of engulfment. With this sudden delivery of actin, the cell most likely also recruits other essential regulating and scaffolding proteins necessary for engulfment. Fluorescently labeling the cells for other actin associated proteins or regulators of the actin cytoskeleton

would perhaps help fill in the missing links between the coordination between cup height and force.

4.4 Methods

4.4.1 Microscopy

Side view fluorescent images were taken using a custom, single-objective, light sheet fluorescent microscope (LSFM) as described previously [55] [57]. Briefly, 561 nm and 488 nm (OBIS, Coherent) lasers combine colinearly into an acousto-optic tunable filter (AOTF) (AOTnC-400.650-TN, AA optoelectronic, France) to control laser intensity and sequential timing. After the AOFT, laser light is passed into a single mode fiber optic cable (FT030-Y, Thorlabs) which guides the light into the AFM hood. The line Bessel light sheet (LBLS) is formed within the AFM hood by passing through beam expanders, a cylindrical lens (LJ1567RM-A, Thorlabs), and an annulus (R1DF200, Thorlabs). The LBLS is able to scan through the specimen using a lateral steering mirror (OIM 101 1", Optics-in-Motion). The axial motion of the LBLS is decoupled from the motion of the objective in Z using an electrically tunable lens (ETL) (EL-16–40-TC, Optotune). Finally, the LBLS arrives within the microscope body (Olympus IX-71, Olympus, USA), passes through the tube lens and objective (UplanSAPO 60×/1.2 NA W (Olympus, USA), then reaches the specimen. AOFT voltages were set such that the laser power at the specimen remained between 1.2-6.5 uW and 1.7-3.9 uW for 561 nm and 488 nm, respectively. A custom dual band pass filter cube assembly (TRF59904-EMOL2 C173202; Chroma, USA) passes 488 nm and 561 nm light to the sample and directs GFP and RFP emission to the camera. Emission light is collected and reflected by a 45-degree mirrored optical prism (described below) back down

through the objective, through a short pass filter (880nm), to another ETL which controls the focus of the image plane independent of the objective height. The imaging pathway terminates in an OrcaFlash4.0 V3 sCMOS (Hamamatsu, Japan).

4.4.2 Environmental control

The specimen is insulated with a custom 3D printed chamber (Thingiverse 2035546) placed on top of the circular sample coverslip to maintain proper environmental conditions. This chamber is secured to the stage with the Asylum Research MFP-3D magnetic petri dish holder and sealed with an FKM membrane on the cantilever holder to shield the specimen against evaporation. The chamber is designed with separate reservoirs for deionized water to maintain humidity as well as a gap which allows the prism to be introduced to the specimen. The sample temperature is controlled using the Asylum Research MFP-3D AFM petri dish heater. To further regulate the sample temperature, the objective is fitted with a Flexible Polyimide Foil Heater (Thorlabs HT10k) operated by a PIV controller (Thorlabs TC200). Both the petri dish heater and the PIV controller were set such that the specimen reached 37.0 °C with a 0.1 °C gradient from the center to the edge of the coverslip.

4.4.3 Substrate Preparation

Round coverslips (40 mm diameter, #1; Fisher Scientific) were acid washed in 1M HCl at 58C for 4 hours, rinsed twice in deionized water, and sonicated in fresh deionized water for 30 min three times. Then, coverslips were sonicated in 70% followed by 95% ethanol for 30 min each and stored in 95% ethanol. Once ready for use, coverslips were dried between sheets of

Whatman filter paper and plasma cleaned. Rings of Polydimethylsiloxane (PDMS) (10:1 Sylgard 184, Dow Corning, USA) were made from a custom PDMS mold (8:1 Sylgard 184), plasma cleaned, and quickly adhered to the round coverslips to form a water-tight, but removeable seal. The PDMS-cloning ring assembly was then UV cleaned for 15 min. Fibronectin (F1141 Sigma-Aldrich, USA; 50 ug/ml) in HBSS (14175095 Gibco, USA) was added to the PDMS ring and incubated at 37 degrees overnight. Prior to use, the sample was rinsed three times in HBSS (14025092 Gibco, USA).

4.4.4 Prism Fabrication

Mirrored right-angle prisms (part #8531-607-1; Precision Optics Corporation, Inc., USA) were glued (Norland optical adhesive 81; Norland Products, USA) onto glass capillary tubes (part #5010-100 and 3530-050; Wale Apparatus, USA) which were affixed to a compact table clamp (part #CL3; Thorlabs, USA). The UV polymerizing glue attached the flat side of prism to capillary tube, leaving the mirrored surface exposed. Prior to use, the prisms were rinsed in 70% ethanol and deionized water. If needed, accumulated debris was removed with First Contact polymer cleaner (Photonic Cleaning, USA).

4.4.5 Prism Alignment

To ensure that the prism is in line with the LBSL and lands on the coverslip at 45 degrees, a two layered calibration slide was used. The bottom layer contains 40nm fluorescent Rhodamine beads for visualizing the LBLS tilt and the top layer contains 15 um TetraSpeck beads for verifying the angle of the prism. Using translation micrometers, the prism edge is

brought onto the surface of the coverslip near a 15 um bead and the steering mirror and ETL are adjusted such that a side view image is formed. The prism-capillary tube-table clamp assembly was mounted to a 3D rotation stage equipped to control the pitch, roll, and yaw (TTR001, Thorlabs). Before each experiment, these controls are adjusted such that the side view image is aligned with the prism edge, ensuring that the prism is angled at 45 degrees with respect to the coverslip. For imaging, the AFM cantilever was first positioned over the cell of interest and the prism was then positioned over but not touching the AFM cantilever or the cell. The position of the prism edge was optimized as to not collide with the AFM cantilever in z, but close enough in y to the cell and cantilever such that the ETL has a sufficient working range to position the LBLS beam waist through the specimen in side view.

4.4.6 IgG Bead Functionalization

An aliquot of Polybead carboxylate 6um microspheres (17141; Polysciences Inc., USA) were washed three times in HBSS by centrifugation in an Eppendorf tube (6000 g, 1 min). To activate the carboxyl groups on the surface, the beads were resuspended in an EDAC (1-ethyl-3-(-3-dimethylaminopropyl) carbodimide; 171440010 Thermo Scientific, USA; 10 mg/ml) and NHS (N-hydroxysuccinimide); 24500 Thermo Scientific, USA; 10 mg/ml) solution in HBSS and rotated for 15 min at room temperature. The beads were again centrifuged and resuspended in and solution of AF488 Goat anti-Mouse IgG (A11001 Invitrogen, USA; 15 ug/ml) and Human IgG (I4506 Sigma-Aldrich, USA; 1.5 ug/ml) and rotated for 60 min in the dark. The IgG solutions were centrifuged (10,000 g, 5 min) prior to use in the functionalization steps. Finally, the beads were washed three times as described above.

4.4.7 Cantilever-Bead Attachment

Tipless cantilevers (Nanoworld TL1-Arrow-50; Nanoworld, Switzerland) were plasma cleaned and then treated with 0.1% APTES (aminopropyl triethoxysilane; Sigma) in toluene () via vapor deposition at 80 degrees for 60 min. The treated cantilever was then placed in the AFM chip holder and onto the AFM head for calibration in air followed by beading in imaging media. Following calibration, the plated cell sample was placed on the stage, the PDMS ring was removed, and IgG functionalized beads were added at a concentration of 2.5x10^4 beads/ml. Using the AFM head manual z translation stage, the cantilever was lowered onto a suitable bead and then raised to pick the bead off the surface. The sample was then moved to a cell and the beaded cantilever was lowered again before imaging. This beading process was repeated for each cell.

4.4.8 Cantilever Calibration

The spring constant and optical lever sensitivity (OLS) of the AFM cantilevers were performed using the Sader method in air [79]. Because the tip of the cantilever is positioned partially beneath the PRISM, the super luminescent diode (SLD) spot was aligned further back on the cantilever tip. After submerging the cantilever in the imaging media of the sample, the OLS in liquid was calculated by taking a thermal noise spectrum and fitting the peak using the built in Igor software. [80]

4.4.9 Cell Line Transfection and Constructs

F-tractin-Halo RAW 264.7 cells were generated as described in a previous publication, including the complete transfection protocols and reagents [57]. Briefly, macrophage cell line RAW 264.7 were obtained from ATCC (TIB-71) and the final stable cell line was made by two successive transfections followed by antibiotic selection. First, a stable RAW 264.7 cell line expressing reverse tetracycline-controlled transactivator (rtTA) was produced to create an inducible expression system. Then, that cell line was used to produce a stable cell line expressing F-tractin-Halo under the control of the tetracycline-dependent promoter. Both cell lines were generated using a PiggyBac transposon system and transfected with Viromer Red transfection reagent (Lipocalyx, Weinbergweg, Germany) according to the manufacturer protocol. PiggyBac plasmids PB-rtTA and PB-miRE-tre-Puro were generously gifted by Mauro Calabrese (The University of North Carolina at Chapel Hill). The plasmid PB-tre-F-tractin-Halo-Hygro was constructed as previously described [57]. All plasmid were confirmed by sequencing (Genewiz, USA) prior to transfection.

4.4.10 Cell Culture

Stable F-tractin-Halo RAW 264.7 cells were maintained in RPMI 1640 media (61870036; Gibco, USA) supplemented with GlutaMax (; Gibco, USA) and 10% heat inactivated (56C, 30 min) fetal bovine serum (;VWR, USA). Subcultures were prepared with cell detachment using Accutase (; StemPro, USA) and gentle scraping. Cells were used between passage number 9-22. Prior to imaging, the cell imaging media (describe media) was supplemented with doxycycline (50 nM, 48 hrs; ;) in order to induce F-tractin-Halo expression. For phagocytic experiments, cells

were plated onto fibronectin coated coverslips within the PDMS rings. One hour before imaging, JaneliaFluor 549 (JF549) HaloTag ligand in imaging media (concentration 30 min; Janelia Farms, USA) was added to the cells followed by three subsequent washes in imaging media every 10 min to remove unbound dye.

4.4.11 Imaging and AFM settings for side view phagocytosis experiment

Using the oculars, AFM head wheel, and stage micrometers of the microscope, the cantilever was beaded and the sample was moved to an appropriate cell displaying lamellipodia and filopodia. The bead of the cantilever was positioned over the cell of interest and lowered to less than 8um above the cell. Then, the prism was positioned over the cantilever and the cell with the bottom edge of the prism touching down on the coverslip less than 50 um beneath the cell. The lateral position of the prism was set such than the prism did not obscure the SLD laser spot on the back of the cantilever. Using the imaging application (HCImage Live) for the camera, the LBLS position was honed to pass through the center of the cell using the mirror voltage. Fine adjustments of the cantilever height above the cell as well as the LBLS waist position (excitation ETL voltage) and image focus (emission ETL voltage and objective height) height were made once in side view. The camera was set to accept external trigger and a custom LabView program was used to communicate between the AFM, AOFT, camera, and steering mirror. When the force curve began, the AFM controller also triggered the start of the custom synchronization script (Igor) within the Asylum Research Software synchronizing the AFM and the camera. The 561 nm and 488 nm lasers had a 300 ms exposure and 100 ms delay sequentially. Laser power at the sample was chosen to provide sufficient SNR with a maximum

of 30 and 15 µW for 561 nm and 488 nm, respectively. Before each experiment, a virtual deflection curve was taken using the Asylum Research Software. The AFM was set to closed loop feedback and the velocity of the approach and retraction of the cantilever was set to 1 µm/s. Using the Igor software dwell mode, the Z-piezo was directed to approach the sample until a defined trigger was reached, stop (dwell) for 800 s, retract, and stop (dwell) for 200 s. This trigger was measured before each experiment such that the cantilever would be within 0.5 µm of the cell. During the dwell, the Z-piezo position remained fixed allowing the cantilever tip to move freely.

4.4.12 Minimum Bead Pull-Off Measurements

An adhesive substrate was prepared by placing a section of silicone transfer film (ARclad IS-7876) onto the center of a 40 mm coverslip. The coverslip was positioned for imaging and 2.5x10^4 beads/ml in HBSS were added to the sample atop the adhesive film. IgG functionalized 6 µm beads and APTES-treated, calibrated, and beaded cantilevers were prepared as described for engulfment experiments. After beading the cantilever, the sample was moved to the edge of the adhesive layer using the manual stage micrometers. The manual focus was raised to the top of the adhesive layer and the beaded cantilever was centered into view. The cantilever was lowered to within a few micrometers of the adhesive surface and a single force curve was taken using the Asylum Research Software. The approach and retraction velocity were set to 1 µm/s. The success or failure of the bead 'pulled off' from the cantilever was confirmed in brightfield. Regardless, the cantilever was then re-beaded with a new bead

and the process was repeated. The same cantilever was used for a maximum of 8 pull-off measurements.

4.4.13 Correlation of force signal and local actin activity

The cross-correlation analysis was performed on our AFM force time series, F(t), and the phagocytic cup height derived from the F-tractin fluorescence intensity outside of the IgG bead, H(t). For each image in the timelapse, the center of the bead was collected via a custom image segmentation script. Then, the intensity profile along a line segment centered through the bead was collected. This line segment was rotated about the bead center in increments of 2 degrees. The intensity values for 5 pixels from the bead edge were averaged for each angle value to generate an average actin intensity as a function of the position around the outside of the bead. The average intensity from each frame was plotted versus time as a circular kymograph. The cup edge was extracted with edge detection in Matlab using the first order derivative, resulting in the arc length, s. The cup height, h, was then calculated via the following equation, assuming spherical symmetry. (This is also known as the sagitta of a circle)

$$h = R\left(1 - \cos\frac{s}{2R}\right)$$

Prior to cross-correlation analysis, the force and cup height data were high pass filtered (frequency cut off = 0.5mHz) to remove offset and slope. Downward forces, toward the cell, are denoted as negative and upward forces, away from the cell, are denoted at positive. Therefore, positive correlations between the force and the cup height represent events where a. the cup width increases and the forces are upward (cell is pushing) or b. the cup width decreases and the forces are downward. Similarly, negative correlations represent events where a. the cup

width increases and the forces are downward (cell is pulling) or b. the cup width decreases and the forces are upward.

Since phagocytosis is a multistage process, we performed our cross-correlation calculations on subsets of the data, allowing for local assessment of the correlation strength. We chose a time window of 240 s and stepped through the dataset at increments of 2 s. Thus, the correlation strength at each time as a function of time lag of cup width relative to force is described below.

$$(F \star H)(t,\tau) = \int_{t-\frac{t_w}{2}}^{t+\frac{t_w}{2}} F(t')H(t'+\tau)dt'$$

where (F⋆H) signifies the unnormalized cross-correlation strength of force and cup height, t represents lab time, t_w is the time window, and τ is the time lag with τ=0 revealing the correlation strength without allowing time lag. The cross-correlation calculation is unnormalized to show a correlation strength that is proportionate to the increase in cup height magnitude.

4.4.14 Derivation of the PCLE2 model

In order to understand what force is actually being measured by the AFM, we need to sum all the forces on the bead in the z direction. Assuming the dominate contribution to the force on the bead lies within the contacts at the leading edge of the cup perimeter (red arrows and dots), and assuming these forces are circularly symmetric, the sum of the forces in the x-direction cancel, leaving only the z-component of the force of the cell on the bead. When the force on the bead is in the positive z-direction (green arrow), the bead experiences a downward

force from the cantilever, F_{AB}, and an upward force from the cell, F_{CBz}. Since the net acceleration of the bead is negligible, these two forces must sum to zero.

$$\sum F_z = -F_{AB} + F_{CBz} = 0$$

The contractile-ring model proposes a line tension, T, that acts horizontal to the z-axis of the bead at each height. However, contact forces on spheres must act normal to the surface so the magnitude of the force acting orthogonal to the bead surface (x'-direction), due to the tension in the contractile-ring, is $T_{x'} = T \sin\theta$. Forces that oppose the motion of the bead, due to molecular adhesions between the intracellular receptors of the cell to the ligands on the bead surface can be summarized as an effective friction force. When the force on the bead is in the positive z-direction (green arrow), the force from the cell on the bead, f_{CB}, points in the positive y'-direction, tangent to the bead surface and the force from the bead on the cell, f_{BC}, point in the negative y'-direction. The contributions from $T_{x'}$ and f_{CB} to F_{CBz} can be found by

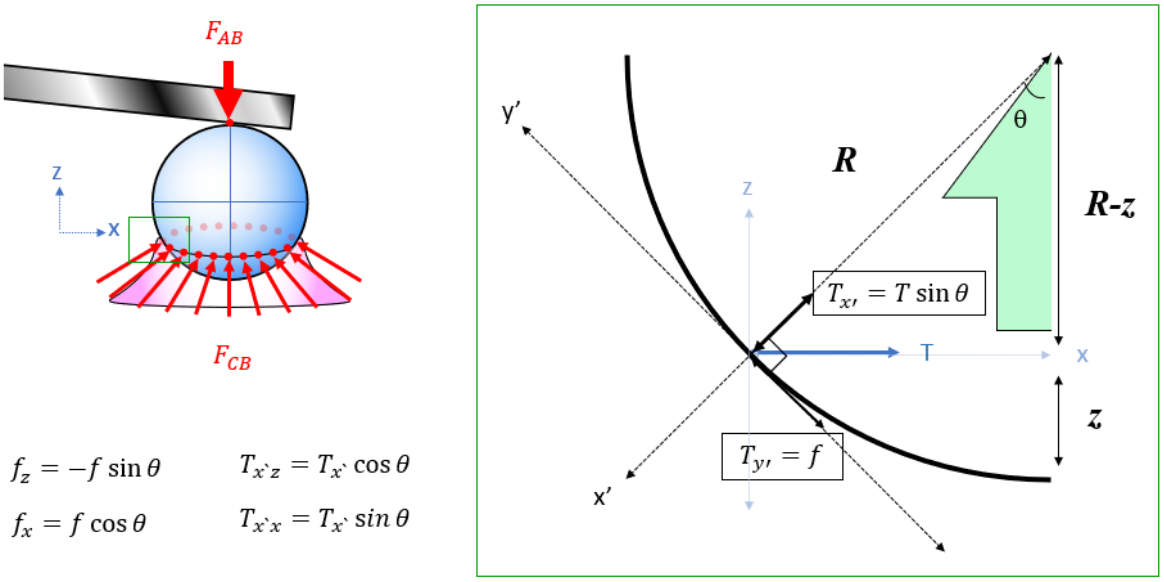

Figure 4.7. Diagram of Forces Acting on the Bead in the PCLE2 Model.

breaking both into components along the z-direction. The sum of the forces in the z-direction then becomes:

$$\sum F_z = -F_{AB} + (f_{CB} + T_{x`z}) = 0$$

$$\sum F_z = -F_{AB} - f\ sin\,\theta + T\ sin\,\theta\ cos\,\theta = 0$$

$$F_{AB} = sin\,\theta\,(f - T\ cos\,\theta)$$

By Newton's third law, the force of the AFM cantilever on the bead is equal and opposite to the force from the bead on the cantilever.

$$F_{BA} = sin\,\theta\,(T\ cos\,\theta - f)$$

Thus, the force from the bead on the AFM cantilever, the output of the AFM measurement, in terms of the cup height, z, bead radius, R, ring tension, T, and effective frictional force, f, is given below.

$$F_{BA} = \left(\sqrt{\frac{2z}{R} - \left(\frac{z}{R}\right)^2}\right)\left(T\left(1 - \frac{z}{R}\right) - f\right)$$

Before the engulfment is complete, the force from the bead on the AFM is equal to the force from the cell on the bead. After engulfment and internalization, the readout from the AFM is the force of the cell directly on the cantilever.

Chapter 5: Deformable Polyacrylamide Beads for Future Phagocytosis Studies

5.1 Actin Structures in the Phagocytic Cup

Though there is much we can learn from the plethora of information gathered from studying the actin cytoskeleton in cell migration, phagocytosis exhibits its own set of unique actin structures. With the onset of advanced microparticle technology [81] and high-resolution 3D imaging, the actin network composing the phagocytic cup has been revealed to contain dynamic clustered sites of F-actin. [82] [26] [68] [83] [56] [84] (**Fig. 5.1A-F**). As the presence of discrete actin spots within the phagocytic cup is still an active area of research, they have many different names. Ostrowski et al. identified these puncta (**Fig. 5.1A**) as 'podosome-like structures' and also reported that, unlike focal adhesions, the Arp2/3 complex was localized to the core of the podosome-like structure. Podosomes are small (<1um) actin structures composed of a branched F-actin core surrounded by a ring of adhesion and scaffolding proteins. They function as sites of adhesion and extracellular matrix degradation for migrating macrophages. Given their dynamic protrusions of different stiffness substrates, podosomes have also been implicated in mechanosensation [85] [86]. In a deformable target model, phagocytes were seen to assemble F-actin 'teeth' and aid in compressing the target during phagocytosis (**Fig. 5.1B**). In agreement with Ostrowski et al., inhibiting the Arp2/3 complex led to a decrease in the number of phagocytic teeth and thus the compressive force on the

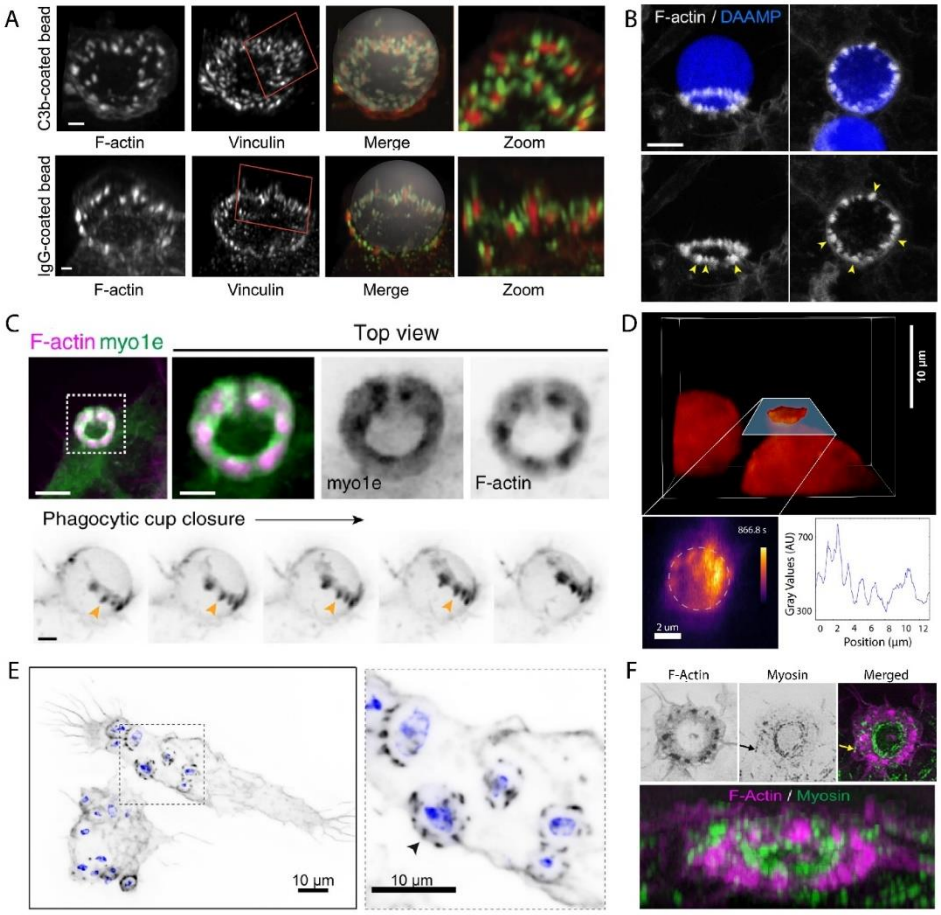

Figure 5.1. Actin Puncta or clusters within phagocytic cups formed by phagocytes. A 3D reconstruction of F-Actin (red) and Vinculin (green) in the phagocytic cup of Human macrophages introduced to complement C3b or IgG opsonized beads (shown in a grey overlay in the 'Merge' column). Images were captured using STED super-resolution microscopy. Scale bar 1um. Data from Ostrowski et al. *[84]*. **B** F-actin (white) of RAW macrophages engulfing 1.4kPa deformable microparticles (blue) opsonized with IgG. Yellow arrows point out individual "teeth." Images represent maximum intensity projections of confocal z-stacks captured using a Spinning Disc Confocal system. Scale bar 5um. Data from © 2021, Vorselen et al. *[68]*. **C** 3D representation of the actin (magenta) and myosin (green) within the phagocytic cup of a RAW macrophage engulfing an IgG coated bead (not shown). Imaged with a Spinning Disc Confocal system (top, Scale bar 5um and 2um) or a lattice light sheet microscope (bottom, Scale bar 4um). Copyright © 2019, Barger, et al **D** Volumetric representation of the F-actin (red/inferno) distribution of a RAW macrophage during phagocytosis of an IgG functionalized bead (not shown). Images were collected using line-bessel light sheet microscopy. Data from Copyright © 2020, Nelsen et al. *[56]*. **E** F-actin (black) labeled Human macrophages after ingestion of IgG-opsonized latex beads. Images were captured using an Airyscan super-resolution microscope. Data from © 2021, Tertrias et al. *[87]*. **F** 3D view of a Raw macrophage adhered to a 3-3.5um micropatterned IgG disc and labeled for F-actin (magenta) and myosin (green). Images were captured using 3D structured illumination microscopy. Data from Herron & Hu et al. *[83]*.

target[3] [84]. They report that this force of squeezing orthogonal to the target surface is balanced by an inward force towards the cell from the base of the cup in early cup formation and by myosin-II 'purse-string' contractility in late-stage cup formation.[4] A different lab found similar structures (**Fig. 5.1C**) while exploring the role of two molecular motors (myosin 1e and 1f) in phagocytosis of antibody-opsonized target. Like the Arp2/3 complex, removing these class 1 myosins prevented these actin 'plumes' from organizing correctly and thus disrupting proper internalization, though early-stage cup formation was unaffected [82]. Using line-bessel light sheet microscopy, Nelsen et al. were able to resolve punctate actin structures (**Fig. 5.1D**) in the phagocytic cup during the early stages of phagocytosis [56]. In an effort to distinguish the actin puncta that they observed (**Fig. 5.1E**), coined 'phagosome-associated podosome' from true podosomes, Tertrias et al. challenged macrophage cells with latex beads unfunctionalized with antibody. They found that phagosome-associated podosomes were not formed without IgG, the phagocytic cup did not mature into a phagolysosome, and furthermore, podosomes on other areas of the cell did not disassemble as they saw in the antibody case [87]. This implies that the pool of actin and adhesion proteins within the cell is shared between phagosome-associated podosomes and true podosomes. In an interesting two-dimensional geometry, Herron & Hu et al. introduced macrophages to flat, micropatterned IgG discs and observed the corresponding actin and other adhesion protein architecture (**Fig. 5.1F**). The authors fearlessly

[3] Though Tertrias et al. found the opposite to be true. Their phagosome-associated podosomes were resistant to the Arp2/3 inhibitor CK666, like podosomes [87].

[4] This is in conflict with what Waterman says. [164] She argues that the engulfment mechanism is dominated by an actin-generated protrusive force and the restoring force provided by the cortical tension. If a phagocytic cup can make it past the midpoint, it will always be engulfed, therefore not requiring a purse string mechanism. A pulling force originating from the base of the phagocytic cup is also unlikely due to the disassembly of actin puncta observed in Ostrowski et al [84].

identify the discrete actin structures forming around the perimeter of the IgG discs as 'phagocytic podosomes' and characterize the actin structure of these podosomes in revolutionary detail using localization-based super resolution microscopy. Using 3D Structured Illumination Microscopy (SIM), myosin II was revealed to organize in an expanding, inner ring between the podosomes and the IgG disc, potentially to aid in podosome protrusive forces necessary for phagocytic cup progression [83]. As self-sustaining structures, podosome assembly does not require contractility, though myosin can indirectly modulate podosome growth and protrusion [88]. As 3D imaging techniques improve, the organization of these phagocytic podosomes and the interplay with adhesion proteins will emerge to increase our understanding of the mechanism by which phagocytes engulf.

5.2 Results

5.2.1 Three-Dimensional Bead Segmentation

I have developed a segmentation algorithm to automatically define the shape boundary of deformable polyacrylamide beads from a fluorescent 3D dataset. **Figure 5.2a** shows a single slice of a volumetric dataset of macrophage cells engulfing antibody coated deformable beads. Each of these beads are labeled for reference later in other sections. To begin visualizing, a field of view containing a single bead is selected from the volumetric dataset as shown in **b**. **c** Each slice of the volume is then passed through a series of image processing steps in order to isolate the perimeter of the bead. The edges of the bead are first identified using Laplace of Gaussian edge detection. The identified edges are then dilated to create continuity between neighboring line segments. Then, the entire shape is filled to remove internal edges. Watershed, dilating,

filling, area exclusion steps are then implemented to remove extraneous artifactual shapes not associated with the bead. Finally, the edges are eroded to return to the original size, and the perimeter of the solid shape is determined. **Fig 5.2d** shows the result of this segmentation algorithm used on each of the four beads. All image processing and 3D visualization was done in Matlab and ImageJ.

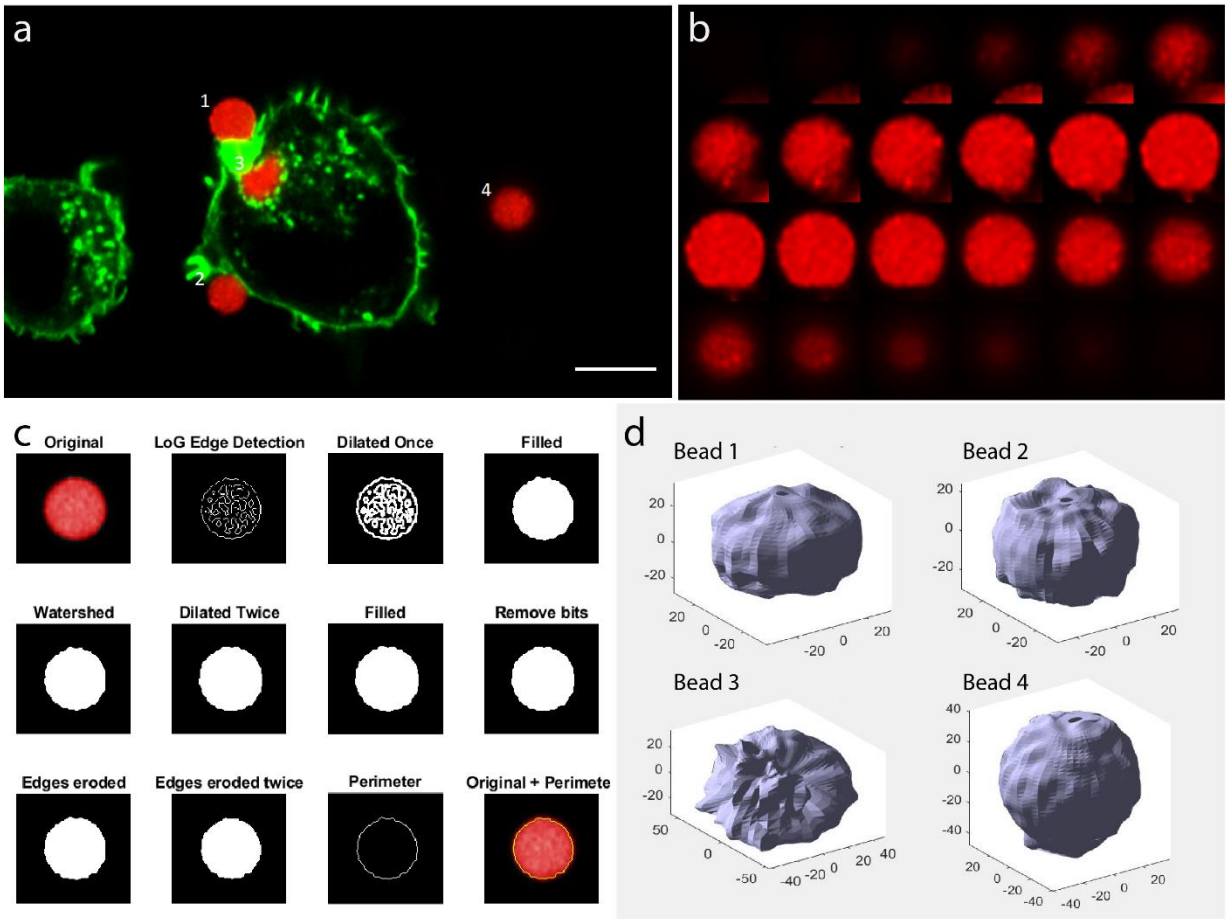

Figure 5.2. Three-dimensional deformable bead segmentation. a Composite fluorescent image of RAW 264.7 macrophages (green) stained with Alexa Fluor 488 Phalloidin and 6um polyacrylamide beads labeled with Janelia Fluor 549 IgG. The four beads in the field of view are labeled for reference. Note that this image is one cross-section in a dual-color volumetric dataset taken using a Zeiss Ariyscan. Scale bar: 10um. b Montage of the confocal slices through Bead 1 which make up the volumetric set. c Image processing steps in the segmentation algorithm to automatically determine the bead edge. d 3D visualization of each of the four beads from the volume described in a. Units are arbitrary.

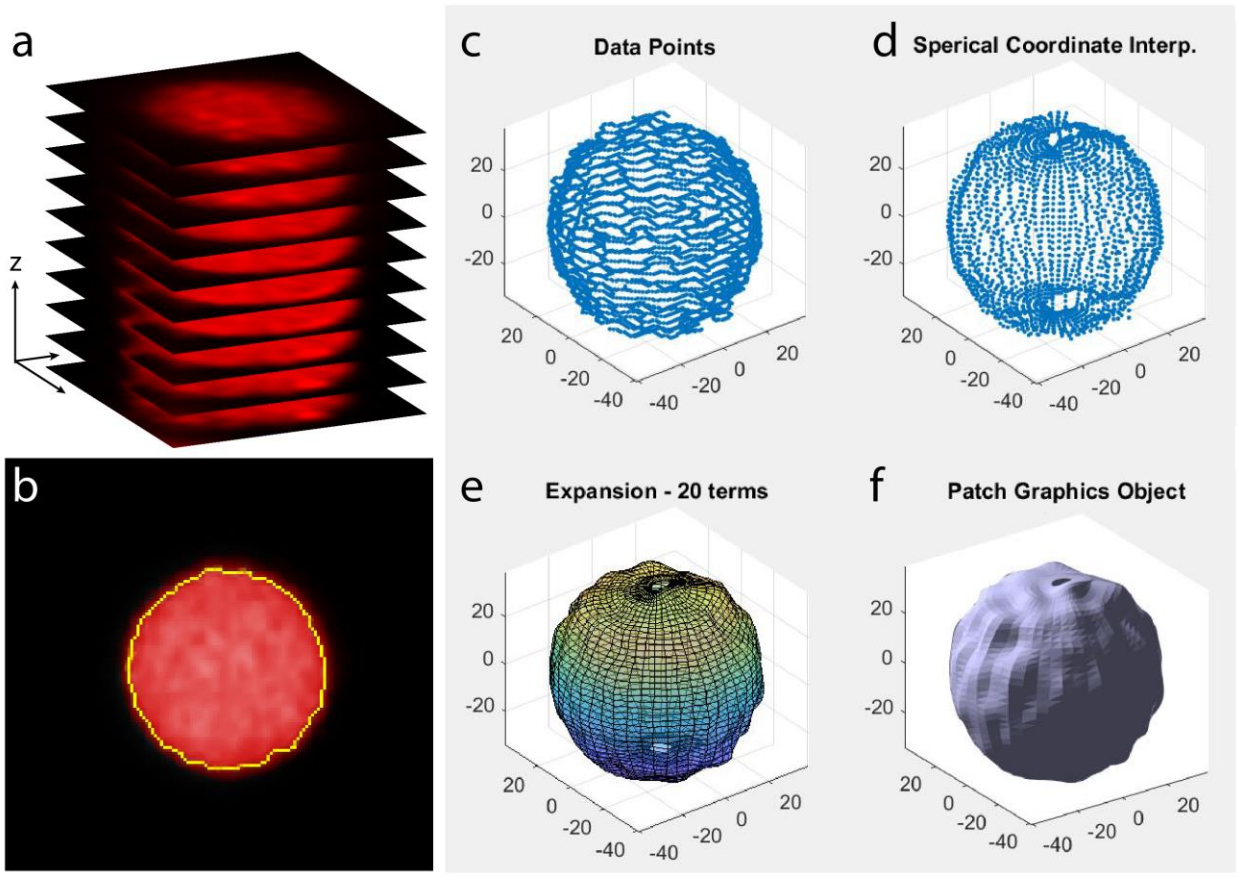

Figure 5.3. Computing a surface from spherical harmonic expansion. **a,b** A volumetric tiff stack of images is read into our custom Matlab script to identify the edges of each slice. **c** The edges from each slice are represented in a cartesian coordinate system to form a point cloud. **d** The point cloud is interpolated into spherical coordinates for a defined number of phi and theta coordinates. **e** The surface of the bead is computed up to 20 terms in the spherical harmonic expansion. **f** The final bead surface displayed using the Matlab patch graphics object.

5.2.2 Spherical Harmonic Fitting of the Surface

In collaboration with Dr. Moslem Moradi, I have described the surface of these deformable beads using spherical harmonic expansion. After the segmentation described in **Fig 5.2**, the point cloud is interpolated from cartesian coordinates to spherical coordinates, **Fig 5.3a-d**. To calculate spherical harmonics, we find Y1 for positive m, and Y2 for negative m. The expansion coefficients ax, ay, az (for positive m), and ax2, ay2, and az2 (for negative m) are then

calculated by integration. The integration is done by summing over the values of the integrand multiplied by weights:

$$\int_0^{\pi}\int_0^{2\pi} x(\theta,\varphi)Y^*_{\ell,m}(\theta,\varphi)\,\sin\theta \mathrm{d}\theta\,\mathrm{d}\varphi = \sum_{i=1}^{N_\theta}\sum_{j=1}^{N_\varphi} x(\theta_i,\varphi_j)Y^*_{\ell,m}(\theta_i,\varphi_j)\,w_\theta^i w_\varphi^j$$

Where N is a normalization prefactor.

5.2.3 Preliminary Shape Analysis for Bead Deformation

In order to compare the indentations we observed on our beads during phagocytosis to the deformations caused by podosomes, we measured the indentation depth, indentation width, and indentation spacing for each bead (**Fig 5.4a,b,c,e**). There was no significant difference between the width or spacing of the indentations for all four beads. Furthermore, these width values are consistent with the average diameter range of podosome indentations cited by van den Dries, et al. [86] The indentation depth of bead 1, 2, and 4 showed no significant difference, however, the indentation depth of bead 3 was significantly different than bead 1, 2, and 4. It's important to note that bead 3 is the only bead completely internalized by the cell as well as the only bead with obvious punctate actin spots surrounding the bead and coincident with the indentations. Using the Hertz model for force we can estimate the forces exerted by these podosomes. Assuming the protrusive heights, δ_{Ref}, and elastic modulus, E_{ref}, from Bouissou et al., we can see that the force necessary to indentor our significantly softer beads is 10^4 less than that needed to indent the 2.3GPa formvar sheets used in Bouissou et al. This implies that the actin structures causing these indentations are mechanosensitive and adapt to the stiffness of their target, only exerting as much force as necessary.

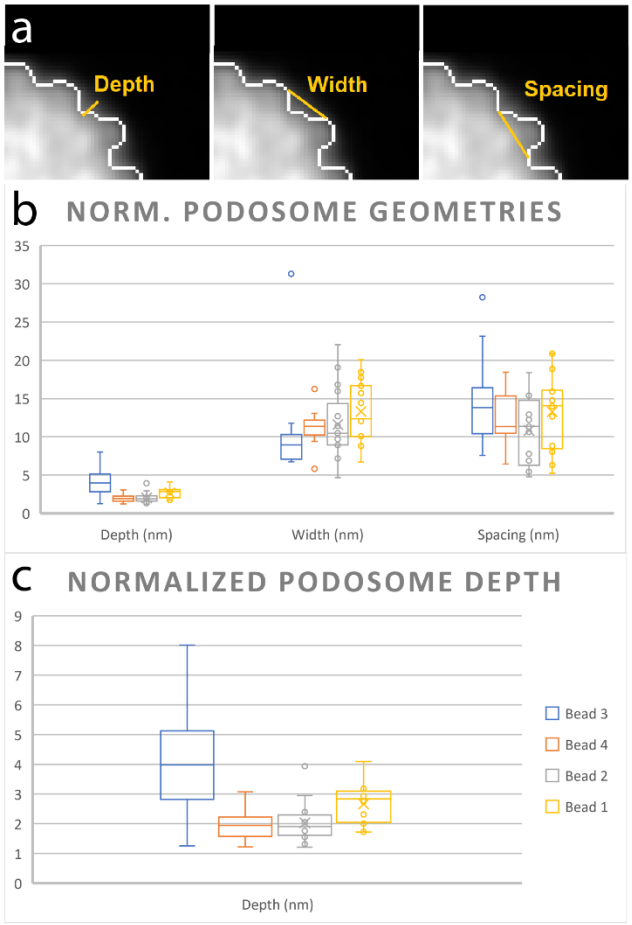

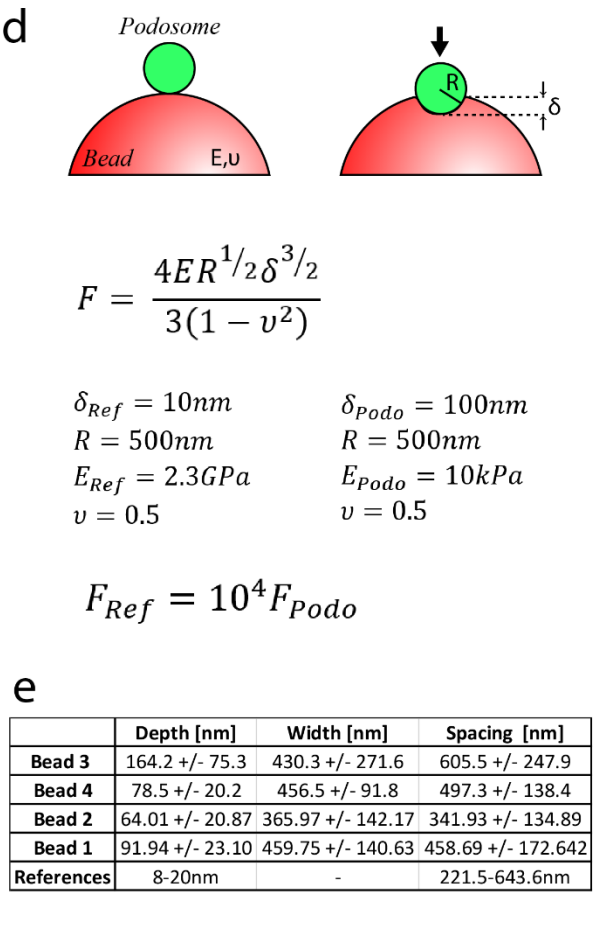

e

	Depth [nm]	Width [nm]	Spacing [nm]
Bead 3	164.2 +/- 75.3	430.3 +/- 271.6	605.5 +/- 247.9
Bead 4	78.5 +/- 20.2	456.5 +/- 91.8	497.3 +/- 138.4
Bead 2	64.01 +/- 20.87	365.97 +/- 142.17	341.93 +/- 134.89
Bead 1	91.94 +/- 23.10	459.75 +/- 140.63	458.69 +/- 172.642
References	8-20nm	-	221.5-643.6nm

Figure 5.4. Relating bead indentations to podosome geometries. **a** Shows an example of how the shape descriptors; depth, width, and spacing, were measured for each bead. The three panels are taken from the central slice of Bead 4. **b,c** Plots of the indentation depth, indentation width, and indentation spacing for all four beads, described in **Fig 5.2a**. In a t-test assuming unequal variance with a significance level of 0.05, Bead 3 indentation depth is significantly different from beads 1, 2, and 4. **d** Cartoon illustrating how a spherical indentor of radius, R, (green, podosome) may deform the bead (red) of Young's Modulus, E, and poisson ratio, υ, causing an indentation depth, δ. Using the Hertz model and our approximate bead elastic modulus and measured indentations, we can approximate the force.

5.3 Conclusion and Future Work

This is the beginning of a new dimension to the force measurements during phagocytosis. Using soft targets is nothing new in the field of immunology, however, combining the deformable beads with the AFM cantilever experiments would provide net forces on the

target as well local forces on the target. Future phagocytosis experiments combining this technique with the “bead pull off” experiments described in Chapter 4 would provide both local deforming forces as well as net downward forces. In this way, we could correlate the behavior of the cell in the decision-making process of engulfment. Does it deform the target before deciding to engulf it? If the target is too well-adhered to the substrate, does the cell decide to undergo trogcytosis [43] instead of full engulfment? This technique will open the door to an expanded breadth of force resolution.

Chapter 6: Guanine Nucleotide Exchange Factor (GEF-H1) Activation in RAW 264.7 Macrophage Cell Protrusions and Phagocytic Spreading

Phagocytosis is a complex cellular process that requires precise spatial and temporal remodeling of the actin cytoskeleton. It is well documented that the actin driven engulfment process depends on upstream GTPase activation, but it is still unclear how phagocytosis relies on the activation of GEFs. Active GEF-H1 has recently been associated with regulating force response and leading-edge dynamics during migration. Using a single-chain FRET biosensor we are able to correlate relative changes in the activation state of GEF-H1. The GEF-H1 biosensor consists of a yPet and mCerulean3 FRET pair inserted into the hinge of the autoinhibitory domain to signal the change in conformation of the protein upon activation. We have made a RAW 264.7 murine macrophage cell line stably expressing this biosensor as well as Ftractin-Halo in order to study the dynamics of GEF-H1 activation during phagocytosis. We have captured the actin distribution and GEF-H1 activity during frustrated phagocytic spreading of cells on IgG functionalized substrates. Within an average of 3 minutes after contact, the macrophage cells spread to their maximum area. During this spreading, GEF-H1 activation is highest at the leading edge of the phagocytic cup. This suggests that GEF-H1 activation plays a role in the mechanosensory process of phagocytosis.

6.1 Rho Family GTPases and GEF Signaling in Phagocytosis

Many fundamental cellular processes are regulated by members of the Rho family GTPases, including division, migration, adhesion, and phagocytosis. Rho GTPases and their associated signaling proteins often cooperate or antagonize each other to orchestrate cellular tasks. This results in a complex molecular dialogue between signaling proteins at many levels of their signaling pathways dynamically regulated in space and time. This crosstalk between members of the signaling network effects protein activation conformation, protein expression and stability, and regulation of downstream signaling pathways.

In order for cells to move, the underlying actin cytoskeleton is remodeled by multiple signaling cascades coordinated in space and time. The Rho family Guanosine Triphosphatases (GTPases) act as critical regulators of this signaling network by activating downstream effectors of the dynamic actin cytoskeleton. [89] GTPases are highly conserved proteins that act as molecular switches by cycling between a guanosine diphosphate (GDP)-bound, inactive state

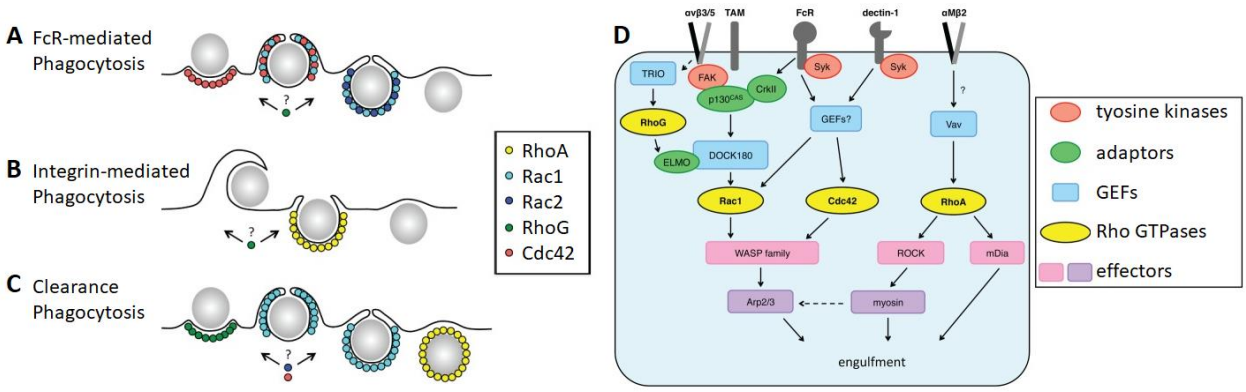

Figure 6.1. Rho GTPase Signaling in Phagocytosis. **A** Schematic of the location of CDC42, Rac1, and Rac2 at different stages of FcR-dependent phagocytosis. **B** The location of RhoA during Integrin ($\alpha M\ \beta 2$)-mediated phagocytosis. **C** The location of RhoG, Rac1, and RhoA at different stages of clearance phagocytosis. **D** Phagocytosis signaling network diagram for several surface receptors. Note that the GEFs are upstream of the GTPases and engulfment is downstream of the GTPases. *[99]* Copyright © 2014, Mao & Finnemann.

and a guanosine triphosphate (GTP)-bound, active state. [90] The activation state of GTPases is altered by several regulatory proteins such as GTPase-activating proteins (GAPs), which turn off signaling via induced GTP hydrolysis, and Guanine nucleotide exchange factors (GEFs), which turn on signaling by promoting the exchange from GDP to GTP. [91] In the active state, GTPases 'turn on' a signaling network that can lead to processes such as formin-mediated actin polymerization [92] [93], ARP2/3-mediated branched actin polymerization [94] [95], cofilin-mediated severing and actin depolymerization [96] [97], and actomyosin contractility [98]. These fundamental actin processes form a toolset from which cells can orchestrate the formation and dismantlement of complex cytoskeletal structures.

The roles of several Rho family GTPases have been implicated in Fcγ Receptor (FcR)-mediated, Complement Receptor (CR3)-mediated, and clearance phagocytosis. [99] **Figure 6.1A** summarizes the essential GTPases reported for each type of phagocytosis. Early on, phagocytosis was thought to proceed through distinct methods of internalization depending on receptor-ligand pathway. FcR-mediated phagocytosis was marked by membrane ruffles and a phagocytic cup that wrapped around the target like a 'zipper.' Particles undergoing CR3-mediated phagocytosis were observed to 'sink' into phagosome with little to no protrusions from the membrane. [19] [18] Though both processes were mediated by actin polymerization, several studies sought to uncover the molecular events behind these morphological differences [21] [22]. Rho Family GTPases had recently been well characterized in the context of cell migration, and therefore ideal candidates. See **Figure 6.1B** for a visual summary of the GTPases and their upstream and downstream effectors. Rac1 and CDC42 were found to be required for FcR-mediated phagocytosis [21] [22], and RhoA was found to be required for CR3-mediated

phagocytosis [21]. FcR-mediated phagocytosis was assumed to be driven by branched actin networks given that ARP2/3 is downstream of both Rac1 and CDC42 activation, and the 'sinking' observed in CR3-mediated phagocytosis was predicted to be contraction caused by formin-mediated actin bundles joined to myosin-II due to mDia1 and ROCK being downstream of RhoA [23]. However, advances in detailed imaging of the engulfment process revealed ruffling and protrusions were also present in CR3-mediated phagocytosis [24], suggesting CR3-mediated phagocytosis also utilized Rac1 and/or CDC42 signaling upstream of phagocytosis. Furthermore, inactivation of the ARP2/3 complex affected both FcR and CR3-mediated phagocytosis [27] [28], supporting the notion that both types of phagocytosis required Rac1 and CDC42-medated branched actin and RhoA-mediated linear actin networks [100] [101] [102].

Consistent with this hypothesis, Jaumouille et al. used high resolution microscopy to show that both ARP2/3 (branched actin) and formin mDia1 (linear actin) are involved in the assembly of actin structures required for CR3-mediated phagocytosis [26]. While the exact role of mDia1 has yet to be discovered, one could reasonably assume that the linear actin bundles it generates play a role in reinforcing the branched actin network and providing opportunities to form additional links from integrins to the cytoskeleton. As there are no known direct or indirect mechanical linkages between the more specific phagocytic receptors (such as FcR) and f-actin, these secondary connections via integrins become critical for both pathways of target internalization [103]. In other words, each pathway may be initialized by distinct molecular interactions (**Fig 6.1A**), however, in order to physically surround and engulf the target, they may

both employ a shared set of integrin-based adhesions and molecular clutch driven branched-actin polymerization (**Fig 6.1B**).

While the dynamics of Rho GTPases in phagocytosis have been well characterized, not much is known about the spatiotemporal sequence of events leading to GTPase activation. From in vitro and live cell studies, we know that GEFs are one of several classes of regulatory molecules that modulate the activation state of multiple downstream GTPases. This added degree of complexity in the signaling network allows GTPases to perform their functionally distinct actions in different areas of the cell. However, this also exposes the need to explore these uncharacterized upstream activation dynamics in space and time within living cells. In the context of cell migration, RhoA has been shown to initiate both protrusions and retractions in different areas of the cell [104] [105] [106] and GEF-H1 was identified as a major GEF controlling the activation state of RhoA. [57] GEF-H1 is also the reported to localize to microtubules in its inactive conformation and activates after microtubules detachment [107]

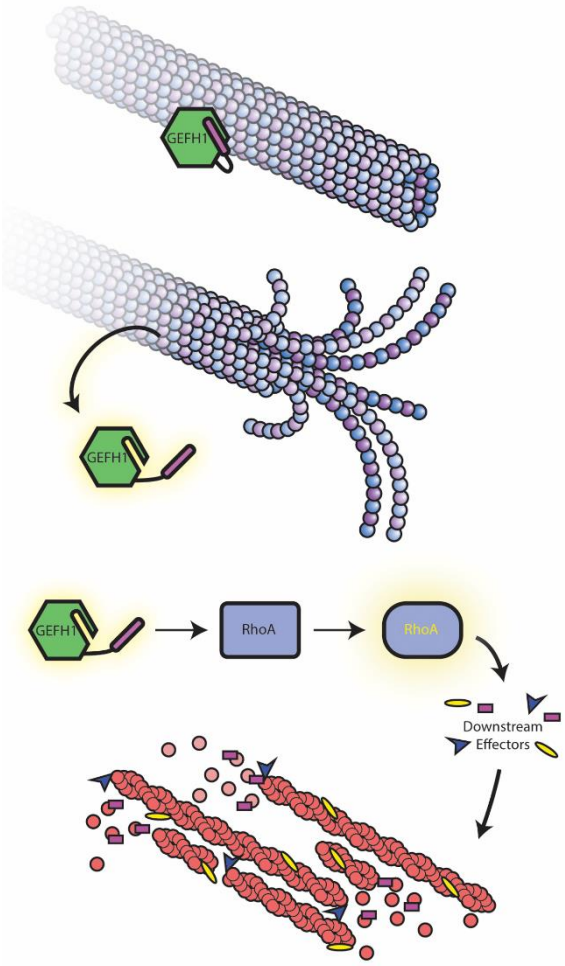

Figure 6.2. GEF-H1 and RhoA Regulate the Microtubule and Actin Cytoskeleton. Shows GEF-H1 bound to a microtubule in its inactive state, activating upon microtubule disassembly, catalyzing RhoA into its active form, and RhoA interacting with downstream effectors to modulate the actin cytoskeleton.

[108] allowing it to then encourage RhoA activation and subsequent actin remodeling. (**Fig 6.2**) Therefore, GEF-H1 is considered a critical regulator between the dynamics of the microtubule and actin cytoskeleton. [109]

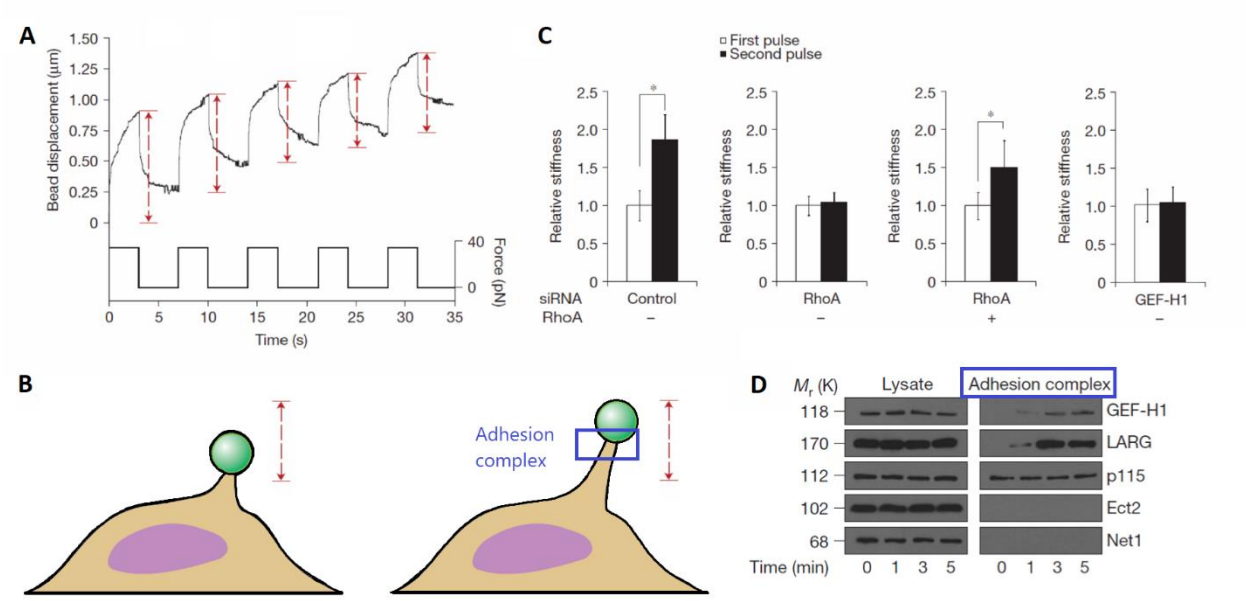

Figure 6.3. Cell Stiffening in Response to Force. **A** The bead displacement after successive force pulses shows a decrease in the overall amplitude, implying the cell is stiffening in response to the pull. **B** Cartoon representation of the force pulsing experiment. **C** Bar graphs summarize the effect of RhoA or GEF-H1 knockdowns. Cells without RhoA or GEF-H1 did not exhibit a stiffening response. **D** Comparing the amount of protein in the whole cell lysate versus the adhesion complex versus pulse number. As the number of pulses increased, more GEF-H1 and LARG were recruited to the adhesion complex, while the amount in the whole remained constant. Copyright ©2011, Guilluy et al. *[78]*

Perhaps not surprisingly, GEFH1 has also been found to play a role in mechanotransduction, the process wherein cells perceive the mechanical properties of their environment and react appropriately to perform cellular tasks. [110] In three-dimensional cell invasion, the microtubules of breast epithelial cells were found to be destabilized by a stiff extracellular matrix. This in turn led to an increase in GEF-H1 activation followed by RhoA activation. [111] In 2D cell migration, GEF-H1 was found to be required for neutrophil motility and migration under fluid shear stress. [112] [113] Finally, Guilluy et al. found that GEF-H1 was

recruited to the site of force application (**Fig 6.3D**) under integrin-stimulated tensional force cycles, implementing GEF-H1 as a key regulator of cellular force adaptation. [78] **Figure 6.3** shows how the cell stiffened in response to repeated force cycles. Given the recent work on phagocytes adapting to the geometrical and mechanical properties of their target [41] [114] [115], we sought to investigate the role of GEF-H1 in regulating mechanotransduction during phagocytosis.

In 2018, Azoitei et al., designed an activation GEF-H1 FRET biosensor to correlate RhoA activation, GEF-H1 activation, and edge motion in migrating cells. [116] Fluorescent biosensors provide the ability to observe the relative distribution of protein activity throughout the cell during the cellular phenomenon under study. [105] [117] The Authors found that GEF-H1 activation is sensitive to local changes in microtubule dynamics during cellular protrusions. I have used this same biosensor in RAW 264.7 macrophages to investigate the role of GEF-H1 in coordinating the actin cytoskeleton during phagocytosis.

6.2 Results

6.2.1 Stable Cell Line of Raw 264.7 Macrophages Expressing the GEF-H1 Biosensor

With extensive guidance from Dr. Takashi Watanabe, Raw 264.7 murine macrophage cells were transfected with a FRET Biosensor that reports the activity of GEF-H1. GEF-H1 has an autoinhibitory domain that obscures its active site in the inactive conformation. Azoitei et al. exploited the hinge region which connects the autoinhibitory domain to the Dbl homology (DH) of GEF-H1 by inserting a FRET pair. [116] (**Fig 6.4A-B)** In addition to the biosensor, these cells were also stably expressing F-tractin-Halo in order to correlate the actin cytoskeleton with GEF-

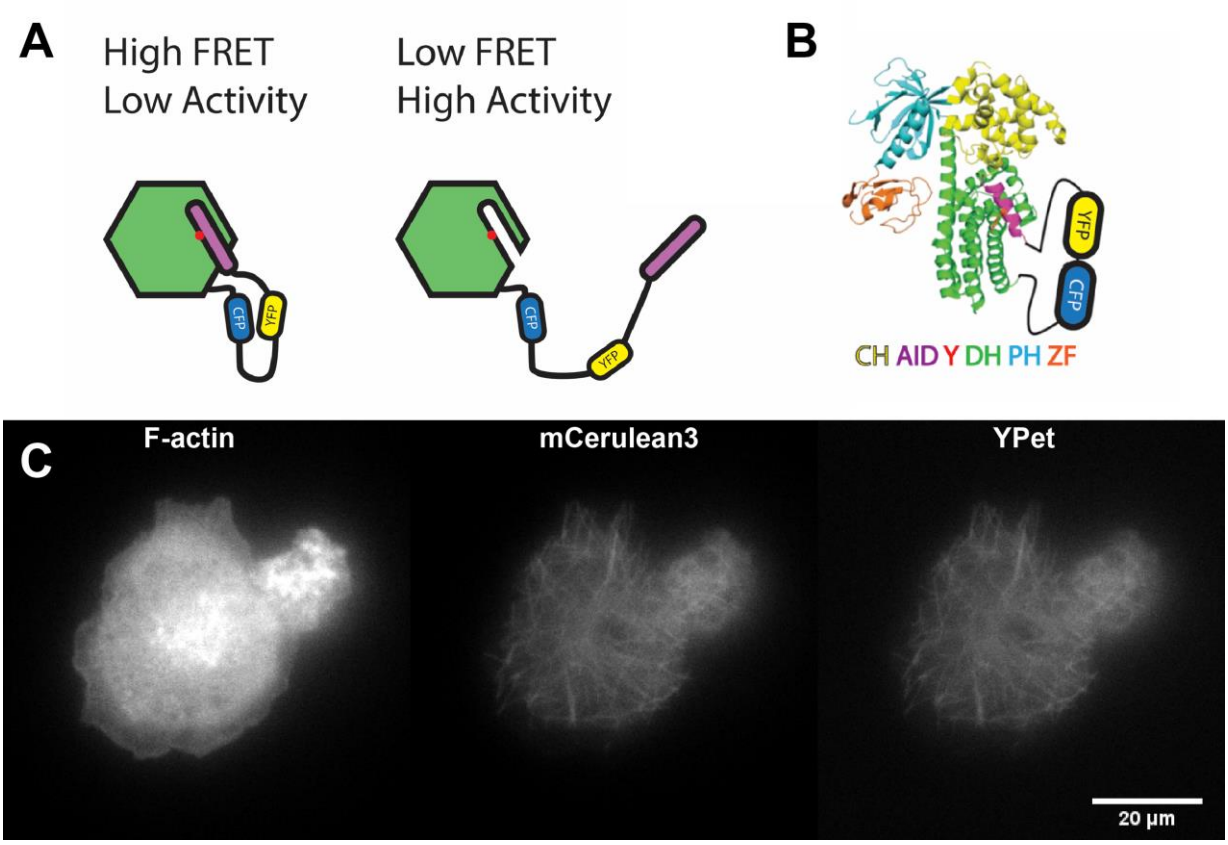

Figure 6.4. GEF-H1 Biosensor in Raw 264.7 Macrophage Cell Labels Microtubules. **A** The GEF-H1 biosensor design includes FRET pair added to the hinge region of the autoinhibitory domain of the protein. In this way, the FRET efficiency is high when GEF-H1 is in the inactive state and low when GEF-H1 is in the active state. **B** Ribbon diagram of GEF-H1 showing the autoinhibitory domain in purple, DH domain in green, and the FRET pair inserted in the hinge region between them. **C** Example three channel images of the Raw_Ftractin-Halo_GEFH1-BS stable cell line. F-actin is labeled by JF549 (left), mCeruclean3 acts as the donor of the FRET pair (middle), and YPet acts as the acceptor of the FRET pair (right). Note that the Ypet shown here is direct excitation, not FRET emission. Copyright © 2019, Azoitei, et al.

H1. **Figure 6.4C** shows the F-actin labeled by Ftractin-Halo and the microtubules of the cell labeled by the GEF-H1 BS. Direct activation of YPet in the FRET pair reports the distribution of all GEF-H1, active or inactive. Exciting mCerulean3 results in both mCerulean3 emission (when GEF-H1 is inactive and the FRET pair are separated) and FRET emission from YPet (when GEF-H1 is in its active conformation and the FRET pair are within Forster radius). Therefore, the ratio of mCerulean3 emission to FRET emission reports the relative activity of GEF-H1 within the cell.

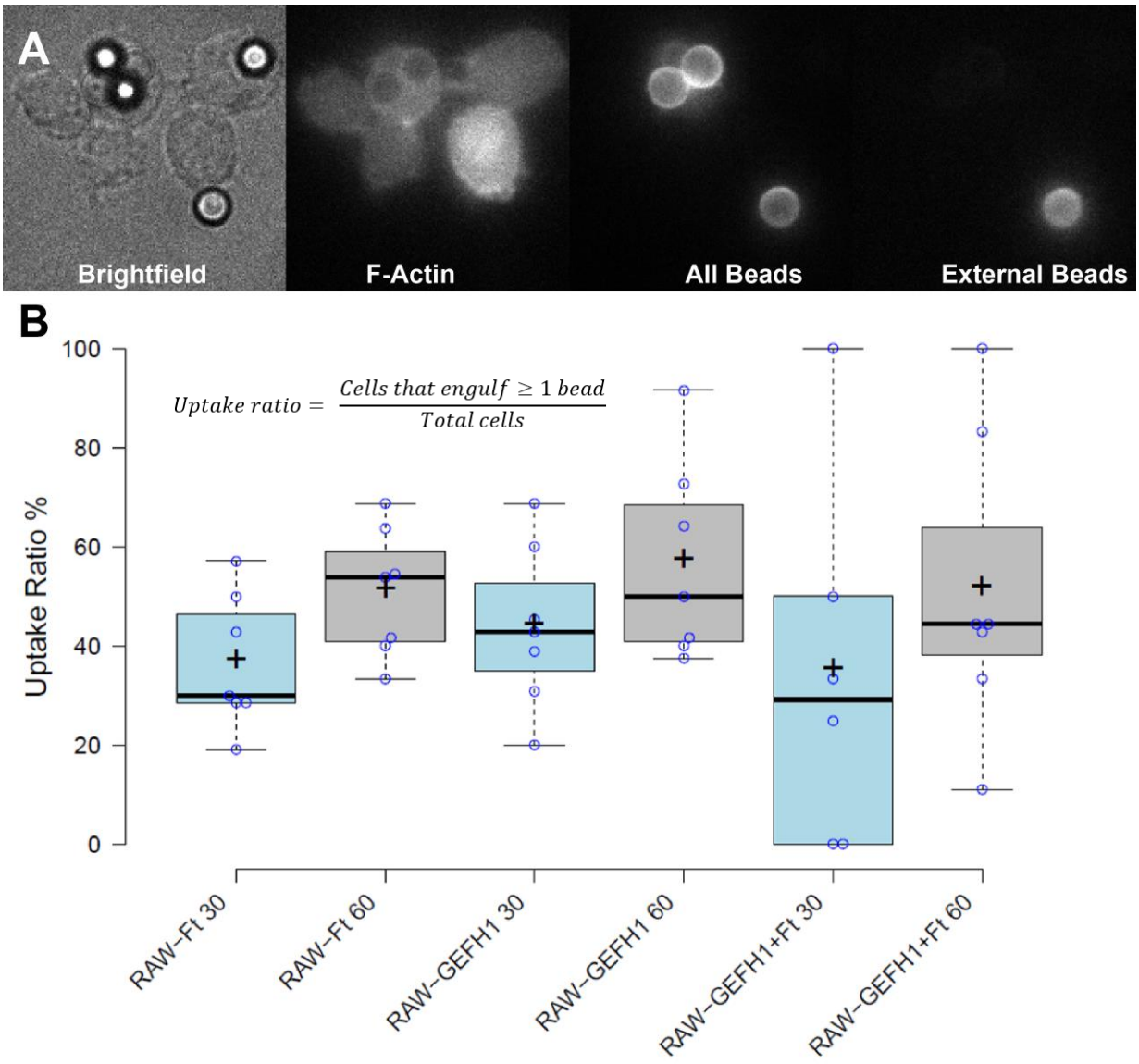

Figure 6.5 Phagocytic Uptake Assay of Stable Cell lines Reveal No Significant Effect on Phagocytic Ability. **A** Microscopy Images of the Uptake Assay. Both the cells and beads are visible in brightfield, the cells are shown in the F-actin channel, and the two bead channels reveal which beads were not internalized. **B** Boxplots of the uptake ratio for controls cells (RAW-Ft) and transfected cells (RAW-GEFH1 and RAW-GEFH1+Ft) at 30- and 60-minutes incubation. Black plus signs represent the mean while the horizontal black line represents the sample medians. Whiskers extend from the min to the max datapoint. Using Wilcoxon rank sum test, no significant difference was found between any of the cell treatments. The mean uptake percentage (engulfing cells/total cells) was about 46%.

Both the F-tractin-Halo and GEF-H1 BS constructs were under the control of a tetracycline-

dependent promoter to reduce potential adverse effects of GEF overexpression within the cell.

6.2.2 Verification of Macrophage Unperturbed Phagocytic Ability

In order to gauge the effect of GEFH1 expression on phagocytosis, particle uptake ratio assays were performed at 30 and 60 minutes incubation. **Figure 6.5A** shows representative microscopy images of the end point of the uptake assay. Phagocytic targets were differentially labeled with fluorescent IgG to distinguish all beads from external beads. Then, using a custom macro written in FIJI by myself, Oheneba Boateng, and Luca Menozzi, the total number of internalized beads and cells within each field of view were counted. With this, the 'uptake ratio' defined as the percentage of cells that engulfed at least one bead, was determined for each cell treatment. In each case, the GEFH1 expression had an insignificant effect on particle uptake (**Fig 6.5B**), meaning the GEF-H1 BS did not perturb the biological phenomena we set out to study.

6.2.3 GEF-H1 is Activated on the Cell Periphery During Frustrated Phagocytic Spreading

Frustrated phagocytic spreading is a regime of phagocytosis where phagocytes encounter infinitely large targets and attempt to engulf them more or less symmetrically from the point of contact. This form of phagocytosis has many advantages including constraining the phagocytosis-related proteins to the imaging plane and allowing for integration of other techniques such as micropatterning and traction force microscopy. For example, a handful of studies have used frustrated phagocytic spreading to measure the stress generated by the leading edge of the phagocytic cup [26] [118] [119] [88] as an analogue for the three-dimensional case. For my study, frustrated phagocytic spreading is the ideal technique to use when pairing phagocytic assays with 2D ratiometric FRET imaging. (Though there has been a recent study that performed FRET analysis in 3D, [120])

Figure 6.6A-C show the timeseries of a frustrated phagocytic spreading event in the brightfield channel, f-actin channel, and ratiometric FRET channel. Upon contact with the IgG-coated substrate, the macrophage quickly spreads in all directions until it reaches about 3.5x its

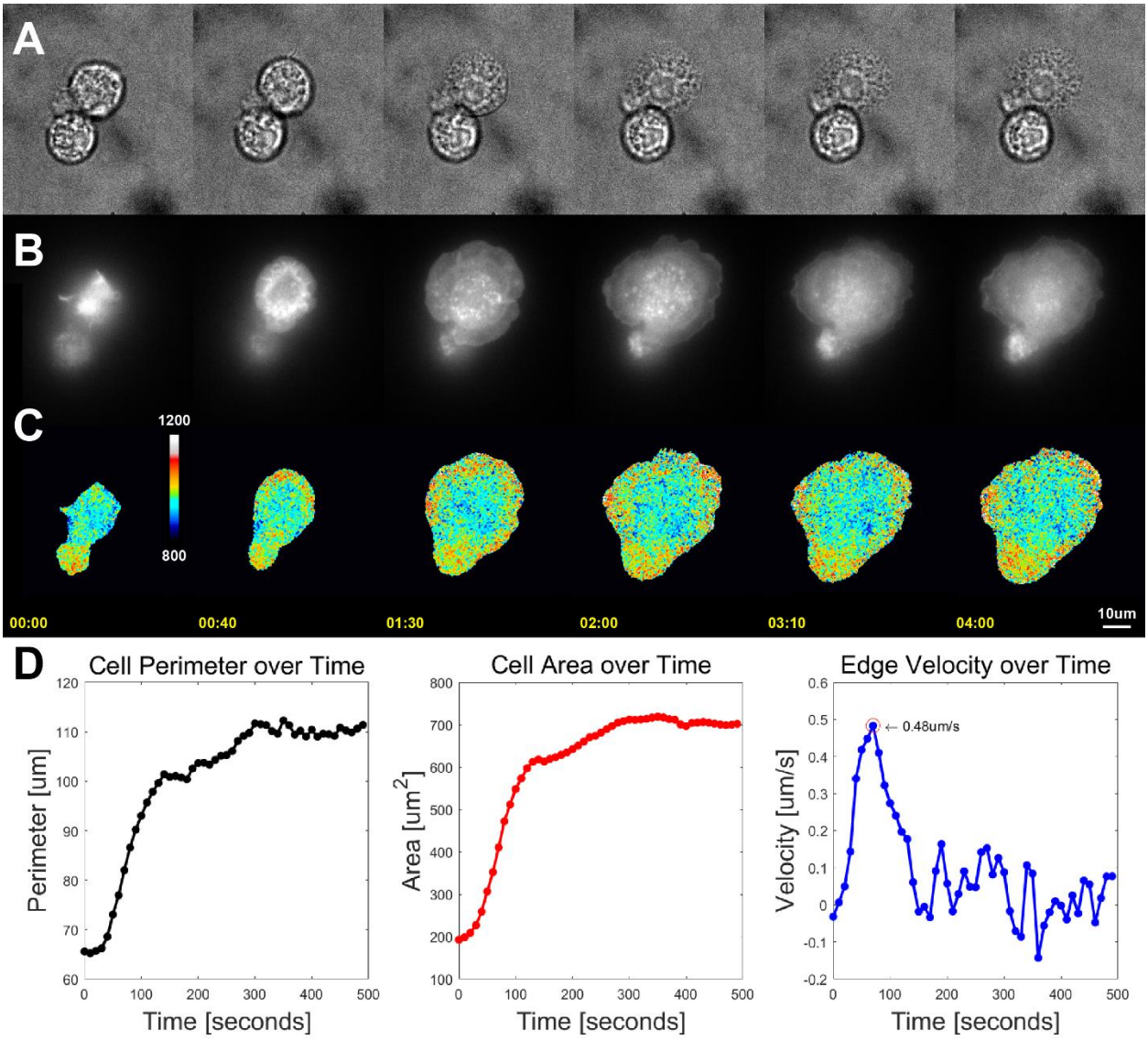

Figure 6.6 Frustrated Phagocytic Spreading Assays Reveal GEF-H1 Activation at the Leading Edge of the Phagocytic Cup. **A** Brightfield images of the timelapse of the spreading event. From this perspective, you can see one cell spreads and one does not. **B** F-Actin during spreading. **C** FRET ratio of Donor/Acceptor. Values have been inverted such that high values on the look up table (red/white) correspond to higher GEF-H1 activity and lower values correspond (blue/cyan) to lower activity. Elapsed time are in minutes. **D** Quantification of spreading perimeter, area, and velocity over time. The maximum velocity reached is 0.48um/s.

original size. The changes in the cell perimeter, spread area, and average edge velocity are quantified in **Figure 6.6D**. Consistent with other studies [118] [119] [88], I observed an initial rapid increase in the spread area followed by a plateau where, presumably, the cell has run out membrane. I observed that GEF-H1 activity was consistently 1.4-fold higher at the phagocytic periphery than at the origin of first contact during the entirety of the spreading event. (**Fig 6.6C**) This zone of GEF-H1 activity overlaps with the 'delimited stress zones' and 'peripheral ring force' reported by Rougerie and Cox, [119] suggesting GEF-H1 is present on the periphery of the phagocytic rim either to help generate these high stresses or in response to them.

6.2.4 GEF-H1 Control does not Associate with Microtubules nor Exhibit Peripheral Activation

In order to verify that the distribution of GEF-H1 activity I observed in Raw cells was not simply a consequence of imaging artifacts, I generated, with extensive help from Dr. Daniel Marston, a GEF-H1 BS control construct with the FRET pair inserted on the C-terminus (GEF-H1 associates with microtubules via its N-terminus [121]) of the protein instead of in the autoinhibitory domain. The design of the control construct is such that there will be FRET but it will be completely uncoupled from the activation state of GEF-H1. (**Fig 6.7A**) Therefore, we expect to see a random distribution of GEF-H1 'activity' unassociated with spreading or protrusions. Furthermore, since inactive GEF-H1 is known to localize to microtubules and active GEF-H1 is cytosolic, there should be no visible association of the control construct with microtubules. Both of these requirements were found to be true. **Figure 6.7B** shows the timeseries of a Raw cell expressing the GEF-H1 BS control construct. In the FRET channel, there are no distinguishable microtubule features, and in the FRET ratio channel, GEF-H1 activity is

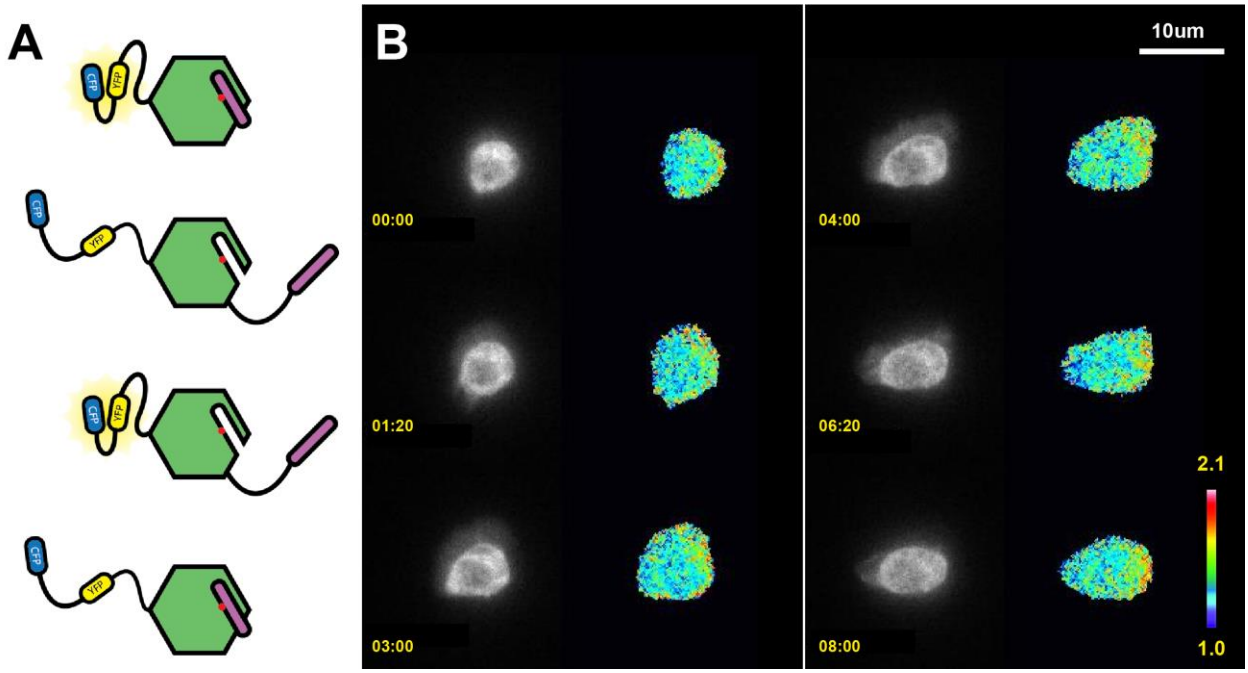

Figure 6.7 GEF-H1 Biosensor Control Construct. **A** The Four possible conformation states of the GEF-H1 Biosensor control. 1. High FRET/Inactive Conformation 2. Low FRET/Active Conformation 3. High FRET/Active Conformation 4. Low FRET/Inactive Conformation. **B** Timelapse of Raw 26.7 cells stably expressing the control construct. FRET emission from YPet is on the left and the FRET ratio is on the right. Elapsed time are in minutes.

not correlated to protrusion events and is relatively flat across the cell. Taken together, I am confident that the results in **Figure 6.7** are indicative of the native GEF-H1 activity within the cell. These results show that the GEF-H1 BS designed by Azoitei et al., has a promising application in the phagocytic model and could be used to further elucidate the role of GEF-H1 in the upstream signaling controlling mechanotransduction and engulfment.

6.2.5 Side View Imaging: GEF-H1 is Active in Cellular Protrusions

Now that the GEF-H1 BS is well characterized in Raw 264.7 cells, and we have seen a convincing role for GEF-H1 activity in the phagocytic cup, the natural next step is translate this force assay to 3D and incorporate forces. I set out to use the AFM-LS system to correlated GEF-H1 activity with force stimuli from the cantilever tip. **Figure 6.8** shows a RAW cell stably

expressing the GEF-H1 BS in sideview. During this time series, cellular protrusions exhibited 1.5 fold higher activity than the cell body. To my knowledge, this was the first XZ cross section of GEF-H1 activity in living cells. This result not only confirms the previous findings that GEF-H1 is active in cell protrusions for cell migration, but also suggests that this signaling pattern is conserved in macrophage cell types, though macrophages have been shown to have a distinctly different form of migration [122]. These results set the stage for future work in 3D FRET imaging of GEF-H1 activity during phagocytosis as well as in force response assays.

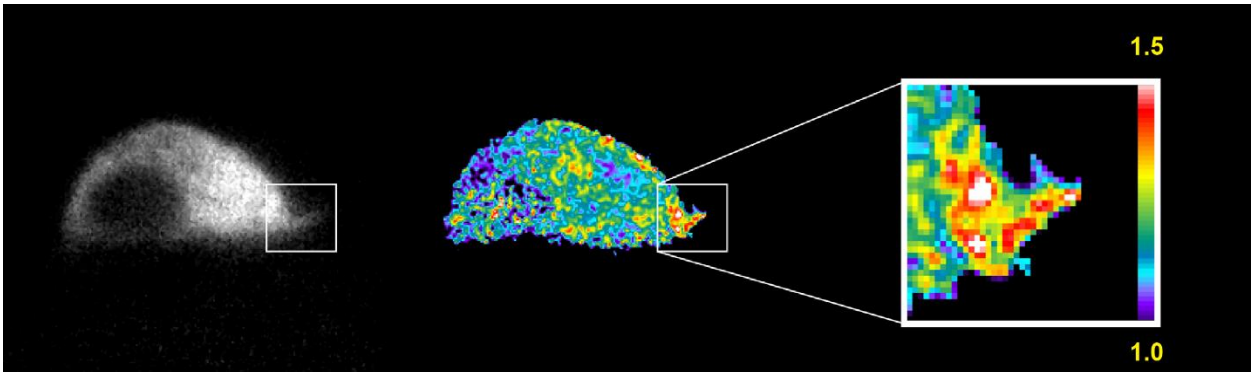

Figure 6.8 Vertical Light Sheet Imaging Reveals GEF-H1 is Active in Cell Protrusions in the XZ Plane. FRET emission (left) and FRET ratio (right) of a cell in side view. Inset shows a close up of the FRET ratio in the cellular protrusion.

6.3 Discussion of GEF-H1 Coordinating Microtubule and Actin Dynamics

A connection I find very exciting is the interplay between the microtubule and actin cytoskeleton. GEF-H1 one of the very few GTPases which interact with microtubules and also acts as the major regulator of RhoA activation. This crucial role bridges signaling from both cytoskeletons to coordinate distinct cellular tasks. What we know thus far is that GEF-H1 localizes to microtubules in the inactive form and while there, GEF-H1 was shown to promote microtubules stability resulting in microtubule acetylation. [121] Acetylated microtubules are more compliant to forces, longer-lived, and have a shorter persistence length. Both ARP2/3

[123] [124] and talin [110] have been reported to effect acetylation levels of microtubules. GEF-H1 is then known to activate RhoA resulting in mDia1 and myosin-II mediated actomyosin contractility driving engulfment.

While the signaling pathway downstream of GEF-H1 activation is fairly well established, the sequence of events leading to GEF-H1 activation is still unclear. Seetharaman et al. report that microtubule acetylation increases with increasing substrate rigidity. [110] In direct conflict with this result, Heck et al. report that higher matrix stiffness led to less acetylated tubulin. [111] However, both papers find that increased external stiffness led to increased active GEF-H1. This suggests that perhaps the method of GEF-H1 activation is not simply release from microtubules, but is instead related to microtubule acetylation itself. If you look closely at the results from Seetharaman et al., you will see that only on stiff substrates did knocking down the alpha tubulin acetylase have an effect on the amount of active GEF-H1 in the cytosol. My theory is that GEF-H1 plays a redundant role for maintaining microtubules stability in the absence of other microtubules stabilizing agents. As microtubules are important physical links to the intramembrane mechanosensitive ion channels, GEF-H1 leaves microtubules and activates RhoA and actomyosin contractility only when microtubules are sufficiently acetylated.

What is missing from both of these results in the timing of these relative changes. Both paper report end point assay but don't show the time course of cell decision making and adaptation to the substrate. Neither consider the fact that GEF-H1 could re-bind to newly polymerized microtubules after the matrix stiffness has been 'sensed' by the cell. Real-time FRET ratiometric imaging could provide the insight needed to answer the question: is GEF-H1

active because it fell off the destabilized microtubule or did GEF-H1 activation cause microtubules destabilization? More about microtubule acetylation in the next chapter!

6.4 Conclusion and Future Work

GEF-H1 has proven to be an important regulator of microtubule stability, RhoA activation, and mechanotransduction. Extending the roles GEF-H1 plays in cell migration to phagocytosis has a promising outlook but required further investigation. Whether active GEF-H1 localizing to the leading edge of the phagocytic cup is purely coincidental of microtubules disassembly or it is actually playing an important role in coordinating the actin scaffolding producing the cup remains to be elucidated. Lack of evidence observing RhoA in the leading edge of the phagocytic cup during FcR-mediated phagocytosis confuses the canonical picture of GEF-H1 signaling. Just as Azoitei et al., found that GEF-H1 is mediated by Src signaling at the leading edge, there may be other undiscovered downstream effectors of GEF-H1 at the leading edge of cup. Exactly what part in the force response sequence GEF-H1 becomes activated in is still unclear. Is it the part of the initial evaluation of mechanical properties, informing the cell on how to respond? Is it part of the response? Both? The results from Guilly et al., would suggest the latter but this has yet to be fully fleshed out. What we know is that when cells encounter force, GEF-H1 will be there.

6.5 Methods

6.5.1 Generation and Culture of Raw 264.7 macrophages stably expressing GEF-H1 Biosensor

The generation of RAW 264.7 murine macrophage cells expressing F-tractin-Halo and the GEF-H1 biosensor was performed according to the protocol in Nelsen et al. [57] Briefly, RAW 264.7 cells were obtained from ATCC (TIB-71) and maintained in RPMI 1640 medium (ThermoFisher Scientific, cat# 61870036, MA) supplemented with GlutaMAX and 10% heat-inactivated fetal bovine serum (Gemini Bio-Product, CA). Cells expressing F-tractin-Halo and GEF-H1 biosensor were generated using a PiggyBac transposon system via three sequential transfections. We first produced a stable macrophage cell line expressing reverse tetracycline-controlled transactivator (rtTA) and then used those cells to produce a stable cell line expressing F-tractin-Halo and later GEF-H1 biosensor under the control of a tetracycline-dependent promoter. The transfection was performed using the Viromer Red transfection reagent (Lipocalyx, Weinbergweg, Germany) according to the manufacturer's instructions. Briefly, 2.5 × 10^5 cells were seeded into one well of a six-well plate, and the cells were transfected the following day. For each well, we used 1.2 µL of Viromer Red transfection reagent, 2.5 µg piggyBac transgene plasmid (PB-rtTA or PB-tre—F-tractin—Halo-Hygro or PB-tre-GFH1BS10) and 0.5 µg of piggyBac transposase plasmid (ratio at 5:1). After 24 hours, the medium was replaced with fresh culture medium and the cells were allowed to recover for 24 hours. Stable transfectants were selected by gradually increasing antibiotic concentrations; geneticin (G418) to a concentration of 500 µg/ml for PB-rtTA, hygromycin to 100 µg/ml for PB-F-tractin-Halo, and Blasticidin to 50 µg/ml for PB-tre-GFH1BS10. To induce the expression of F-

tractin-Halo and the GEF-H1 biosensor, the cells were grown in medium containing 50 nM doxycycline for 48 hours.

On the day of imaging, 4 µL of 10^−8 M JaneliaFluor 549 (JF549) HaloTag ligand was added to the cells for a 30 minute incubation. The dye containing media was replaced with imaging media three times every 10 minutes to removed unbound dye.

6.5.2 Plasmid construction

pTriEx4-GFH1BS10-yPet-mCerulean3 was a gift from Klaus Hahn. PiggyBac plasmids PB-rtTA and PB-miRE-tre-Puro were kindly provided by Mauro Calabrese (The University of North Carolina at Chapel Hill). GEF-H1-BS10 was amplified using the primers (forward primer, tgaaccgtcagatcgcctggaccggtgccaccatgtctcggatcgaatccctcacg; reverse primer, aggcacagtcgaaacgcattgtcgacttagctctcggaggctacagcct), and cloned between AgeI and SalI sites of PB-tre-HygroB, yielding PB-tre-GEF-H1-BS-Hygro. Those plasmids were confirmed by sequencing before use. The primers were synthesized by Integrated DNA Technologies (CA) and sequences were performed by Genewiz (NJ).

6.5.3 IgG Functionalization of 6um Microspheres

6um IgG-coated beads were produced according to the previously published protocol. [125] Briefly, Polybead carboxylate 6um microspheres CAT# 17141 (2.65% solids) were rotated in a EDAC/NHS solution (1-Ethyl-3-(3-dimethylaminopropyl)carbodiimide (EDAC); 10 mg/mL and 1-Hydroxy-2,5-pyrrolidinedione (NHS); 10 mg/mL) for 15 min, rinsed three times, and resuspended in a solution of 1.5ug/ml Rabbit IgG (I5006, Sigma) and 15ug/ml AF488 IgG

(thermofisher) in PBS and rotated in the dark for 60 min. Beads were then rinsed three times and stored in PBS until ready to use.

6.5.4 IgG Functionalization of coverslips

40mm round coverslips were cleaned in a UV chamber followed by a plasma cleaner and vapor treated with 0.1% TPMA (Tris(2-pyridylmethyl) amine; Sigma) in toluene at 80 deg for 60 min. A solution of (1-Ethyl-3-(3-dimethylaminopropyl)carbodiimide (EDAC); 10 mg/mL and 1-Hydroxy-2,5-pyrrolidinedione (NHS); 10 mg/mL) in PBS was then added to the coverslips 15 min at 37 deg. The PBS/EDAC was then removed, and 10 ug/mL rabbit IgG (I5006, Sigma) in PBS was added for 60 min at 37 °C. This was replaced by PBS for storage, or media for immediate use with cells.

6.5.4 Fibronectin Functionalized Polyacrylamide Gels

The polyacrylamide gels functionalized with fibronectin that were used in the side view imaging and uptake ratio experiments were fabricated according to our previously published protocol. [57]

6.5.5 Uptake Assay Experiments

Uptake Assay experiments were performed according to a previously publish protocol. [125] Briefly, macrophages were plated at 2.5x10^5 cells per ml and incubated at 37C for one hour. A concentration of 5x10^6 beads per ml was added to each cloning ring and the sample was put on ice for 30min to allow the beads to all settle. Phagocytosis was then synchronized

by placing the sample into the 37C incubator for 30 or 60 min depending on the time point. External beads (those which were not engulfed) were labeled with a secondary antibody on ice for 30 min. Finally, samples were fixed with 4% paraformaldehyde and imaged in one channel for actin, one channel for all beads, and one channel for external beads. The uptake ratio, the number of cells that engulfed at least one bead divided by the total number of cells, was determined using a FIJI.

6.5.6 Side view FRET Imaging Experiments

Side view imaging experiments were performed as described in Chapter 4. One difference is the implementation of the W-VIEW GEMINI Image Splitting Optics using CFP (FF01-483/32-25) / YFP(FF01-542/27-25) and Dichroic (FF509-FDi01-25x36) filters. Left- and right-hand sides of the split image were aligned prior to each experiment.

6.5.7 Phagocytic Spreading FRET Experiments

Experiments were performed using an Olympus IX-80 inverted microscope with a 60x 1.3NA oil objective. Samples were illuminated with a white LED and excitation filters 445/30 and 572/35 for mCerulean3 and JF549, respectively. Images were collected sequentially at 200ms exposure at 1 fps. FRET image processing was performed using 2dfretimgproc-master-v1 courtesy of the Hahn Lab (http://hahnlab.com/tools/software.html).

Chapter 7: Microtubule Acetylation Broadly Controls Mechanosensation and Regulates the Rigidity of Drosophila S2 cells

The mechanical properties of the cell are known to depend on the cytoskeleton. It is well studied that interventions preventing the proper assembly of the actin cytoskeleton have altered the mechanical stiffness of cells. The components of the cell's cytoskeleton are formed and disassembled into load bearing polymerous filaments with the aid of regulator proteins. These regulator proteins depend on the high specificity of interaction between components, disruptions to which can have downstream consequences to the mechanical stability of the filament as a whole. In 2019, we explored how mutating the K40 acetylation site on α -tubulin to prevent acetylation caused the entire cell to increase in stiffness. Microtubules depend on acetylation to allow for a more flexible and compliant filament that can withstand cell shape changes. Without this flexibility, we speculate that preventing acetylation caused each microtubule to become more brittle leading to an increase in the elastic modulus of the entire microtubule cytoskeleton.

7.1 Mechanosensation and Microtubule Acetylation

Mechanical stimuli applied to cells within the peripheral nervous system terminate in the electrochemical signals that mediate hearing, balance, vibrations, gravity, body movements, touch, and pain in a signal transduction process known as mechanosensation. [126] This signal conversion is a consequence of direct activation of mechanically gated ion channels, catalyzing

the transition between an inactive and active protein conformation. [127] [128] [129] The mechanism of this activation has been separated into two principal contributions; 'force-from-lipid' [130] [131] [132] or 'force-from-filament.' [133] The 'force-from-lipid' principal presumes that the conformational change of the ion channel is mediated by forces on the surrounding lipid bilayer of the membrane. In the 'force-from-filament' principal, mechanical forces applied to the ion channel are attributed to displacements of the channel with respect to tethered protein filaments that provide a mechanical link to the extracellular matrix or the greater cellular cytoskeleton. [134] [135] [136] [137] In this model, the compliant tether connecting the membrane-bound ion channel to the immobile greater structure acts as a gating spring which opens the channel under sufficient tension. These proteins that relay extracellular stimuli to intracellular components resulting in signal transduction via a compliant element known as a gating spring are termed mechanoreceptors.

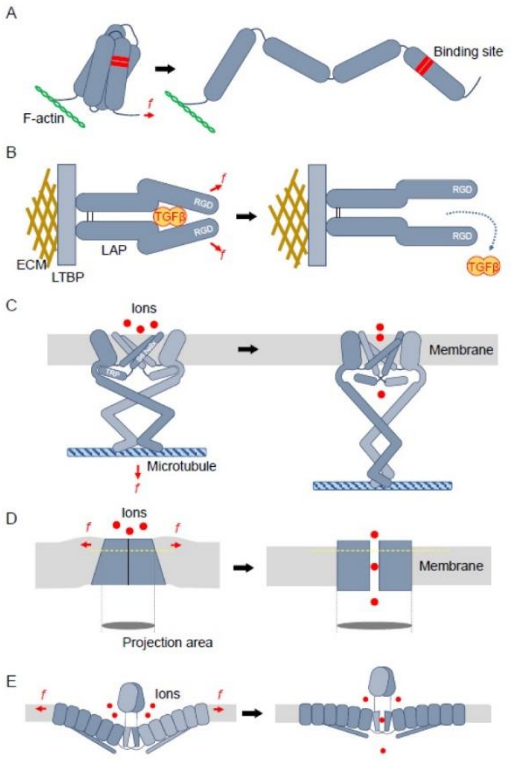

Figure 7.1. Schematic Model of Several Proposed Mechanoreceptor Force Transmission Strategies. Copyright © 2018 Lim et al. Korean Society for Biochemistry and Molecular Biology. All rights reserved.

Figure 7.1 shows several conformation changes of mechanoreceptors under force: **Fig 7.1A-C** illustrate the 'force-from-filament' principal and **Fig 7.1D-E** illustrate the 'force-from-lipid' principal.

Much of the current understanding surrounding mechanoreceptors and their interaction with the cellular cytoskeleton comes from the study of a group of ion channels found in the plasma membrane of numerous animal cell types known as transient receptor potential (TRP) channels. In particular, mammalian transient receptor potential vanilloid type-1 (TRPV1) and Drosophila TRPM/No mechanoreceptor potential C (NOMPC) have garnered widespread attention for their role as the mechanotransduction channel for osmosensory [138] and gentle touch [139], and their direct interact with microtubules. [140] [138] Using superresolution microscopy, Prager-Khoutorsky et al. found that in mammalian osmosensory neurons, an interwoven scaffold of microtubules bind to the C-terminus of TRPV1 channels. As the cell undergoes shrinking, the cell membrane applies a pushing force on the microtubules, in turn compressing and activating the channels. This activation leads to induced depolarization and increased neuron electrical activity. [138] Conversely, microtubules bind to the cytoplasmic N-terminus of NOMPC which is made up of 29 tandem ankyrin repeats (AR). [140] [141] Using a resolved cryo-EM structure and molecular dynamic simulations, Wang et al. reported that NOMPC could be opened by compression of the intracellular AR domain but not by stretch. The helical AR domain behaves like a spring compressing by ~13 pN/nm and transmits the compression to the TRP domain causing it to rotate clockwise and thus open the channel. [142] NOMPC has been shown to mediate mechanotransduction of touch sensation, requiring both the AR domains and binding of microtubules and thus the helical AR domain is considered a putative gating spring of NOMPC. [143] [135] [136] [141] Both TRPV1 and NOMPC have been shown to require direct interaction with microtubules in order to function as

mechanoreceptors, therefore, these channels may be sensitive to changes in the mechanical properties of microtubules.

Post-translational modifications (PTM) are the covalent modification of proteins after protein synthesis, allowing cells to alter existing proteins in response to various stimuli. PTMs effectively extend the functional multiplicity of the extant proteome by modifying functional groups or introducing new ones to proteins. [144] Acetylation, the introduction of an acetyl group (CH_3CO) onto a molecule, is a powerful PTM that can affect the hydrophobicity, solubility, and surface properties of a protein and thus impact a protein's conformation and ability to interact with other binding agents. [145] The effect of the microtubule modification on mechanosensation has been studied in many model systems including muscle tissue [146], C. elegans [147], zebrafish [148], and mice. [149] [150] [151] Coleman et al. showed that upregulation of acetylated α-tubulin in cardiomyocytes and skeletal myofibers slowed the rates of contraction and relaxation. [146] Chalfie and Au examined an array of mutations affecting the development and function of six touch receptor neurons in C. elegans and identified 18 genes responsible for touch sensation, including MEC-17. [147] MEC-17 is a gene that encodes the major α -tubulin acetylase, ATat1, and possesses conserved homologs found in all ciliated cells. When Akella et al. generated a MEC-17 depleted zebrafish, they found reduced touch responses and a variety of defects in the developing embryos. [148] Similarly, Morley et al. found that mice lacking ATat1 were insensitive to touch and pain. [150] This evidence strongly suggests that microtubule acetylation is a conserved process across species and key regulator of mechanosensation.

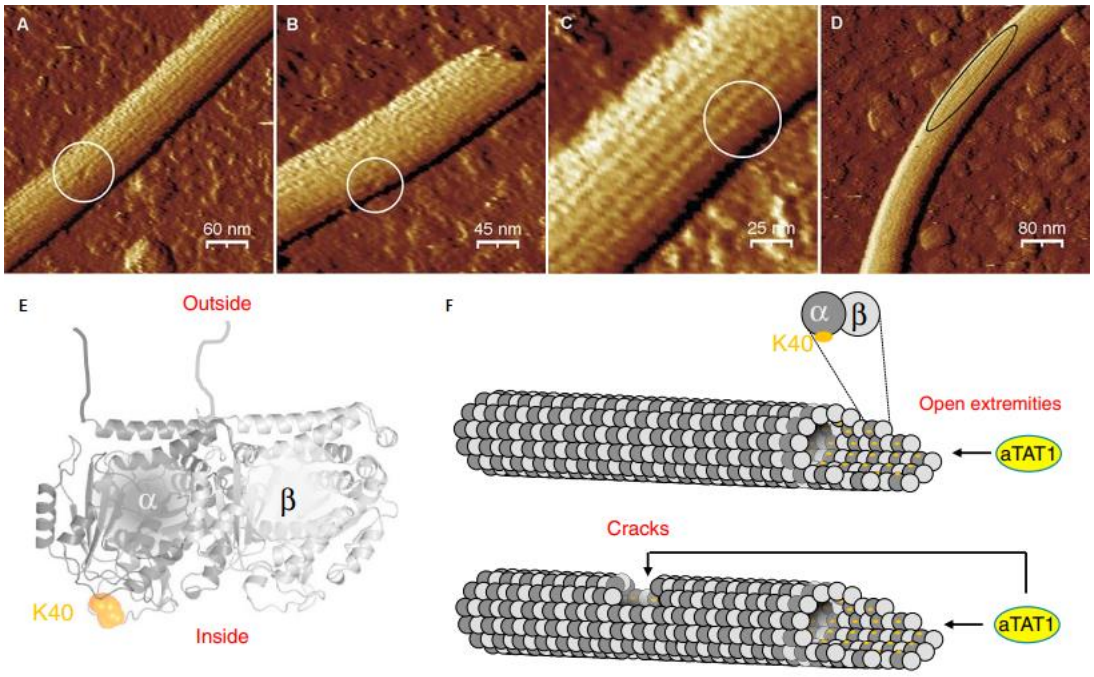

Figure 7.2 AFM images Reveal Defects in the Microtubule Lattice. **A-B** show two small holes in the MT wall. **C** shows a lateral offset in one or more protofilaments or a 'crack' in the lattice. **D** shows a split between two protofilaments. The split is likely related to the unusually strong bend in this MT (radius of curvature 650 nm). *[154]* **E** shows the alpha and beta tubulin dimer and the location of the K40 residue, the target for acetylation. **F** shows how ATat1 is only able to enter the lumen of flawless microtubules through open extremities but when there are defects in the lattice, such as a 'crack,' Atat1 can also enter the lumen. *[152]*

Unlike most PTMs of microtubules which take place on the outer surface of the hollow tubulin lattice, microtubule acetylation occurs on lysine 40 (K40) of α -tubulin, a residue only exposed on the inner lumen of the microtubule. [152] Piperno et al. reported that the catalytic activity of ATat1 is more than 100 times higher towards tubulin in its polymerized state, when the binding site is obscured, compared to its unpolymerized state. [153] This presents a spatial puzzle for how ATat1 can reach their modification sites within the microtubule lumen. As shown in **Figure 7.2A-D**, microtubules routinely develop defects in their lattice structure [154], leading to the theory ATat1 is able to acetylate the K40 residues on the inner lumen of the microtubules by entering through these 'cracks.' [155] These lattice defects are most likely due

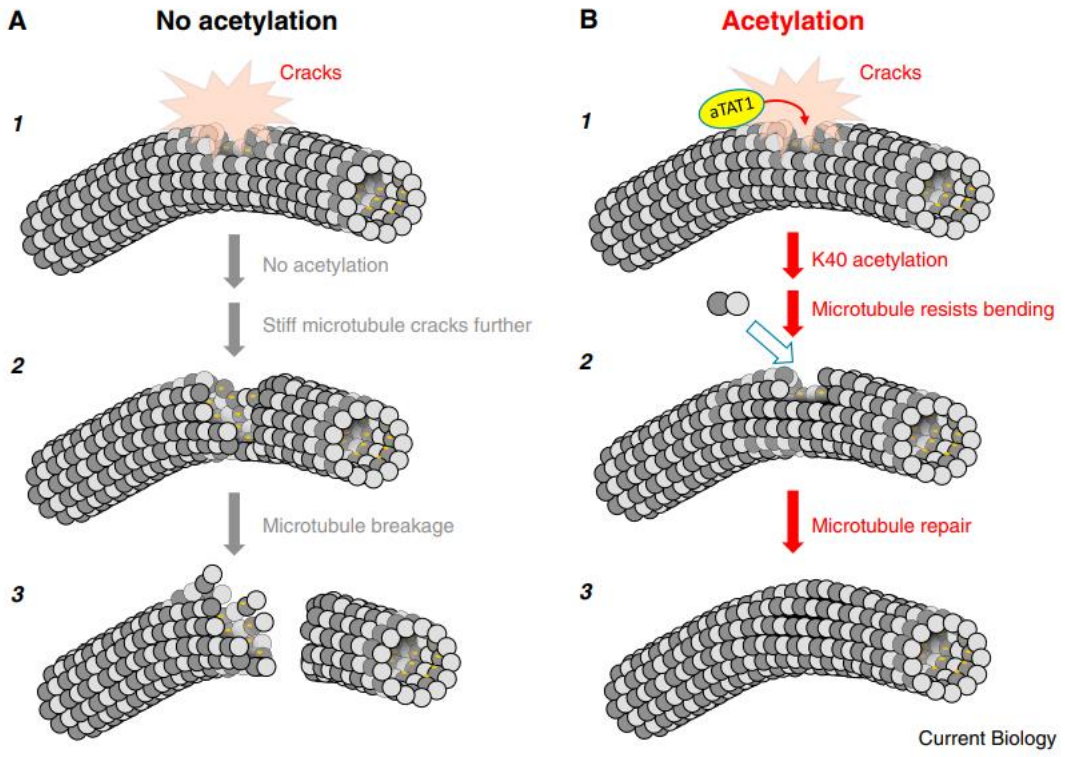

Figure 7.3. K40 acetylation protects microtubules from mechanical stress. **A** In the absence of aTAT1 and K40 acetylation, cracks in the microtubule lattice can lead to microtubules breakage and depolymerization. **B** In the presence of aTAT1, the acetylase is able to enter the lumen via the cracks in the lattice and acetylate the K40 in the α-tubulin subunits. This acetylation stabilizes the microtubule allowing for more time for self-repair. *[152]*

to the intracellular mechanical stress that bends microtubules. To understand the material properties of microtubules, several studies have performed repeated cycles of microtubule bending and reported a decrease in microtubule stiffness consistent with material fatigue. [156] [157] By introducing K40 acetylation and therefore altering the lattice structure, microtubules experience increased flexibility and resilience, making them more compliable to forces and preventing breakage. [158] Microtubule acetylation has generally been associated with stable and long-lived microtubules [152] and these recent mechanical studies suggest that α -tubulin acetylation regulates the mechanical resilience of microtubules. **Figure 7.3A-B** depict the fate of microtubules upon bending and cracking with and without K40 acetylation. K40 acetylation

reinforces the microtubule lattice and allows the microtubule to heal thus increasing its longevity. Since the function of K40 acetylation is to alter microtubules mechanical properties, and K40 acetylation is required for mechanosensation, how do the material properties of microtubules contribute to mechanosensation?

In a collaboration with Dr. Stephen Rogers at the University of North Carolina at Chapel hill, I investigated how K40 acetylation affects the mechanical properties of Drosophila S2 cells. Leading up to this study, Yan et al. identified Drosophila α -tubulin acetylase (dTAT), a Drosophila homolog to the known mammalian acetylase, ATat1, as the major Drosophila acetylase and characterized its role in mechanosensation. [159] In larval Drosophila, *dTat* mutants, a phenotype lacking *dTat*, were tested for gentle and harsh touch sensitivity defects, vibration response and gravitaxis. They report that gentle touch responses decreased by 67% as a result of the mutation. This defect was correlated to microtubule acetylation by mutating the K40 residue on α -tubulin to prevent acetylation leading to a comparable loss of gentle touch responses. [159] Furthermore, they found that dTAT is required for NOMPC-dependent mechanically induced membrane depolarization, but surprisingly, dTAT does not regulate NOMPC-mediated gentle touch responses. Instead, dTAT was found to control gentle touch responses and other forms of mechanosensation via modulations in microtubule stability. First, hyperacetylation or taxol-induced microtubule stabilization sensitized larvae to gentle touch. Second, taxol treatment rescues mechanosensory behavior defects of dTat and non-acetylatable mutants. Finally, in response to mechanical stimuli and during development as a whole, sensory dendrites lacking dTAT contained more microtubules plus ends than control cells. The prevalence of microtubule plus ends implies a higher degree of mechanically induced

breakages or increased microtubule dynamics. Taken together, these results establish that modulations of microtubule stability are a key regulator of mechanosensation. [159] Consistent with Morely et al., I found that Drosophila S2 cells lacking dTAT have an increased elastic modulus, though the role cellular stiffness plays in the overall mechanosensation of the animal remains to be revealed. [151]

7.2 Methods to Measure the Elastic Modulus of *dTat* depleted Drosophila S2 cells

7.2.1 S2 cells Culture and Sample Preparation

Culture and RNAi of Drosophila S2 cells were performed as previously described. [160] S2 cells (Drosophila Genomics Resource Center, Bloomington, IN) were cultured in SF900II medium supplemented with 100x antibiotic-antimycotic (Invitrogen, Carlsbad, CA). After seven days of RNAi, S2 cells were treated with dsRNA every other day to maintain protein depletion. On the day of an experiment, confluent cells from each population (control or *dTat* RNAi) were plated on cleaned glass poly L-lysine-coated coverslips such that adherent cells were spaced about 2-3 cell diameters apart once attached. Stiffness measurements were acquired 45 min to 120 min after plating at room temperature. Parallel samples of control or *dTat* RNAi cells were plated and an approximately equivalent number of data points were acquired during each trial. The order of data acquisition was varied for each experiment.

7.2.2 Atomic Force Microscopy Measurements

The elastic moduli of control- and *dTat* RNAi-treated cells were measured using an MFP-3D Bio AFM (Asylum Research, Santa Barbra, CA). The AFM head was mounted on an Olympus

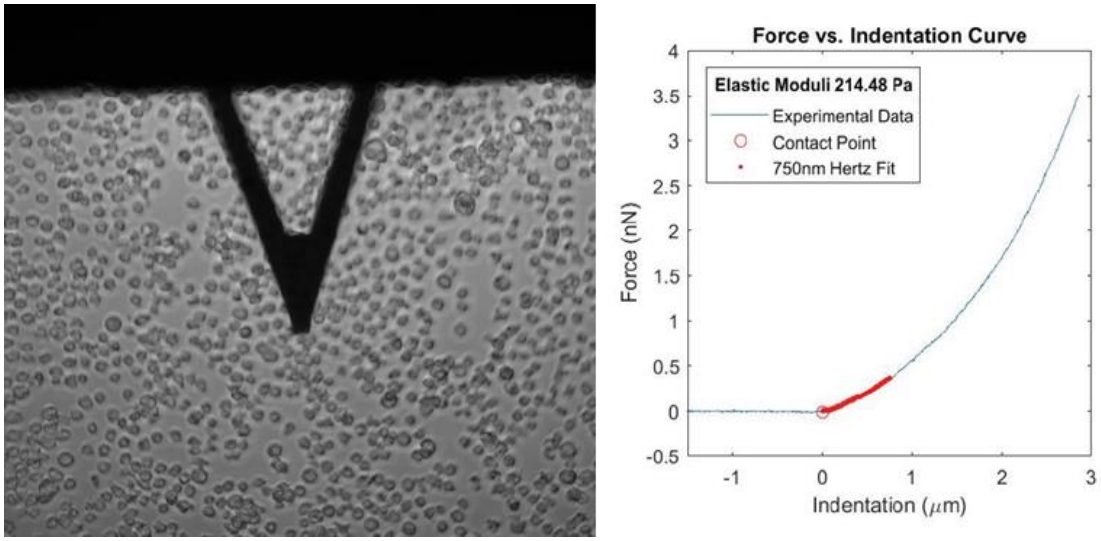

Figure 7.4. AFM Indentation Experiments. **A** Brightfield image of the triangular cantilever positioned over a sample of plated S2 cells. **B** Representative Force vs. Indentation curve used to determine the elastic modulus of each cell by fitting to the Hertz model. The plot shows the entire force-indentation curve in blue, a red circle for the contact point, and the Hertz model fit for 750 nm indent in red. Within the Hertz model, force increases as the 3/2 power of indentation. Here this fitting resulted in a cell modulus of 214 Pa.

IX71 inverted optical microscope to aid in accurately positioning the cantilever probe directly above a single cell (**Fig 7.4A**). Cells were probed using a Novascan silicon nitride AFM cantilever of nominal spring constant 0.03N/m with a 4.5um polystyrene bead attached. Before force measurements were made on each sample, the cantilever spring constant (0.039-0.042N/m) was calibrated using the built-in thermal tune method in the IGOR/Asylum Software.

For force versus indentation measurements the cantilever was moved at a velocity of 5 mm/s toward the cell until a force of 3 nN was reached. The cantilever was then retracted at the same rate. For most cells, this was equivalent to an indentation of 3-4 mm. For each cell, two force curves were collected and one was chosen, based on clearly defined points of contact and flat baseline approaches. The first curve was picked in approximately 80% of all cells. Force

measurements were acquired for 300 cells of each type over a period of three days of experiments. Calibrated cantilever deflection and piezo displacement data collected were converted to produce force versus indentation curves (**Fig 7.4B**). Using a custom MATLAB code, force-indentation data were fit to the Hertzian contact mechanics model to determine elastic moduli (stiffness) for each cell [55] [161]. The force versus indentation data were fit up to indentations of 750nm which corresponded to less than 10% of the cell height. The entire dataset was screened for relative RMS fitting errors greater than two sigma above the mean. Then, elastic moduli values that were above or below two sigma of the mean were excluded within each trial. [162]

7.3 Results of AFM stiffness measurements on *dTat* depleted S2 cells

7.3.1 The effect of acetylation on S2 cell microtubules

The microtubules of healthy S2 cells were labeled for all tubulin (**Fig 7.5A**) and acetylated tubulin (**Fig 7.5B**) in order to observe the morphological differences between these

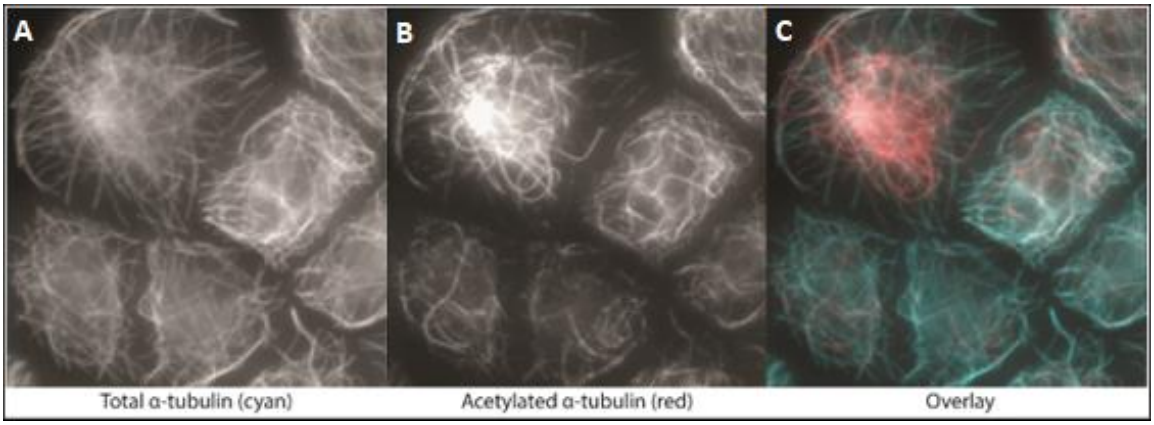

Figure 7.5. Morphology of microtubules with acetylated α-tubulin. S2 cells double stained for acetylated α -tubulin (left, red) and total a-tubulin (right, cyan). Microtubules with acetylated α -tubulin show a higher curvature and lower persistence length. (Experiment by S. Rogers, 2018)

two states of the microtubules as well as the respective localization of each type of microtubule within the cell. The acetylated phenotype exhibits higher curvature consistent with K40 acetylation increasing the flexibility of microtubules, while the non-acetylated phenotypes appear to have a higher persistence length. The acetylated microtubules also appear to be clustered in the center of the cell as opposed to 'framing' the perimeter of the cell as seen in the non-acetylated case. (**Fig 7.5C**)

To ensure that RNAi treatment against dTAT did not affect the amount of tubulin transcribed by the cell, an immunoblot was performed to test for the amount of dTAT, acetylated α-tubulin, and total α -tubulin. From **Figure 7.6**, we can see that the RNAi was effective in depleting dTAT from the *dTat* mutants (empty band at ~34kD for the *dTat* column). As expected, without *dTat*, the amount of acetylated α-tubulin was essentially zero for the *dTat* mutants. However, the amount of total tubulin (acetylated or not) remained unaffected by RNAi treatment. Therefore, both the control and *dTat* cells have sufficient α-tubulin to polymerize microtubules, but the *dTat* mutants are not able to acetylate them.

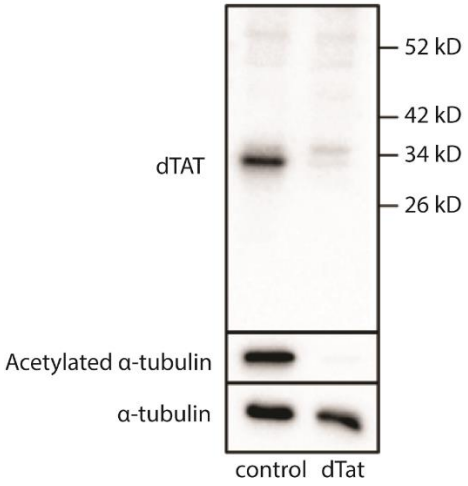

Figure 7.6. Immunoblot of RNAi against dTAT performed on S2 cells. RNAi on S2 cells dramatically depleted the major α-tubulin acetylase (dTAT), thereby preventing the acetylation of α-tubulin. However, the total α-tubulin level when compared to the controls were unaffected. (Experiment by S. Rogers)

7.3.2 dTat depleted S2 cells exhibit higher cortical stiffness

Our studies thus far support a model in which microtubule acetylation by *dTat* broadly regulates mechanosensation via effects on microtubule stability. We next examined whether dTAT regulates cellular rigidity, which could contribute to *dTat* mutant mechanosensation defects. Loss of the microtubule acetylase α-tubulin N-acetyltransferase 1 (ATAT1) results in

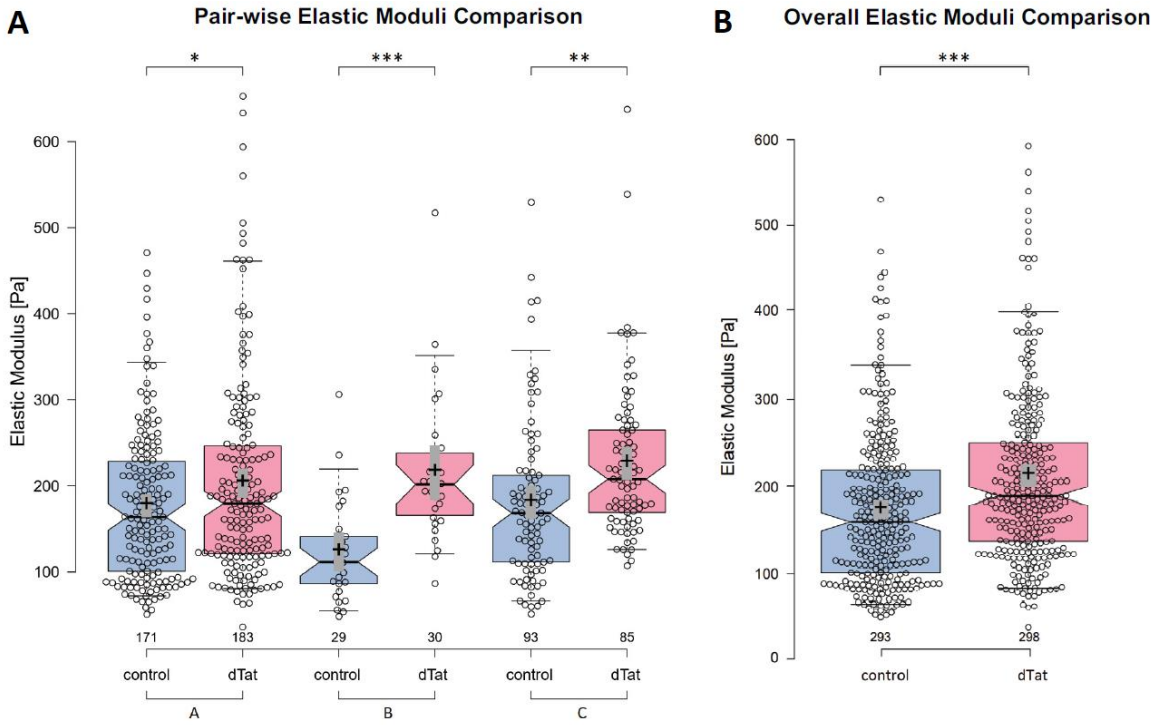

Figure 7.7. dTAT regulates cellular rigidity in S2 cells. **A** Plots show the pattern of stiffness data for a combined 3 days of experiments, with the median (central bar) and mean (+sign) shown. Means of 172 Pa for control and 211 Pa for dTat RNAi are significantly different to $p < 0.0001$. The medians of each were control: 158.5 Pa; dTat RNAi: 187.9 Pa, and the Mann Whitney comparison was also significant > 0.0001. **B** The paired comparisons of the cellular stiffness data shown in **A**. The waist of the boxplots indicates the median and the height of the notches represents the 95% confidence interval of the median. The mean is denoted by the plus sign and the grey box represents the 95% confidence interval of the mean. The whiskers extend from the 5th to the 95th percentile. Statistical significance is marked as follows: "***" for a p-value < 0.001, "**" for a p-value between 0.001 and 0.005, and "*" for a p-value < 0.05. Significance levels for each pair, based on the student's t-test, assuming unequal variance, are indicated in **Table 7.1**. Each pair was derived from cells separately grown and maintained; no wells were re-used.

	Pair A		Pair B		Pair C	
Mean [Pa]	176.8	203.0	123.2	215.3	180.7	226.1
Median [Pa]	163.8	179.3	111.5	201.6	168.4	207.7
p (same mean)	0.016		1.08E-05		9.88E-04	
	*		***		**	

Table 7.1. Means, medians and significance values for AFM measurements. Significance levels for each pair were calculated with the Student's t-test assuming unequal variance. Statistical significance is marked as follows: "***" for a p-value < 0.001, "**" for a p-value between 0.001 and 0.005, and "*" for a p-value < 0.05.

increased cellular rigidity of cultured mouse DRG neurons. [151] To test whether this biophysical function was conserved in Drosophila, we used atomic force microscopy (AFM) to examine the elastic moduli of dTAT-depleted S2 cells and compared them to control-treated cells. We found that *dTat* RNAi-treated cells exhibited a statistically significant increase in cortical stiffness, with *dTat* RNAi cells exhibiting a 22% increase in stiffness (**Figure 7.7; Table 7.1**). Means of 172 Pa for control and 211 Pa for *dTat* are significantly different to $p < 0.0001$. The medians of each were control: 158.5 Pa; *dTat*: 187.9 Pa, and the Mann Whitney comparison was also significant > 0.0001. These results indicate that the role of dTAT/ATAT1 in regulating the mechanical properties of cells is conserved; whether this activity contributes to its role in mechanosensation remains to be determined.

7.4 Discussion on Microtubule Acetylation and Cellular Stiffness

We have shown that the regulation of cellular stiffness by is a conserved function for microtubule acetylases. These results have since been reproduced in cardiomyocytes and flexor digitorum brevis (FDB) fibers. [146] Coleman et al. showed, via nanoindentation, that microtubules enriched in acetylated α-tubulin increase cytoskeletal young's modulus and

viscoelastic resistance. [146] In mice, acetylated microtubules of the peripheral sensory neurons are enriched in a submembranous band in the soma that is distinct from the cytoplasmic microtubule network. [151] This submembranous band appears to confer rigidity to the plasma membrane, and cultured DRG neurons from *Atat1* knockout mice exhibited increased membrane stiffness. [151] The localization of acetylated microtubules is similar to what we have observed in our S2 cells. (**Fig 7.5**) The authors proposed that in this system, microtubule acetylation tunes the mechanical properties of the membrane and, in its absence, cells are less elastic and require more force to trigger mechanosensitive channels.

Our results support a model in which unacetylated microtubules are brittle and prone to breakages without repair. Mechanosensitive ion channels tethered to the cytoskeletal network via microtubules are then unable to stretch into their active conformations and transmit electrical signals in response to mechanical stimulations. (**Figure 7.8**) The lack of acetylation reduces the flexibility and curvature of microtubules, leading to microtubules that brittle and prone to breakages without repair. This difference in morphology may contribute to an overall increased cellular rigidity where in the *dTat* mutant cells, the force probes encounter a stiff matrix of linear microtubules which crack under compression later leading to disassembly and

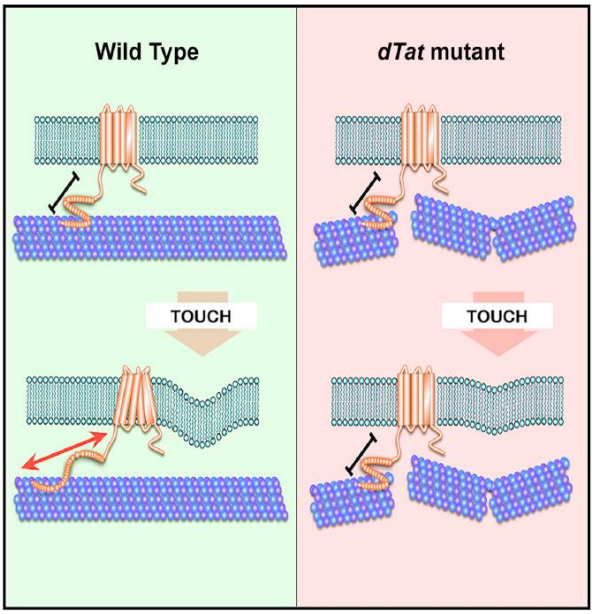

Figure 7.8. Proposed model for decreased mechanosensation in the absence of *dTat* and microtubule acetylation. Copyright © 2018 Yan et al. Published by Elsevier Inc. All rights reserved. *[159]*

preventing the gating-spring of the TRP channel from stretching. In the healthy case, the force probes encounter a curly meshwork of flexible microtubules whose defects after compression are self-repaired, preserving the mechanical link to transmit mechanical signals via ion channels.

However, the molecular mechanism linking microtubule acetylation to cellular stiffness and the extent to which this alteration of cellular stiffness contributes to mechanosensation are unknown. To address these important outstanding issues, it will be necessary to identify the molecular components that link microtubules to the mechanical properties of the cell cortex and examine their contribution to mechanosensation independently of microtubule function. Although we have found no evidence for a specialized submembranous network of acetylated microtubules in Drosophila PNS neurons, it will be interesting to determine whether *dTat* regulates cellular elasticity in these cells as well. It is therefore possible that microtubule acetylation regulates mechanosensitivity through multiple mechanisms: by regulating microtubule structure and by tuning the mechanical properties of neurons.

7.5 Conclusions and Future Work

The results of the AFM force measurements on S2 cells indicate that the regulation of overall cell stiffness is a conserved function for microtubule acetylases. Further investigation is required to determine how this change in cell stiffness contributes to mechanosenstion. It would be interesting to study if changes in cellular stiffness alone cause changes in perceived mechanosensation. This could be further investigated by measuring the cellular stiffness of different cells of the PNS which have distinct roles in mechanosensation.

Chapter 8: Conclusion

In this project, I used an advanced AFM-LS system to simultaneously image and record sensitive force data on single, living cells. The system was applied to three projects; phagocytosis, GEF-H1, and microtubules acetylation. In the phagocytosis experiment, I developed a new protocol which allowed for full bead internalization as well as an image processing pipeline to track the leading edge of the phagcoytic cup while simultaneously recording force data. I used these outputs to identify three distinct scaling relationships between the force and the cup height based on the underlying biochemistry of the dynamic actin cytoskeleton. Furthermore, I correlated force and cup height to investigate their casual behavior. Both analyisis techniques are able to draw conclusions despite cell to cell variablily. In the GEF-H1 project, generated a stable macrophage cell line expressing both a GEF-H1 biosensor and an actin label for studies correlating actin cytoskeletal dynammics with one of its mechanosensitive regulalors, GEF-H1. I showed GEF-H1 activation at the leading edge of the cellular protrusions and the phagocytic cup in macrophages. I also recorded the first ratiometric FRET imaging on our AFM-LS system. In the microtubules acetyaltion project, I found that S2 that are not able to acetylate their microtubules result in an overall increase in the whole cell elastic modulus. This suggests that the microtubules become stiff and less compliant to forces, resulting in their ultimate breakage and therefore loss of mechanotransduction.

The field of mechanobiology is rich with overlap between the actin cytoskeleton and the microtubule cytoskeleton. My biggest regret is not using this multifacetted system for more

intentional studies on the crosstalk between the actin cytoskeleton and microtubules during phagocytosis. However, I believe I am leaving the project in a position primed to be pick up by an impassioned individual ready to investigate. Jim Fan has made great strides towards a QGel traction force substrate for cup closure experiments (**Fig 8**). Using TIRFM (Total Internal Reflection Fluorescence Microscopy) combined with TFM (Traction Force Microscopy), one can observe the changes in protein distribution and the traction forces applied to the surface. In 2018, I propsed (but never completed) a project combining TIRFM, TFM, and FRET ratio imaging

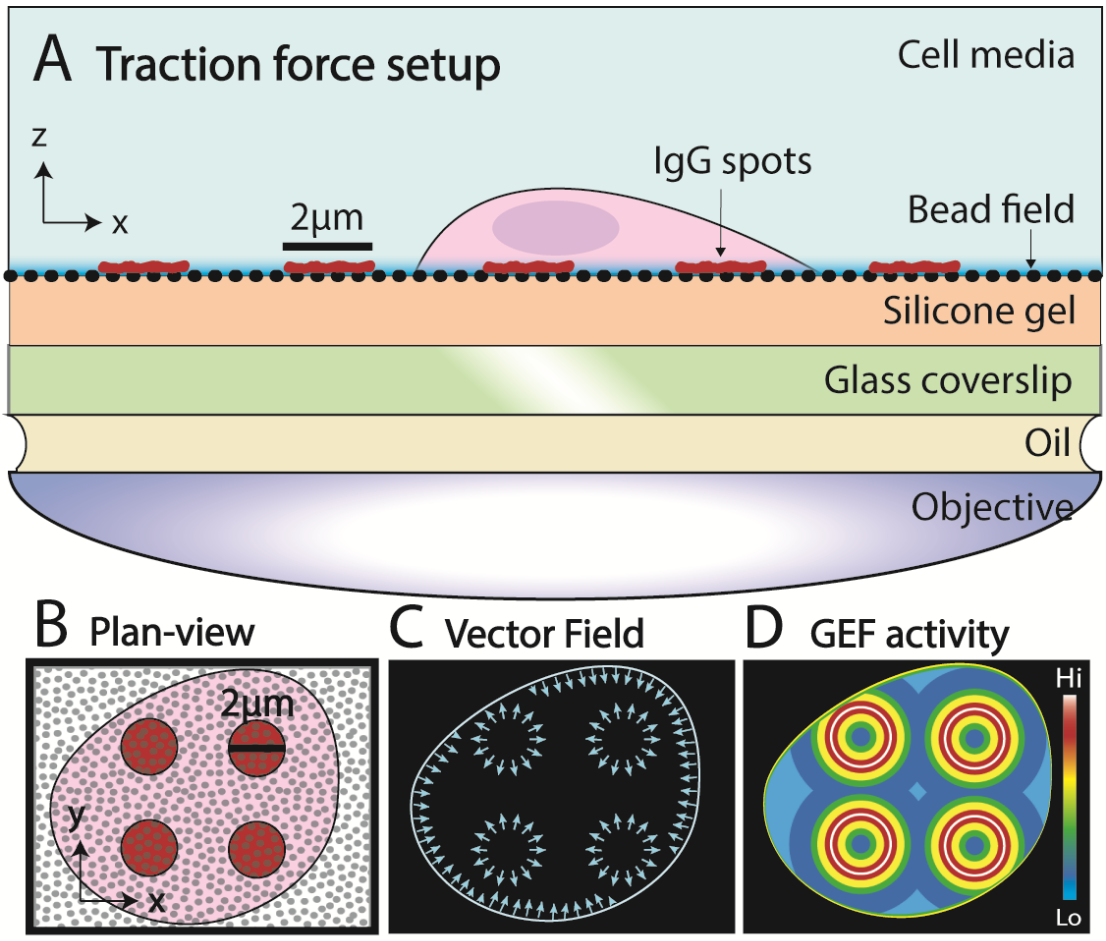

Figure 8. Proposed Future Experiment Combining TIRFM, TFM, FRET, and MP. **A** XZ Cross-section of the unique QGel-TFM-MP substrate. **B** XY plane view cartoon of the cell in **A**. **C** Mock vector field calculated from the displacements of the TFM beads. **D** Mock ratiometric FRET activity.

on micropatterned (MP) IgG substrates. **Figure 8A** shows the cross section of the specimen components and **Figure 8B-D** show the intended outputs; the local of the patterns and traction force beads, strain field for calculating the traction force, and the ratiometric FRET activation. I bbelieve a project like this combined with side view would be very powerful. Actin, Microtubules, and Mechanosensation are all tied to gether with GEF-H1. I am excited for where this project will go and future discoveries using this unique system.

APPENDIX A: ALTERNATIVE STRATEGIES FOR FUTURE PHAGOCYTOSIS ASSAYS

A.1 Live Cell and Bead Cantilever Attachment

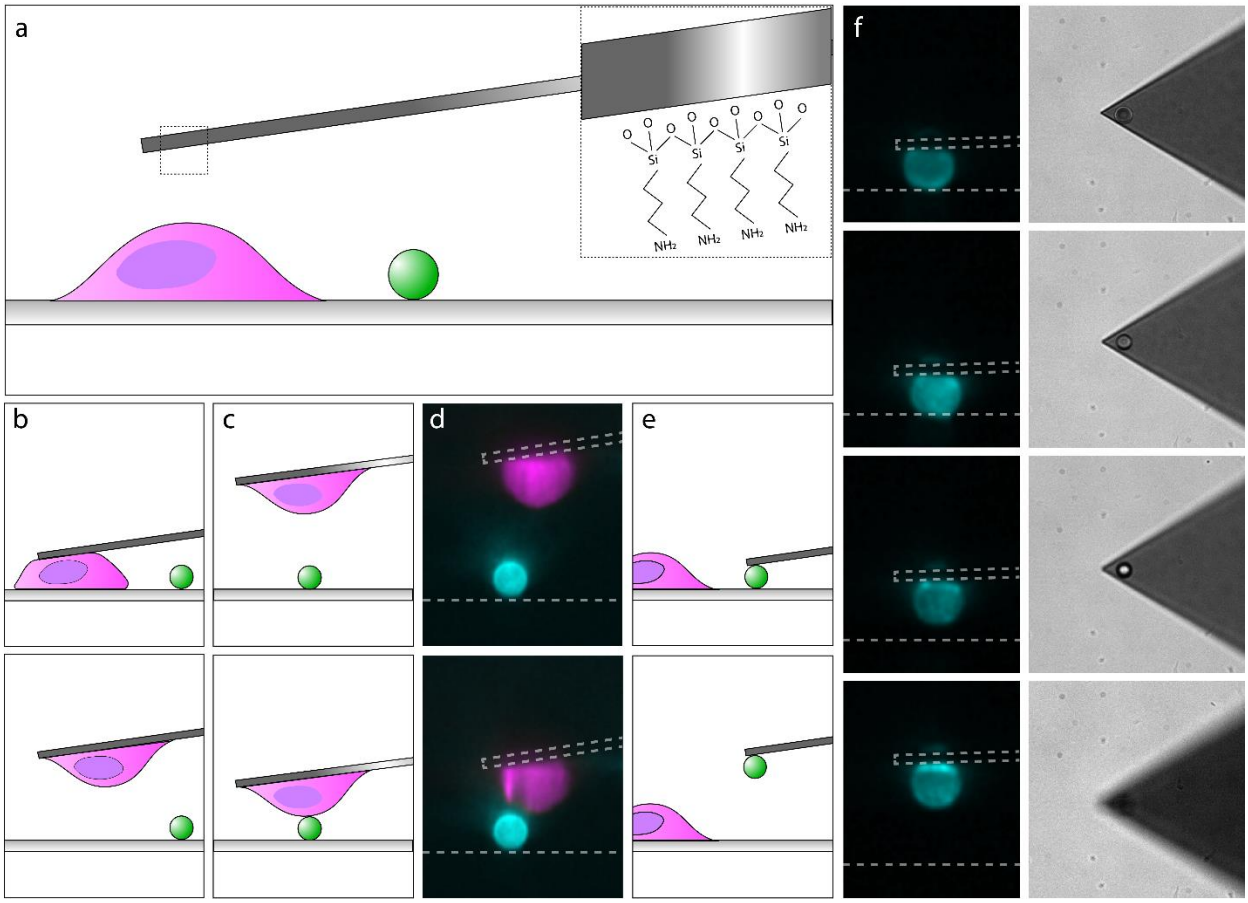

Figure A.1. New Target Attachment Protocol for Complete Engulfment**. a** Diagram of the sample space with cells and beads plated on a coverslip and the AFM cantilever treated with (3-Aminopropyl) triethoxysilane (APTES), an aminosilane, as shown in the inset. **b** Shows the cell attaching to the cantilever, then later engaging a bead in **c-d**. The coverslip surface and the cantilever position are noted by the white dotted line for reference in the fluorescence images. **e-f** Show the treated cantilever is also able to pick up IgG-coated beads. **f** Shows the cantilever picking up the bead in side view (left) and in brightfield (right). Once the bead is picked off the surface, it appears out of focus in the brightfield image along with the cantilever tip.

We have developed a new protocol for attaching IgG-functionalized polystyrene beads as well as cells to the AFM cantilever. Commercial, tipless, single-crystal silicon cantilevers with triangular free ends are first plasma cleaned to remove surface residues and then treated with 1% APTES in toluene via vapor deposition. The treated cantilevers are then calibrated for their

spring constants in air and submerged into the sample containing the cells of interest and a low dilution of IgG functionalized polystyrene beads, **Fig A.1a**. As shown in **Fig A.1b-d**, cells will readily attach to the cantilever surface and can then engage a nearby IgG-coated bead for inverted engulfment studies. This technique also opens the door for introducing the attached macrophage cell to cancer cells on the substrate or other targets. Our current application takes advantage of the intermediate bond strength between the bead and the cantilever for phagocytosis studies. As **FigA.1e-f** show, after contact with the APTES-treated cantilever, the IgG-functionalized bead is easily removed from the substrate. The bond between the bead and cantilever is strong enough to allow for lateral motion in the sample media as the user searches for a suitable cell to engage, but weak enough that the macrophage cells are able to fully engulf and remove the beads from the cantilever.

A.2 Lateral Bead Attachment and Engulfment

We have demonstrated the introduction of a target to a macrophage and its subsequent complete engulfment. Attaching the bead onto the cantilever laterally allows us flexibility in terms of where on the cell the target gets introduced, such as the lamellipodia shown in **FigA.2a-b**. In this case, the bead moves about 0.5um in y and 4um in x during engulfment, which can also be seen in the fluorescence images, **FigA.2c-d**. We can see an increasing displacement in the beginning of engulfment that eventually levels off in the net displacement plot, **FigA.2e**. Likewise, the maximum velocity of the bead reaches 0.08um/s in the beginning

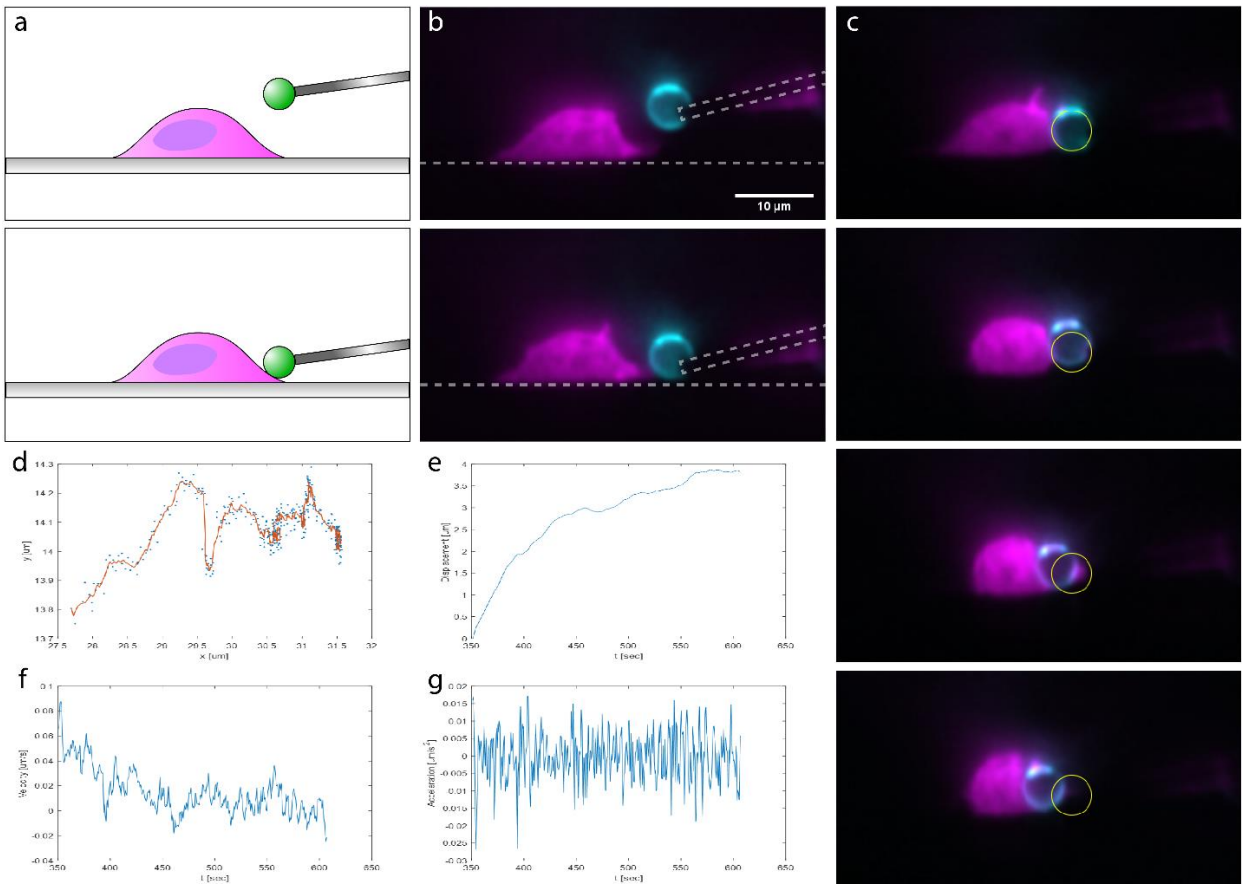

Figure A.2. Lateral Bead Engulfment and Quantifying Bead Detachment. **a** Diagram of a bead attached laterally to the cantilever engaging a cell. **b** Fluorescence images of **a** with the coverslip and cantilever noted by the white dotted lines for reference. **c** Timelapse of the engulfment in **b**. The cantilever is fixed and original location of the bead is overlayed in yellow on each frame to show total displacement. **d** Plot of bead displacement in y versus displacement in x. The orange line is the result of a moving average filter to the data points shown in blue. **e** Net displacement of the bead over time. **f** Velocity of the bead over time. **g** Acceleration of the bead over time.

and then decreases to zero, while the acceleration remains relatively constant around zero,

FigA.2f-g.

APPENDIX B: BEAD TRACKING SOFTWARE FOR DYNAMIC INTENSITY ANALYSIS

B.1 Software to Extract Bead Position and Generate Circular Kymographs

In order to quantify the actin intensity forming the phagocytic cup, we created a series of image processing tools to dynamically track the bead location for each frame and then measure the actin intensity around the bead. To find the bead 'origin' for each frame, the bead channel was blurred with a 2 pixel gaussian blur, intensity thresholded, convert to a mask, dilated by 2pixels, hole filled, eroded by 2pixels, and the maximum inscribed circle was fit to the mask. As you can see from **FigB.1a**, the polystyrene bead distorts the illumination creating a teardrop shape instead of a circle. This makes the maximum inscribed circle a critical step in locating the true bead 'origin.' This 'origin' is used to update the location of the line profile. Due to small variations in the bead sizes, it is also important to measure the diameter of the bead for each experiment. In order to do this, we took the gradient of the line profiles through the bead and identified the maximum and minimum locations corresponding to the steepest slopes in the line profile, or in our case, the edges of the bead, **FigB.1b**. This diameter fluctuates with the distorted bead illumination, as shown in **Figure B.1c**, so for each bead, the maximum bead diameter was chosen. With the bead 'origin' and diameter calculated for each frame, we then designed a radial line profile tool to measure the intensity through the bead 'origin' from 0 to 360 degrees. **Figure B.1d** shows the first four frames of an experiment where the yellow line profile rotates through 180 degrees, measuring the intensity at each angle and plotting each line profile as a vertical line as shown in **Figure B.1e** and **B.1f** with intensity represented by the color bar. The left side of the line records angles 0-180 degrees and the right side of the line record angles 181-360 degrees. With this, we have designed a robust tool to study the actin

intensity surrounding the bead during engulfment and detachment from the cantilever.

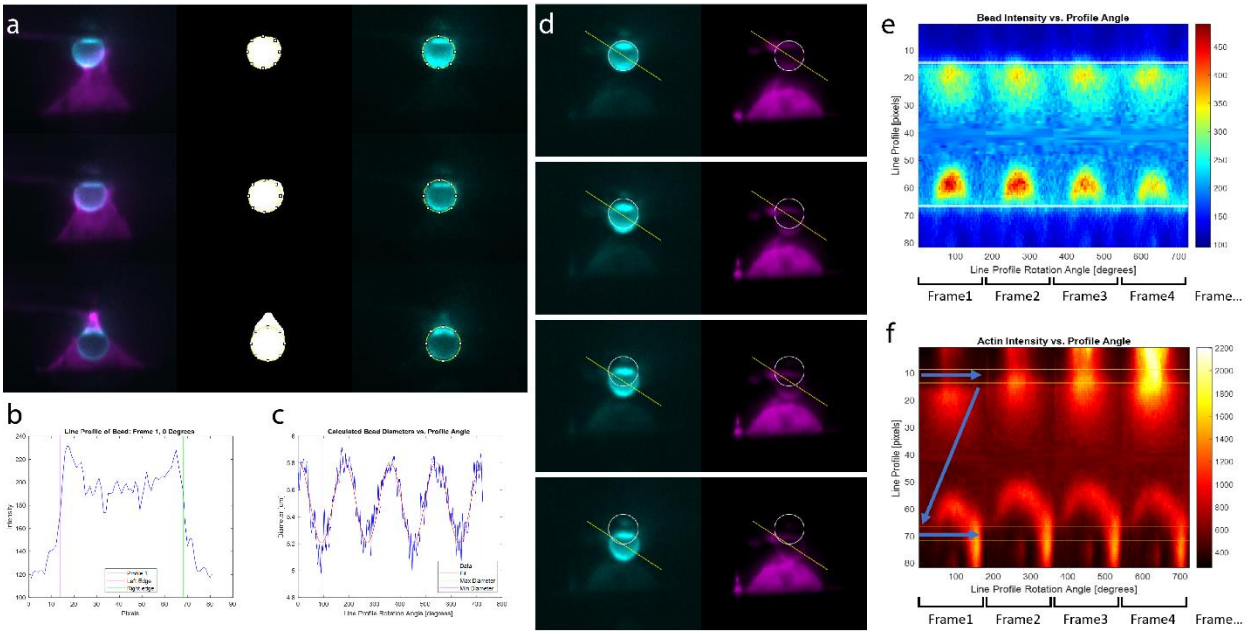

Figure B.1. Bead Tracking and Radial Line Profiles to Measure Actin Intensity in the Phagocytic Cup**. a** Example fluorescence images of bead detachment, bead segmentation, and the result of the bead segmentation overlayed onto the bead channel. **b** A representative line intensity profile across a bead, the left edge (magenta), and the right edge (green). **c** Fluctuations in the calculated diameter due to nonuniform bead illumination (blue) and the sinusoidal fit (red). **d** First four frames of a phagocytosis experiment where the cantilever and bead are lowered down to the cell. The bead channel is shown in cyan and the actin channel is shown in magenta. The original bead location is shown as a white overlay in both channels for reference. An example line profile for each bead position is shown as a yellow line which rotates through 180 degrees centered on the bead location. The origin of this line is updated for each frame to be centered at the bead. **e** Result of the line profile for the first four frames of the bead channel in **d**. The calculated diameter boundaries for this bead are shown as white horizontal lines. The color bar represents Alexa Fluor 488 IgG intensity on the bead. **f** Results of the line profile for the first four frames of the actin channel in **d**. A five-pixel width area outside of the bead diameter is shown as two yellow lines on the top and the bottom of the plot to measure the actin in the phagocytic cup. The direction of the intensity data from 0 to 360 degrees around the bead is explained by the blue arrows. The color bar indicates Janelia Fluor 549 intensity in the cell.

APPENDIX C: FIGURE PERMISSIONS

Figure 1.1

ELSEVIER LICENSE
TERMS AND CONDITIONS

Jul 24, 2023

This Agreement between Ms. Megan Kern ("You") and Elsevier ("Elsevier") consists of your license details and the terms and conditions provided by Elsevier and Copyright Clearance Center.

License Number	5595430205537
License date	Jul 24, 2023
Licensed Content Publisher	Elsevier
Licensed Content Publication	Current Biology
Licensed Content Title	The cytoskeleton in phagocytosis and macropinocytosis
Licensed Content Author	Sivakami Mylvaganam,Spencer A. Freeman,Sergio Grinstein
Licensed Content Date	May 24, 2021
Licensed Content Volume	31
Licensed Content Issue	10
Licensed Content Pages	14
Start Page	R619
End Page	R632
Type of Use	reuse in a thesis/dissertation
Portion	figures/tables/illustrations
Number of figures/tables/illustrations	1
Format	both print and electronic
Are you the author of this Elsevier article?	No
Will you be translating?	No

Title	Combined Atomic Force Microscopy and Light sheet Microscopy Characterize the Mechanobiology of Phagocytosis
Institution name	University of North Carolina at Chapel Hill
Expected presentation date	Jul 2023
Order reference number	Figure 1.1
Portions	Figure 1
Requestor Location	Ms. Megan Kern 120 E Cameron Ave Phillips Hall CHAPEL HILL, NC 27599 United States Attn: Ms. Megan Kern
Publisher Tax ID	98-0397604
Total	**0.00 USD**

Terms and Conditions

INTRODUCTION

1. The publisher for this copyrighted material is Elsevier. By clicking "accept" in connection with completing this licensing transaction, you agree that the following terms and conditions apply to this transaction (along with the Billing and Payment terms and conditions established by Copyright Clearance Center, Inc. ("CCC"), at the time that you opened your RightsLink account and that are available at any time at https://myaccount.copyright.com).

GENERAL TERMS

2. Elsevier hereby grants you permission to reproduce the aforementioned material subject to the terms and conditions indicated.

3. Acknowledgement: If any part of the material to be used (for example, figures) has appeared in our publication with credit or acknowledgement to another source, permission must also be sought from that source. If such permission is not obtained then that material may not be included in your publication/copies. Suitable acknowledgement to the source must be made, either as a footnote or in a reference list at the end of your publication, as follows:

"Reprinted from Publication title, Vol /edition number, Author(s), Title of article / title of chapter, Pages No., Copyright (Year), with permission from Elsevier [OR APPLICABLE SOCIETY COPYRIGHT OWNER]." Also Lancet special credit - "Reprinted from The Lancet, Vol. number, Author(s), Title of article, Pages No., Copyright (Year), with permission from Elsevier."

4. Reproduction of this material is confined to the purpose and/or media for which permission is hereby given. The material may not be reproduced or used in any other way,

including use in combination with an artificial intelligence tool (including to train an algorithm, test, process, analyse, generate output and/or develop any form of artificial intelligence tool), or to create any derivative work and/or service (including resulting from the use of artificial intelligence tools).
5. Altering/Modifying Material: Not Permitted. However figures and illustrations may be altered/adapted minimally to serve your work. Any other abbreviations, additions, deletions and/or any other alterations shall be made only with prior written authorization of Elsevier Ltd. (Please contact Elsevier's permissions helpdesk here). No modifications can be made to any Lancet figures/tables and they must be reproduced in full.
6. If the permission fee for the requested use of our material is waived in this instance, please be advised that your future requests for Elsevier materials may attract a fee.
7. Reservation of Rights: Publisher reserves all rights not specifically granted in the combination of (i) the license details provided by you and accepted in the course of this licensing transaction, (ii) these terms and conditions and (iii) CCC's Billing and Payment terms and conditions.
8. License Contingent Upon Payment: While you may exercise the rights licensed immediately upon issuance of the license at the end of the licensing process for the transaction, provided that you have disclosed complete and accurate details of your proposed use, no license is finally effective unless and until full payment is received from you (either by publisher or by CCC) as provided in CCC's Billing and Payment terms and conditions. If full payment is not received on a timely basis, then any license preliminarily granted shall be deemed automatically revoked and shall be void as if never granted. Further, in the event that you breach any of these terms and conditions or any of CCC's Billing and Payment terms and conditions, the license is automatically revoked and shall be void as if never granted. Use of materials as described in a revoked license, as well as any use of the materials beyond the scope of an unrevoked license, may constitute copyright infringement and publisher reserves the right to take any and all action to protect its copyright in the materials.
9. Warranties: Publisher makes no representations or warranties with respect to the licensed material.
10. Indemnity: You hereby indemnify and agree to hold harmless publisher and CCC, and their respective officers, directors, employees and agents, from and against any and all claims arising out of your use of the licensed material other than as specifically authorized pursuant to this license.
11. No Transfer of License: This license is personal to you and may not be sublicensed, assigned, or transferred by you to any other person without publisher's written permission.
12. No Amendment Except in Writing: This license may not be amended except in a writing signed by both parties (or, in the case of publisher, by CCC on publisher's behalf).
13. Objection to Contrary Terms: Publisher hereby objects to any terms contained in any purchase order, acknowledgment, check endorsement or other writing prepared by you, which terms are inconsistent with these terms and conditions or CCC's Billing and Payment terms and conditions. These terms and conditions, together with CCC's Billing and

Payment terms and conditions (which are incorporated herein), comprise the entire agreement between you and publisher (and CCC) concerning this licensing transaction. In the event of any conflict between your obligations established by these terms and conditions and those established by CCC's Billing and Payment terms and conditions, these terms and conditions shall control.

14. Revocation: Elsevier or Copyright Clearance Center may deny the permissions described in this License at their sole discretion, for any reason or no reason, with a full refund payable to you. Notice of such denial will be made using the contact information provided by you. Failure to receive such notice will not alter or invalidate the denial. In no event will Elsevier or Copyright Clearance Center be responsible or liable for any costs, expenses or damage incurred by you as a result of a denial of your permission request, other than a refund of the amount(s) paid by you to Elsevier and/or Copyright Clearance Center for denied permissions.

LIMITED LICENSE

The following terms and conditions apply only to specific license types:

15. **Translation**: This permission is granted for non-exclusive world **English** rights only unless your license was granted for translation rights. If you licensed translation rights you may only translate this content into the languages you requested. A professional translator must perform all translations and reproduce the content word for word preserving the integrity of the article.

16. **Posting licensed content on any Website**: The following terms and conditions apply as follows: Licensing material from an Elsevier journal: All content posted to the web site must maintain the copyright information line on the bottom of each image; A hyper-text must be included to the Homepage of the journal from which you are licensing at http://www.sciencedirect.com/science/journal/xxxxx or the Elsevier homepage for books at http://www.elsevier.com; Central Storage: This license does not include permission for a scanned version of the material to be stored in a central repository such as that provided by Heron/XanEdu.

Licensing material from an Elsevier book: A hyper-text link must be included to the Elsevier homepage at http://www.elsevier.com . All content posted to the web site must maintain the copyright information line on the bottom of each image.

Posting licensed content on Electronic reserve: In addition to the above the following clauses are applicable: The web site must be password-protected and made available only to bona fide students registered on a relevant course. This permission is granted for 1 year only. You may obtain a new license for future website posting.

17. **For journal authors:** the following clauses are applicable in addition to the above:

Preprints:

A preprint is an author's own write-up of research results and analysis, it has not been peer-reviewed, nor has it had any other value added to it by a publisher (such as formatting, copyright, technical enhancement etc.).

Authors can share their preprints anywhere at any time. Preprints should not be added to or enhanced in any way in order to appear more like, or to substitute for, the final versions

of articles however authors can update their preprints on arXiv or RePEc with their Accepted Author Manuscript (see below).
If accepted for publication, we encourage authors to link from the preprint to their formal publication via its DOI. Millions of researchers have access to the formal publications on ScienceDirect, and so links will help users to find, access, cite and use the best available version. Please note that Cell Press, The Lancet and some society-owned have different preprint policies. Information on these policies is available on the journal homepage.
Accepted Author Manuscripts: An accepted author manuscript is the manuscript of an article that has been accepted for publication and which typically includes author-incorporated changes suggested during submission, peer review and editor-author communications.
Authors can share their accepted author manuscript:

- immediately
    - via their non-commercial person homepage or blog
    - by updating a preprint in arXiv or RePEc with the accepted manuscript
    - via their research institute or institutional repository for internal institutional uses or as part of an invitation-only research collaboration work-group
    - directly by providing copies to their students or to research collaborators for their personal use
    - for private scholarly sharing as part of an invitation-only work group on commercial sites with which Elsevier has an agreement
- After the embargo period
    - via non-commercial hosting platforms such as their institutional repository
    - via commercial sites with which Elsevier has an agreement

In all cases accepted manuscripts should:

- link to the formal publication via its DOI
- bear a CC-BY-NC-ND license - this is easy to do
- if aggregated with other manuscripts, for example in a repository or other site, be shared in alignment with our hosting policy not be added to or enhanced in any way to appear more like, or to substitute for, the published journal article.

Published journal article (JPA): A published journal article (PJA) is the definitive final record of published research that appears or will appear in the journal and embodies all value-adding publishing activities including peer review co-ordination, copy-editing, formatting, (if relevant) pagination and online enrichment.
Policies for sharing publishing journal articles differ for subscription and gold open access articles:
Subscription Articles: If you are an author, please share a link to your article rather than the full-text. Millions of researchers have access to the formal publications on

ScienceDirect, and so links will help your users to find, access, cite, and use the best available version.
Theses and dissertations which contain embedded PJAs as part of the formal submission can be posted publicly by the awarding institution with DOI links back to the formal publications on ScienceDirect.
If you are affiliated with a library that subscribes to ScienceDirect you have additional private sharing rights for others' research accessed under that agreement. This includes use for classroom teaching and internal training at the institution (including use in course packs and courseware programs), and inclusion of the article for grant funding purposes.
Gold Open Access Articles: May be shared according to the author-selected end-user license and should contain a CrossMark logo, the end user license, and a DOI link to the formal publication on ScienceDirect.
Please refer to Elsevier's posting policy for further information.
18. **For book authors** the following clauses are applicable in addition to the above: Authors are permitted to place a brief summary of their work online only. You are not allowed to download and post the published electronic version of your chapter, nor may you scan the printed edition to create an electronic version. **Posting to a repository:** Authors are permitted to post a summary of their chapter only in their institution's repository.
19. **Thesis/Dissertation**: If your license is for use in a thesis/dissertation your thesis may be submitted to your institution in either print or electronic form. Should your thesis be published commercially, please reapply for permission. These requirements include permission for the Library and Archives of Canada to supply single copies, on demand, of the complete thesis and include permission for Proquest/UMI to supply single copies, on demand, of the complete thesis. Should your thesis be published commercially, please reapply for permission. Theses and dissertations which contain embedded PJAs as part of the formal submission can be posted publicly by the awarding institution with DOI links back to the formal publications on ScienceDirect.

Elsevier Open Access Terms and Conditions
You can publish open access with Elsevier in hundreds of open access journals or in nearly 2000 established subscription journals that support open access publishing. Permitted third party re-use of these open access articles is defined by the author's choice of Creative Commons user license. See our open access license policy for more information.
Terms & Conditions applicable to all Open Access articles published with Elsevier:
Any reuse of the article must not represent the author as endorsing the adaptation of the article nor should the article be modified in such a way as to damage the author's honour or reputation. If any changes have been made, such changes must be clearly indicated.
The author(s) must be appropriately credited and we ask that you include the end user license and a DOI link to the formal publication on ScienceDirect.
If any part of the material to be used (for example, figures) has appeared in our publication with credit or acknowledgement to another source it is the responsibility of

the user to ensure their reuse complies with the terms and conditions determined by the rights holder.

Additional Terms & Conditions applicable to each Creative Commons user license:

CC BY: The CC-BY license allows users to copy, to create extracts, abstracts and new works from the Article, to alter and revise the Article and to make commercial use of the Article (including reuse and/or resale of the Article by commercial entities), provided the user gives appropriate credit (with a link to the formal publication through the relevant DOI), provides a link to the license, indicates if changes were made and the licensor is not represented as endorsing the use made of the work. The full details of the license are available at http://creativecommons.org/licenses/by/4.0.

CC BY NC SA: The CC BY-NC-SA license allows users to copy, to create extracts, abstracts and new works from the Article, to alter and revise the Article, provided this is not done for commercial purposes, and that the user gives appropriate credit (with a link to the formal publication through the relevant DOI), provides a link to the license, indicates if changes were made and the licensor is not represented as endorsing the use made of the work. Further, any new works must be made available on the same conditions. The full details of the license are available at http://creativecommons.org/licenses/by-nc-sa/4.0.

CC BY NC ND: The CC BY-NC-ND license allows users to copy and distribute the Article, provided this is not done for commercial purposes and further does not permit distribution of the Article if it is changed or edited in any way, and provided the user gives appropriate credit (with a link to the formal publication through the relevant DOI), provides a link to the license, and that the licensor is not represented as endorsing the use made of the work. The full details of the license are available at http://creativecommons.org/licenses/by-nc-nd/4.0. Any commercial reuse of Open Access articles published with a CC BY NC SA or CC BY NC ND license requires permission from Elsevier and will be subject to a fee.

Commercial reuse includes:

- Associating advertising with the full text of the Article
- Charging fees for document delivery or access
- Article aggregation
- Systematic distribution via e-mail lists or share buttons

Posting or linking by commercial companies for use by customers of those companies.

20. **Other Conditions**:

v1.10

Questions? E-mail us at customercare@copyright.com.

Figure 1.2A

SPRINGER NATURE LICENSE
TERMS AND CONDITIONS

Jul 24, 2023

This Agreement between Ms. Megan Kern ("You") and Springer Nature ("Springer Nature") consists of your license details and the terms and conditions provided by Springer Nature and Copyright Clearance Center.

License Number
5595440074940
License date
Jul 24, 2023
Licensed Content Publisher
Springer Nature
Licensed Content Publication
Nature Cell Biology
Licensed Content Title
The molecular clutch model for mechanotransduction evolves
Licensed Content Author
Vinay Swaminathan et al
Licensed Content Date
Apr 27, 2016
Type of Use
Thesis/Dissertation
Requestor type
academic/university or research institute
Format
print and electronic
Portion
figures/tables/illustrations
Number of figures/tables/illustrations
1
Would you like a high resolution image with your order?
no
Will you be translating?
no
Circulation/distribution
1 - 29
Author of this Springer Nature content
no
Title

Combined Atomic Force Microscopy and Light sheet Microscopy Characterize the Mechanobiology of Phagocytosis
Institution name
University of North Carolina at Chapel Hill
Expected presentation date
Jul 2023
Order reference number
Figure 1.2A
Portions
Figure 1
Requestor Location
Ms. Megan Kern
120 E Cameron Ave
Phillips Hall

CHAPEL HILL, NC 27599
United States
Attn: Ms. Megan Kern
Total
0.00 USD
Terms and Conditions
Springer Nature Customer Service Centre GmbH Terms and Conditions
The following terms and conditions ("Terms and Conditions") together with the terms specified in your [RightsLink] constitute the License ("License") between you as Licensee and Springer Nature Customer Service Centre GmbH as Licensor. By clicking 'accept' and completing the transaction for your use of the material ("Licensed Material"), you confirm your acceptance of and obligation to be bound by these Terms and Conditions.

1. **Grant and Scope of License**

    1. The Licensor grants you a personal, non-exclusive, non-transferable, non-sublicensable, revocable, world-wide License to reproduce, distribute, communicate to the public, make available, broadcast, electronically transmit or create derivative works using the Licensed Material for the purpose(s) specified in your RightsLink Licence Details only. Licenses are granted for the specific use requested in the order and for no other use, subject to these Terms and Conditions. You acknowledge and agree that the rights granted to you under this License do not include the right to modify, edit, translate, include in collective works, or create derivative works of the Licensed Material in whole or in part unless expressly stated in your RightsLink Licence Details. You may use the Licensed Material only as permitted under this Agreement and will not reproduce, distribute, display, perform, or otherwise use or exploit any Licensed

Material in any way, in whole or in part, except as expressly permitted by this License.

2. You may only use the Licensed Content in the manner and to the extent permitted by these Terms and Conditions, by your RightsLink Licence Details and by any applicable laws.

3. A separate license may be required for any additional use of the Licensed Material, e.g. where a license has been purchased for print use only, separate permission must be obtained for electronic re-use. Similarly, a License is only valid in the language selected and does not apply for editions in other languages unless additional translation rights have been granted separately in the License.

4. Any content within the Licensed Material that is owned by third parties is expressly excluded from the License.

5. Rights for additional reuses such as custom editions, computer/mobile applications, film or TV reuses and/or any other derivative rights requests require additional permission and may be subject to an additional fee. Please apply to journalpermissions@springernature.com or bookpermissions@springernature.com for these rights.

2. **Reservation of Rights**

Licensor reserves all rights not expressly granted to you under this License. You acknowledge and agree that nothing in this License limits or restricts Licensor's rights in or use of the Licensed Material in any way. Neither this License, nor any act, omission, or statement by Licensor or you, conveys any ownership right to you in any Licensed Material, or to any element or portion thereof. As between Licensor and you, Licensor owns and retains all right, title, and interest in and to the Licensed Material subject to the license granted in Section 1.1. Your permission to use the Licensed Material is expressly conditioned on you not impairing Licensor's or the applicable copyright owner's rights in the Licensed Material in any way.

3. **Restrictions on use**

1. Minor editing privileges are allowed for adaptations for stylistic purposes or formatting purposes provided such alterations do not alter the original meaning or intention of the Licensed Material and the new figure(s) are still accurate and representative of the Licensed Material. Any other changes including but not limited to, cropping, adapting, and/or omitting material that affect the meaning, intention or moral rights of the author(s) are strictly prohibited.

2. You must not use any Licensed Material as part of any design or trademark.

3. Licensed Material may be used in Open Access Publications (OAP), but any such reuse must include a clear acknowledgment of this permission visible at the same time as the figures/tables/illustration or abstract and which must indicate that the Licensed Material is not part of the governing OA license but has been reproduced with permission. This may be indicated according to any standard referencing system but must include at a minimum 'Book/Journal title, Author, Journal Name (if applicable), Volume (if applicable), Publisher, Year, reproduced with permission from SNCSC'.

4. **STM Permission Guidelines**

1. An alternative scope of license may apply to signatories of the STM Permissions Guidelines ("STM PG") as amended from time to time and made available at https://www.stm-assoc.org/intellectual-property/permissions/permissions-guidelines/.

2. For content reuse requests that qualify for permission under the STM PG, and which may be updated from time to time, the STM PG supersede the terms and conditions contained in this License.

3. If a License has been granted under the STM PG, but the STM PG no longer apply at the time of publication, further permission must be sought from the Rightsholder.
Contact journalpermissions@springernature.com or bookpermissions@springernature.com for these rights.

5. **Duration of License**

1. Unless otherwise indicated on your License, a License is valid from the date of purchase ("License Date") until the end of the relevant period in the below table:

Reuse in a medical communications project	Reuse up to distribution or time period indicated in License
Reuse in a dissertation/thesis	Lifetime of thesis

Reuse in a journal/magazine	Lifetime of journal/magazine
Reuse in a book/textbook	Lifetime of edition
Reuse on a website	1 year unless otherwise specified in the License
Reuse in a presentation/slide kit/poster	Lifetime of presentation/slide kit/poster. Note: publication whether electronic or in print of presentation/slide kit/poster may require further permission.
Reuse in conference proceedings	Lifetime of conference proceedings
Reuse in an annual report	Lifetime of annual report
Reuse in training/CME materials	Reuse up to distribution or time period indicated in License
Reuse in newsmedia	Lifetime of newsmedia
Reuse in coursepack/classroom materials	Reuse up to distribution and/or time period indicated in license

6. **Acknowledgement**

1. The Licensor's permission must be acknowledged next to the Licensed Material in print. In electronic form, this acknowledgement must be visible at the same time as the figures/tables/illustrations or abstract and must be hyperlinked to the journal/book's homepage.

2. Acknowledgement may be provided according to any standard referencing system and at a minimum should include "Author, Article/Book Title, Journal name/Book imprint, volume, page number, year, Springer Nature".

7. **Reuse in a dissertation or thesis**

    1. Where 'reuse in a dissertation/thesis' has been selected, the following terms apply: Print rights of the Version of Record are provided for; electronic rights for use only on institutional repository as defined by the Sherpa guideline (www.sherpa.ac.uk/romeo/) and only up to what is required by the awarding institution.

    2. For theses published under an ISBN or ISSN, separate permission is required. Please contact journalpermissions@springernature.com or bookpermissions@springernature.com for these rights.

    3. Authors must properly cite the published manuscript in their thesis according to current citation standards and include the following acknowledgement: '*Reproduced with permission from Springer Nature*'.

8. **License Fee**

    You must pay the fee set forth in the License Agreement (the "License Fees"). All amounts payable by you under this License are exclusive of any sales, use, withholding, value added or similar taxes, government fees or levies or other assessments. Collection and/or remittance of such taxes to the relevant tax authority shall be the responsibility of the party who has the legal obligation to do so.

9. **Warranty**

    1. The Licensor warrants that it has, to the best of its knowledge, the rights to license reuse of the Licensed Material. **You are solely responsible for ensuring that the material you wish to license is original to the Licensor and does not carry the copyright of another entity or third party (as credited in the published version).** If the credit line on any part of the Licensed Material indicates that it was reprinted or adapted with permission from another source, then you should seek additional permission from that source to reuse the material.

2. EXCEPT FOR THE EXPRESS WARRANTY STATED HEREIN AND TO THE EXTENT PERMITTED BY APPLICABLE LAW, LICENSOR PROVIDES THE LICENSED MATERIAL "AS IS" AND MAKES NO OTHER REPRESENTATION OR WARRANTY. LICENSOR EXPRESSLY DISCLAIMS ANY LIABILITY FOR ANY CLAIM ARISING FROM OR OUT OF THE CONTENT, INCLUDING BUT NOT LIMITED TO ANY ERRORS, INACCURACIES, OMISSIONS, OR DEFECTS CONTAINED THEREIN, AND ANY IMPLIED OR EXPRESS WARRANTY AS TO MERCHANTABILITY OR FITNESS FOR A PARTICULAR PURPOSE. IN NO EVENT SHALL LICENSOR BE LIABLE TO YOU OR ANY OTHER PARTY OR ANY OTHER PERSON OR FOR ANY SPECIAL, CONSEQUENTIAL, INCIDENTAL, INDIRECT, PUNITIVE, OR EXEMPLARY DAMAGES, HOWEVER CAUSED, ARISING OUT OF OR IN CONNECTION WITH THE DOWNLOADING, VIEWING OR USE OF THE LICENSED MATERIAL REGARDLESS OF THE FORM OF ACTION, WHETHER FOR BREACH OF CONTRACT, BREACH OF WARRANTY, TORT, NEGLIGENCE, INFRINGEMENT OR OTHERWISE (INCLUDING, WITHOUT LIMITATION, DAMAGES BASED ON LOSS OF PROFITS, DATA, FILES, USE, BUSINESS OPPORTUNITY OR CLAIMS OF THIRD PARTIES), AND WHETHER OR NOT THE PARTY HAS BEEN ADVISED OF THE POSSIBILITY OF SUCH DAMAGES. THIS LIMITATION APPLIES NOTWITHSTANDING ANY FAILURE OF ESSENTIAL PURPOSE OF ANY LIMITED REMEDY PROVIDED HEREIN.

10. **Termination and Cancellation**

1. The License and all rights granted hereunder will continue until the end of the applicable period shown in Clause 5.1 above. Thereafter, this license will be terminated and all rights granted hereunder will cease.

2. Licensor reserves the right to terminate the License in the event that payment is not received in full or if you breach the terms of this License.

11. **General**

1. The License and the rights and obligations of the parties hereto shall be construed, interpreted and determined in accordance with the laws of the Federal Republic of Germany without reference to the stipulations of the CISG

(United Nations Convention on Contracts for the International Sale of Goods) or to Germany´s choice-of-law principle.

2. The parties acknowledge and agree that any controversies and disputes arising out of this License shall be decided exclusively by the courts of or having jurisdiction for Heidelberg, Germany, as far as legally permissible.

3. This License is solely for Licensor's and Licensee's benefit. It is not for the benefit of any other person or entity.

Questions? For questions on Copyright Clearance Center accounts or website issues please contact springernaturesupport@copyright.com or +1-855-239-3415 (toll free in the US) or +1-978-646-2777. For questions on Springer Nature licensing please visit https://www.springernature.com/gp/partners/rights-permissions-third-party-distribution

Other Conditions:

Version 1.4 - Dec 2022

Questions? E-mail us at customercare@copyright.com.

Figure 1.2B

SPRINGER NATURE LICENSE
TERMS AND CONDITIONS

Jul 24, 2023

This Agreement between Ms. Megan Kern ("You") and Springer Nature ("Springer Nature")

consists of your license details and the terms and conditions provided by Springer Nature and Copyright Clearance Center.

License Number	5595440387718
License date	Jul 24, 2023
Licensed Content Publisher	Springer Nature
Licensed Content Publication	Nature
Licensed Content Title	Nanoscale architecture of integrin-based cell adhesions
Licensed Content Author	Pakorn Kanchanawong et al
Licensed Content Date	Nov 24, 2010
Type of Use	Thesis/Dissertation
Requestor type	academic/university or research institute
Format	print and electronic
Portion	figures/tables/illustrations
Number of figures/tables/illustrations	1
Would you like a high resolution image with your order?	no
Will you be translating?	no
Circulation/distribution	1 - 29
Author of this Springer Nature content	no
Title	Combined Atomic Force Microscopy and Light sheet Microscopy Characterize the Mechanobiology of Phagocytosis
Institution name	University of North Carolina at Chapel Hill
Expected presentation date	Jul 2023
Order reference number	Figure 1.2B
Portions	Figure 4D
Requestor Location	Ms. Megan Kern 120 E Cameron Ave Phillips Hall CHAPEL HILL, NC 27599

United States
Attn: Ms. Megan Kern

Total **0.00 USD**

Terms and Conditions

Springer Nature Customer Service Centre GmbH Terms and Conditions
The following terms and conditions ("Terms and Conditions") together with the terms specified in your [RightsLink] constitute the License ("License") between you as Licensee and Springer Nature Customer Service Centre GmbH as Licensor. By clicking 'accept' and completing the transaction for your use of the material ("Licensed Material"), you confirm your acceptance of and obligation to be bound by these Terms and Conditions.

1. **Grant and Scope of License**

    1. The Licensor grants you a personal, non-exclusive, non-transferable, non-sublicensable, revocable, world-wide License to reproduce, distribute, communicate to the public, make available, broadcast, electronically transmit or create derivative works using the Licensed Material for the purpose(s) specified in your RightsLink Licence Details only. Licenses are granted for the specific use requested in the order and for no other use, subject to these Terms and Conditions. You acknowledge and agree that the rights granted to you under this License do not include the right to modify, edit, translate, include in collective works, or create derivative works of the Licensed Material in whole or in part unless expressly stated in your RightsLink Licence Details. You may use the Licensed Material only as permitted under this Agreement and will not reproduce, distribute, display, perform, or otherwise use or exploit any Licensed Material in any way, in whole or in part, except as expressly permitted by this License.

    2. You may only use the Licensed Content in the manner and to the extent permitted by these Terms and Conditions, by your RightsLink Licence Details and by any applicable laws.

    3. A separate license may be required for any additional use of the Licensed Material, e.g. where a license has been purchased for print use only, separate permission must be obtained for electronic re-use. Similarly, a License is only valid in the language selected and does not apply for editions in other languages unless additional translation rights have been granted separately in the License.

    4. Any content within the Licensed Material that is owned by third parties is expressly excluded from the License.

5. Rights for additional reuses such as custom editions, computer/mobile applications, film or TV reuses and/or any other derivative rights requests require additional permission and may be subject to an additional fee. Please apply
to journalpermissions@springernature.com or bookpermissions@springernature.com for these rights.

2. **Reservation of Rights**

Licensor reserves all rights not expressly granted to you under this License. You acknowledge and agree that nothing in this License limits or restricts Licensor's rights in or use of the Licensed Material in any way. Neither this License, nor any act, omission, or statement by Licensor or you, conveys any ownership right to you in any Licensed Material, or to any element or portion thereof. As between Licensor and you, Licensor owns and retains all right, title, and interest in and to the Licensed Material subject to the license granted in Section 1.1. Your permission to use the Licensed Material is expressly conditioned on you not impairing Licensor's or the applicable copyright owner's rights in the Licensed Material in any way.

3. **Restrictions on use**

1. Minor editing privileges are allowed for adaptations for stylistic purposes or formatting purposes provided such alterations do not alter the original meaning or intention of the Licensed Material and the new figure(s) are still accurate and representative of the Licensed Material. Any other changes including but not limited to, cropping, adapting, and/or omitting material that affect the meaning, intention or moral rights of the author(s) are strictly prohibited.

2. You must not use any Licensed Material as part of any design or trademark.

3. Licensed Material may be used in Open Access Publications (OAP), but any such reuse must include a clear acknowledgment of this permission visible at the same time as the figures/tables/illustration or abstract and which must indicate that the Licensed Material is not part of the governing OA license but has been reproduced with permission. This may be indicated according to any standard referencing system but must include at a minimum 'Book/Journal title, Author, Journal Name (if applicable), Volume (if applicable), Publisher, Year, reproduced with permission from SNCSC'.

4. **STM Permission Guidelines**

    1. An alternative scope of license may apply to signatories of the STM Permissions Guidelines ("STM PG") as amended from time to time and made available at https://www.stm-assoc.org/intellectual-property/permissions/permissions-guidelines/.

    2. For content reuse requests that qualify for permission under the STM PG, and which may be updated from time to time, the STM PG supersede the terms and conditions contained in this License.

    3. If a License has been granted under the STM PG, but the STM PG no longer apply at the time of publication, further permission must be sought from the Rightsholder.
    Contact journalpermissions@springernature.com or bookpermissions@springernature.com for these rights.

5. **Duration of License**

    1. Unless otherwise indicated on your License, a License is valid from the date of purchase ("License Date") until the end of the relevant period in the below table:

Reuse in a medical communications project	Reuse up to distribution or time period indicated in License
Reuse in a dissertation/thesis	Lifetime of thesis
Reuse in a journal/magazine	Lifetime of journal/magazine
Reuse in a book/textbook	Lifetime of edition
Reuse on a website	1 year unless otherwise specified in the License
Reuse in a presentation/slide kit/poster	Lifetime of presentation/slide kit/poster. Note: publication whether electronic or in print of presentation/slide kit/poster may require further permission.
Reuse in conference proceedings	Lifetime of conference proceedings
Reuse in an annual report	Lifetime of annual report
Reuse in training/CME materials	Reuse up to distribution or time period indicated in License
Reuse in newsmedia	Lifetime of newsmedia

Reuse in coursepack/classroom materials	Reuse up to distribution and/or time period indicated in license

6. **Acknowledgement**

    1. The Licensor's permission must be acknowledged next to the Licensed Material in print. In electronic form, this acknowledgement must be visible at the same time as the figures/tables/illustrations or abstract and must be hyperlinked to the journal/book's homepage.

    2. Acknowledgement may be provided according to any standard referencing system and at a minimum should include "Author, Article/Book Title, Journal name/Book imprint, volume, page number, year, Springer Nature".

7. **Reuse in a dissertation or thesis**

    1. Where 'reuse in a dissertation/thesis' has been selected, the following terms apply: Print rights of the Version of Record are provided for; electronic rights for use only on institutional repository as defined by the Sherpa guideline (www.sherpa.ac.uk/romeo/) and only up to what is required by the awarding institution.

    2. For theses published under an ISBN or ISSN, separate permission is required. Please contact journalpermissions@springernature.com or bookpermissions@springernature.com for these rights.

    3. Authors must properly cite the published manuscript in their thesis according to current citation standards and include the following acknowledgement: '*Reproduced with permission from Springer Nature*'.

8. **License Fee**

    You must pay the fee set forth in the License Agreement (the "License Fees"). All amounts payable by you under this License are exclusive of any sales, use,

withholding, value added or similar taxes, government fees or levies or other assessments. Collection and/or remittance of such taxes to the relevant tax authority shall be the responsibility of the party who has the legal obligation to do so.

9. **Warranty**

1. The Licensor warrants that it has, to the best of its knowledge, the rights to license reuse of the Licensed Material. **You are solely responsible for ensuring that the material you wish to license is original to the Licensor and does not carry the copyright of another entity or third party (as credited in the published version).** If the credit line on any part of the Licensed Material indicates that it was reprinted or adapted with permission from another source, then you should seek additional permission from that source to reuse the material.

2. EXCEPT FOR THE EXPRESS WARRANTY STATED HEREIN AND TO THE EXTENT PERMITTED BY APPLICABLE LAW, LICENSOR PROVIDES THE LICENSED MATERIAL "AS IS" AND MAKES NO OTHER REPRESENTATION OR WARRANTY. LICENSOR EXPRESSLY DISCLAIMS ANY LIABILITY FOR ANY CLAIM ARISING FROM OR OUT OF THE CONTENT, INCLUDING BUT NOT LIMITED TO ANY ERRORS, INACCURACIES, OMISSIONS, OR DEFECTS CONTAINED THEREIN, AND ANY IMPLIED OR EXPRESS WARRANTY AS TO MERCHANTABILITY OR FITNESS FOR A PARTICULAR PURPOSE. IN NO EVENT SHALL LICENSOR BE LIABLE TO YOU OR ANY OTHER PARTY OR ANY OTHER PERSON OR FOR ANY SPECIAL, CONSEQUENTIAL, INCIDENTAL, INDIRECT, PUNITIVE, OR EXEMPLARY DAMAGES, HOWEVER CAUSED, ARISING OUT OF OR IN CONNECTION WITH THE DOWNLOADING, VIEWING OR USE OF THE LICENSED MATERIAL REGARDLESS OF THE FORM OF ACTION, WHETHER FOR BREACH OF CONTRACT, BREACH OF WARRANTY, TORT, NEGLIGENCE, INFRINGEMENT OR OTHERWISE (INCLUDING, WITHOUT LIMITATION, DAMAGES BASED ON LOSS OF PROFITS, DATA, FILES, USE, BUSINESS OPPORTUNITY OR CLAIMS OF THIRD PARTIES), AND WHETHER OR NOT THE PARTY HAS BEEN ADVISED OF THE POSSIBILITY OF SUCH DAMAGES. THIS LIMITATION APPLIES NOTWITHSTANDING ANY FAILURE OF ESSENTIAL PURPOSE OF ANY LIMITED REMEDY PROVIDED HEREIN.

10. **Termination and Cancellation**

1. The License and all rights granted hereunder will continue until the end of the applicable period shown in Clause 5.1 above. Thereafter, this license will be terminated and all rights granted hereunder will cease.

2. Licensor reserves the right to terminate the License in the event that payment is not received in full or if you breach the terms of this License.

11. **General**

1. The License and the rights and obligations of the parties hereto shall be construed, interpreted and determined in accordance with the laws of the Federal Republic of Germany without reference to the stipulations of the CISG (United Nations Convention on Contracts for the International Sale of Goods) or to Germany´s choice-of-law principle.

2. The parties acknowledge and agree that any controversies and disputes arising out of this License shall be decided exclusively by the courts of or having jurisdiction for Heidelberg, Germany, as far as legally permissible.

3. This License is solely for Licensor's and Licensee's benefit. It is not for the benefit of any other person or entity.

Questions? For questions on Copyright Clearance Center accounts or website issues please contact springernaturesupport@copyright.com or +1-855-239-3415 (toll free in the US) or +1-978-646-2777. For questions on Springer Nature licensing please visit https://www.springernature.com/gp/partners/rights-permissions-third-party-distribution

Other Conditions:

Version 1.4 - Dec 2022

Questions? E-mail us at customercare@copyright.com.

Figure 3.2A

Hobson, C. M. (2021). On the biomechanics of cell nuclei: Insights from combined force and light microscopy (Order No. 28411289). Available from Dissertations & Theses @ University of North Carolina at Chapel Hill. (2555684968). Retrieved from http://libproxy.lib.unc.edu/login?url=https://www.proquest.com/dissertations-theses/on-biomechanics-cell-nuclei-insights-combined/docview/2555684968/se-2

Figure 5.1A

ELSEVIER LICENSE
TERMS AND CONDITIONS

Jul 24, 2023

This Agreement between Ms. Megan Kern ("You") and Elsevier ("Elsevier") consists of your license details and the terms and conditions provided by Elsevier and Copyright Clearance Center.
License Number
5595451302773
License date
Jul 24, 2023
Licensed Content Publisher
Elsevier
Licensed Content Publication
Developmental Cell
Licensed Content Title
Dynamic Podosome-Like Structures in Nascent Phagosomes Are Coordinated by Phosphoinositides
Licensed Content Author
Philip P. Ostrowski,Spencer A. Freeman,Gregory Fairn,Sergio Grinstein
Licensed Content Date
Aug 19, 2019
Licensed Content Volume
50
Licensed Content Issue
4
Licensed Content Pages

17
Start Page
397
End Page
410.e3
Type of Use
reuse in a thesis/dissertation
Portion
figures/tables/illustrations
Number of figures/tables/illustrations
1
Format
both print and electronic
Are you the author of this Elsevier article?
No
Will you be translating?
No
Title
Combined Atomic Force Microscopy and Light sheet Microscopy Characterize the Mechanobiology of Phagocytosis
Institution name
University of North Carolina at Chapel Hill
Expected presentation date
Jul 2023
Order reference number
Figure 5.1A
Portions
Figure 1A-B
Requestor Location
Ms. Megan Kern
120 E Cameron Ave
Phillips Hall

CHAPEL HILL, NC 27599
United States
Attn: Ms. Megan Kern
Publisher Tax ID
98-0397604
Total
0.00 USD
Terms and Conditions

INTRODUCTION

1. The publisher for this copyrighted material is Elsevier. By clicking "accept" in connection with completing this licensing transaction, you agree that the following terms and conditions apply

to this transaction (along with the Billing and Payment terms and conditions established by Copyright Clearance Center, Inc. ("CCC"), at the time that you opened your RightsLink account and that are available at any time at https://myaccount.copyright.com).

GENERAL TERMS

2. Elsevier hereby grants you permission to reproduce the aforementioned material subject to the terms and conditions indicated.

3. Acknowledgement: If any part of the material to be used (for example, figures) has appeared in our publication with credit or acknowledgement to another source, permission must also be sought from that source. If such permission is not obtained then that material may not be included in your publication/copies. Suitable acknowledgement to the source must be made, either as a footnote or in a reference list at the end of your publication, as follows:
"Reprinted from Publication title, Vol /edition number, Author(s), Title of article / title of chapter, Pages No., Copyright (Year), with permission from Elsevier [OR APPLICABLE SOCIETY COPYRIGHT OWNER]." Also Lancet special credit - "Reprinted from The Lancet, Vol. number, Author(s), Title of article, Pages No., Copyright (Year), with permission from Elsevier."

4. Reproduction of this material is confined to the purpose and/or media for which permission is hereby given. The material may not be reproduced or used in any other way, including use in combination with an artificial intelligence tool (including to train an algorithm, test, process, analyse, generate output and/or develop any form of artificial intelligence tool), or to create any derivative work and/or service (including resulting from the use of artificial intelligence tools).

5. Altering/Modifying Material: Not Permitted. However figures and illustrations may be altered/adapted minimally to serve your work. Any other abbreviations, additions, deletions and/or any other alterations shall be made only with prior written authorization of Elsevier Ltd. (Please contact Elsevier's permissions helpdesk here). No modifications can be made to any Lancet figures/tables and they must be reproduced in full.

6. If the permission fee for the requested use of our material is waived in this instance, please be advised that your future requests for Elsevier materials may attract a fee.

7. Reservation of Rights: Publisher reserves all rights not specifically granted in the combination of (i) the license details provided by you and accepted in the course of this licensing transaction, (ii) these terms and conditions and (iii) CCC's Billing and Payment terms and conditions.

8. License Contingent Upon Payment: While you may exercise the rights licensed immediately upon issuance of the license at the end of the licensing process for the transaction, provided that you have disclosed complete and accurate details of your proposed use, no license is finally effective unless and until full payment is received from you (either by publisher or by CCC) as provided in CCC's Billing and Payment terms and conditions. If full payment is not received on a timely basis, then any license preliminarily granted shall be deemed automatically revoked and shall be void as if never granted. Further, in the event that you breach any of these terms and conditions or any of CCC's Billing and Payment terms and conditions, the license is automatically revoked and shall be void as if never granted. Use of materials as described in a revoked license, as well as any use of the materials beyond the scope of an unrevoked license, may constitute copyright infringement and publisher reserves the right to take any and all action to protect its copyright in the materials.

9. Warranties: Publisher makes no representations or warranties with respect to the licensed material.
10. Indemnity: You hereby indemnify and agree to hold harmless publisher and CCC, and their respective officers, directors, employees and agents, from and against any and all claims arising out of your use of the licensed material other than as specifically authorized pursuant to this license.
11. No Transfer of License: This license is personal to you and may not be sublicensed, assigned, or transferred by you to any other person without publisher's written permission.
12. No Amendment Except in Writing: This license may not be amended except in a writing signed by both parties (or, in the case of publisher, by CCC on publisher's behalf).
13. Objection to Contrary Terms: Publisher hereby objects to any terms contained in any purchase order, acknowledgment, check endorsement or other writing prepared by you, which terms are inconsistent with these terms and conditions or CCC's Billing and Payment terms and conditions. These terms and conditions, together with CCC's Billing and Payment terms and conditions (which are incorporated herein), comprise the entire agreement between you and publisher (and CCC) concerning this licensing transaction. In the event of any conflict between your obligations established by these terms and conditions and those established by CCC's Billing and Payment terms and conditions, these terms and conditions shall control.
14. Revocation: Elsevier or Copyright Clearance Center may deny the permissions described in this License at their sole discretion, for any reason or no reason, with a full refund payable to you. Notice of such denial will be made using the contact information provided by you. Failure to receive such notice will not alter or invalidate the denial. In no event will Elsevier or Copyright Clearance Center be responsible or liable for any costs, expenses or damage incurred by you as a result of a denial of your permission request, other than a refund of the amount(s) paid by you to Elsevier and/or Copyright Clearance Center for denied permissions.

LIMITED LICENSE

The following terms and conditions apply only to specific license types:
15. **Translation**: This permission is granted for non-exclusive world **English** rights only unless your license was granted for translation rights. If you licensed translation rights you may only translate this content into the languages you requested. A professional translator must perform all translations and reproduce the content word for word preserving the integrity of the article.
16. **Posting licensed content on any Website**: The following terms and conditions apply as follows: Licensing material from an Elsevier journal: All content posted to the web site must maintain the copyright information line on the bottom of each image; A hyper-text must be included to the Homepage of the journal from which you are licensing at http://www.sciencedirect.com/science/journal/xxxxx or the Elsevier homepage for books at http://www.elsevier.com; Central Storage: This license does not include permission for a scanned version of the material to be stored in a central repository such as that provided by Heron/XanEdu.
Licensing material from an Elsevier book: A hyper-text link must be included to the Elsevier homepage at http://www.elsevier.com . All content posted to the web site must maintain the copyright information line on the bottom of each image.

Posting licensed content on Electronic reserve: In addition to the above the following clauses

are applicable: The web site must be password-protected and made available only to bona fide students registered on a relevant course. This permission is granted for 1 year only. You may obtain a new license for future website posting.
17. **For journal authors:** the following clauses are applicable in addition to the above:
Preprints:
A preprint is an author's own write-up of research results and analysis, it has not been peer-reviewed, nor has it had any other value added to it by a publisher (such as formatting, copyright, technical enhancement etc.).
Authors can share their preprints anywhere at any time. Preprints should not be added to or enhanced in any way in order to appear more like, or to substitute for, the final versions of articles however authors can update their preprints on arXiv or RePEc with their Accepted Author Manuscript (see below).
If accepted for publication, we encourage authors to link from the preprint to their formal publication via its DOI. Millions of researchers have access to the formal publications on ScienceDirect, and so links will help users to find, access, cite and use the best available version.
Please note that Cell Press, The Lancet and some society-owned have different preprint policies. Information on these policies is available on the journal homepage.
Accepted Author Manuscripts: An accepted author manuscript is the manuscript of an article that has been accepted for publication and which typically includes author-incorporated changes suggested during submission, peer review and editor-author communications.
Authors can share their accepted author manuscript:

- immediately
    - via their non-commercial person homepage or blog
    - by updating a preprint in arXiv or RePEc with the accepted manuscript
    - via their research institute or institutional repository for internal institutional uses or as part of an invitation-only research collaboration work-group
    - directly by providing copies to their students or to research collaborators for their personal use
    - for private scholarly sharing as part of an invitation-only work group on commercial sites with which Elsevier has an agreement
- After the embargo period
    - via non-commercial hosting platforms such as their institutional repository
    - via commercial sites with which Elsevier has an agreement

In all cases accepted manuscripts should:

- link to the formal publication via its DOI
- bear a CC-BY-NC-ND license - this is easy to do
- if aggregated with other manuscripts, for example in a repository or other site, be shared in alignment with our hosting policy not be added to or enhanced in any way to appear more like, or to substitute for, the published journal article.

Published journal article (JPA): A published journal article (PJA) is the definitive final record of published research that appears or will appear in the journal and embodies all value-adding publishing activities including peer review co-ordination, copy-editing, formatting, (if relevant) pagination and online enrichment.
Policies for sharing publishing journal articles differ for subscription and gold open access articles:
Subscription Articles: If you are an author, please share a link to your article rather than the full-text. Millions of researchers have access to the formal publications on ScienceDirect, and so links will help your users to find, access, cite, and use the best available version.
Theses and dissertations which contain embedded PJAs as part of the formal submission can be posted publicly by the awarding institution with DOI links back to the formal publications on ScienceDirect.
If you are affiliated with a library that subscribes to ScienceDirect you have additional private sharing rights for others' research accessed under that agreement. This includes use for classroom teaching and internal training at the institution (including use in course packs and courseware programs), and inclusion of the article for grant funding purposes.
Gold Open Access Articles: May be shared according to the author-selected end-user license and should contain a CrossMark logo, the end user license, and a DOI link to the formal publication on ScienceDirect.
Please refer to Elsevier's posting policy for further information.
18. **For book authors** the following clauses are applicable in addition to the above: Authors are permitted to place a brief summary of their work online only. You are not allowed to download and post the published electronic version of your chapter, nor may you scan the printed edition to create an electronic version. **Posting to a repository:** Authors are permitted to post a summary of their chapter only in their institution's repository.
19. **Thesis/Dissertation**: If your license is for use in a thesis/dissertation your thesis may be submitted to your institution in either print or electronic form. Should your thesis be published commercially, please reapply for permission. These requirements include permission for the Library and Archives of Canada to supply single copies, on demand, of the complete thesis and include permission for Proquest/UMI to supply single copies, on demand, of the complete thesis. Should your thesis be published commercially, please reapply for permission. Theses and dissertations which contain embedded PJAs as part of the formal submission can be posted publicly by the awarding institution with DOI links back to the formal publications on ScienceDirect.

Elsevier Open Access Terms and Conditions
You can publish open access with Elsevier in hundreds of open access journals or in nearly 2000 established subscription journals that support open access publishing. Permitted third party re-use of these open access articles is defined by the author's choice of Creative Commons user license. See our open access license policy for more information.
Terms & Conditions applicable to all Open Access articles published with Elsevier:
Any reuse of the article must not represent the author as endorsing the adaptation of the article nor should the article be modified in such a way as to damage the author's honour or reputation. If any changes have been made, such changes must be clearly indicated.

Figure 6.1

Taylor & Francis is pleased to offer reuses of its content for a thesis or dissertation free of charge contingent on resubmission of permission request if work is published.

Figure 6.3A, C-D

SPRINGER NATURE LICENSE
TERMS AND CONDITIONS
Jul 24, 2023

This Agreement between Ms. Megan Kern ("You") and Springer Nature ("Springer Nature") consists of your license details and the terms and conditions provided by Springer Nature and Copyright Clearance Center.
License Number
5595470201108
License date
Jul 24, 2023
Licensed Content Publisher
Springer Nature
Licensed Content Publication
Nature Cell Biology
Licensed Content Title
The Rho GEFs LARG and GEF-H1 regulate the mechanical response to force on integrins
Licensed Content Author
Christophe Guilluy et al
Licensed Content Date
May 15, 2011
Type of Use
Thesis/Dissertation
Requestor type
academic/university or research institute
Format
print and electronic
Portion
figures/tables/illustrations
Number of figures/tables/illustrations
2
Would you like a high resolution image with your order?

no
Will you be translating?
no
Circulation/distribution
1 - 29
Author of this Springer Nature content
no
Title
Combined Atomic Force Microscopy and Light sheet Microscopy Characterize the Mechanobiology of Phagocytosis
Institution name
University of North Carolina at Chapel Hill
Expected presentation date
Jul 2023
Order reference number
Figure 6.3
Portions
Figure 1C, Figure 2
Requestor Location
Ms. Megan Kern
120 E Cameron Ave
Phillips Hall

CHAPEL HILL, NC 27599
United States
Attn: Ms. Megan Kern
Total
0.00 USD
Terms and Conditions
Springer Nature Customer Service Centre GmbH Terms and Conditions
The following terms and conditions ("Terms and Conditions") together with the terms specified in your [RightsLink] constitute the License ("License") between you as Licensee and Springer Nature Customer Service Centre GmbH as Licensor. By clicking 'accept' and completing the transaction for your use of the material ("Licensed Material"), you confirm your acceptance of and obligation to be bound by these Terms and Conditions.

1. **Grant and Scope of License**

    1. The Licensor grants you a personal, non-exclusive, non-transferable, non-sublicensable, revocable, world-wide License to reproduce, distribute, communicate to the public, make available, broadcast, electronically transmit or create derivative works using the Licensed Material for the purpose(s) specified in your RightsLink Licence Details only. Licenses are granted for the specific use

requested in the order and for no other use, subject to these Terms and Conditions. You acknowledge and agree that the rights granted to you under this License do not include the right to modify, edit, translate, include in collective works, or create derivative works of the Licensed Material in whole or in part unless expressly stated in your RightsLink Licence Details. You may use the Licensed Material only as permitted under this Agreement and will not reproduce, distribute, display, perform, or otherwise use or exploit any Licensed Material in any way, in whole or in part, except as expressly permitted by this License.

2. You may only use the Licensed Content in the manner and to the extent permitted by these Terms and Conditions, by your RightsLink Licence Details and by any applicable laws.

3. A separate license may be required for any additional use of the Licensed Material, e.g. where a license has been purchased for print use only, separate permission must be obtained for electronic re-use. Similarly, a License is only valid in the language selected and does not apply for editions in other languages unless additional translation rights have been granted separately in the License.

4. Any content within the Licensed Material that is owned by third parties is expressly excluded from the License.

5. Rights for additional reuses such as custom editions, computer/mobile applications, film or TV reuses and/or any other derivative rights requests require additional permission and may be subject to an additional fee. Please apply to journalpermissions@springernature.com or bookpermissions@springernature.com for these rights.

2. **Reservation of Rights**

Licensor reserves all rights not expressly granted to you under this License. You acknowledge and agree that nothing in this License limits or restricts Licensor's rights in or use of the Licensed Material in any way. Neither this License, nor any act, omission, or statement by Licensor or you, conveys any ownership right to you in any Licensed Material, or to any element or portion thereof. As between Licensor and you, Licensor owns and retains all right, title, and interest in and to the Licensed Material subject to the license granted in Section 1.1. Your permission to use the Licensed Material is expressly conditioned on you not impairing Licensor's or the applicable copyright owner's rights in the Licensed Material in any way.

3. **Restrictions on use**

1. Minor editing privileges are allowed for adaptations for stylistic purposes or formatting purposes provided such alterations do not alter the original meaning or intention of the Licensed Material and the new figure(s) are still accurate and representative of the Licensed Material. Any other changes including but not limited to, cropping, adapting, and/or omitting material that affect the meaning, intention or moral rights of the author(s) are strictly prohibited.

2. You must not use any Licensed Material as part of any design or trademark.

3. Licensed Material may be used in Open Access Publications (OAP), but any such reuse must include a clear acknowledgment of this permission visible at the same time as the figures/tables/illustration or abstract and which must indicate that the Licensed Material is not part of the governing OA license but has been reproduced with permission. This may be indicated according to any standard referencing system but must include at a minimum 'Book/Journal title, Author, Journal Name (if applicable), Volume (if applicable), Publisher, Year, reproduced with permission from SNCSC'.

4. **STM Permission Guidelines**

1. An alternative scope of license may apply to signatories of the STM Permissions Guidelines ("STM PG") as amended from time to time and made available at https://www.stm-assoc.org/intellectual-property/permissions/permissions-guidelines/.

2. For content reuse requests that qualify for permission under the STM PG, and which may be updated from time to time, the STM PG supersede the terms and conditions contained in this License.

3. If a License has been granted under the STM PG, but the STM PG no longer apply at the time of publication, further permission must be sought from the Rightsholder.
Contact journalpermissions@springernature.com or bookpermissions@springernature.com for these rights.

5. **Duration of License**

1. Unless otherwise indicated on your License, a License is valid from the date of purchase ("License Date") until the end of the relevant period in the below table:

Reuse in a medical communications project	Reuse up to distribution or time period indicated in License

Reuse in a dissertation/thesis	Lifetime of thesis
Reuse in a journal/magazine	Lifetime of journal/magazine
Reuse in a book/textbook	Lifetime of edition
Reuse on a website	1 year unless otherwise specified in the License
Reuse in a presentation/slide kit/poster	Lifetime of presentation/slide kit/poster. Note: publication whether electronic or in print of presentation/slide kit/poster may require further permission.
Reuse in conference proceedings	Lifetime of conference proceedings
Reuse in an annual report	Lifetime of annual report
Reuse in training/CME materials	Reuse up to distribution or time period indicated in License
Reuse in newsmedia	Lifetime of newsmedia
Reuse in coursepack/classroom materials	Reuse up to distribution and/or time period indicated in license

6. **Acknowledgement**

    1. The Licensor's permission must be acknowledged next to the Licensed Material in print. In electronic form, this acknowledgement must be visible at the same time as the figures/tables/illustrations or abstract and must be hyperlinked to the journal/book's homepage.

    2. Acknowledgement may be provided according to any standard referencing system and at a minimum should include "Author, Article/Book Title, Journal name/Book imprint, volume, page number, year, Springer Nature".

7. **Reuse in a dissertation or thesis**

    1. Where 'reuse in a dissertation/thesis' has been selected, the following terms apply: Print rights of the Version of Record are provided for; electronic rights for use only on institutional repository as defined by the Sherpa guideline (www.sherpa.ac.uk/romeo/) and only up to what is required by the awarding institution.

2. For theses published under an ISBN or ISSN, separate permission is required. Please contact journalpermissions@springernature.com or bookpermissions@springernature.com for these rights.

3. Authors must properly cite the published manuscript in their thesis according to current citation standards and include the following acknowledgement: '*Reproduced with permission from Springer Nature*'.

8. **License Fee**

You must pay the fee set forth in the License Agreement (the "License Fees"). All amounts payable by you under this License are exclusive of any sales, use, withholding, value added or similar taxes, government fees or levies or other assessments. Collection and/or remittance of such taxes to the relevant tax authority shall be the responsibility of the party who has the legal obligation to do so.

9. **Warranty**

1. The Licensor warrants that it has, to the best of its knowledge, the rights to license reuse of the Licensed Material. **You are solely responsible for ensuring that the material you wish to license is original to the Licensor and does not carry the copyright of another entity or third party (as credited in the published version).** If the credit line on any part of the Licensed Material indicates that it was reprinted or adapted with permission from another source, then you should seek additional permission from that source to reuse the material.

2. EXCEPT FOR THE EXPRESS WARRANTY STATED HEREIN AND TO THE EXTENT PERMITTED BY APPLICABLE LAW, LICENSOR PROVIDES THE LICENSED MATERIAL "AS IS" AND MAKES NO OTHER REPRESENTATION OR WARRANTY. LICENSOR EXPRESSLY DISCLAIMS ANY LIABILITY FOR ANY CLAIM ARISING FROM OR OUT OF THE CONTENT, INCLUDING BUT NOT LIMITED TO ANY ERRORS, INACCURACIES, OMISSIONS, OR DEFECTS CONTAINED THEREIN, AND ANY IMPLIED OR EXPRESS WARRANTY AS TO MERCHANTABILITY OR FITNESS FOR A PARTICULAR PURPOSE. IN NO EVENT SHALL LICENSOR BE LIABLE TO YOU OR ANY OTHER PARTY OR ANY OTHER PERSON OR FOR ANY SPECIAL, CONSEQUENTIAL, INCIDENTAL, INDIRECT, PUNITIVE, OR EXEMPLARY DAMAGES, HOWEVER CAUSED, ARISING OUT OF OR

IN CONNECTION WITH THE DOWNLOADING, VIEWING OR USE OF THE LICENSED MATERIAL REGARDLESS OF THE FORM OF ACTION, WHETHER FOR BREACH OF CONTRACT, BREACH OF WARRANTY, TORT, NEGLIGENCE, INFRINGEMENT OR OTHERWISE (INCLUDING, WITHOUT LIMITATION, DAMAGES BASED ON LOSS OF PROFITS, DATA, FILES, USE, BUSINESS OPPORTUNITY OR CLAIMS OF THIRD PARTIES), AND WHETHER OR NOT THE PARTY HAS BEEN ADVISED OF THE POSSIBILITY OF SUCH DAMAGES. THIS LIMITATION APPLIES NOTWITHSTANDING ANY FAILURE OF ESSENTIAL PURPOSE OF ANY LIMITED REMEDY PROVIDED HEREIN.

10. **Termination and Cancellation**

1. The License and all rights granted hereunder will continue until the end of the applicable period shown in Clause 5.1 above. Thereafter, this license will be terminated and all rights granted hereunder will cease.

2. Licensor reserves the right to terminate the License in the event that payment is not received in full or if you breach the terms of this License.

11. **General**

1. The License and the rights and obligations of the parties hereto shall be construed, interpreted and determined in accordance with the laws of the Federal Republic of Germany without reference to the stipulations of the CISG (United Nations Convention on Contracts for the International Sale of Goods) or to Germaný s choice-of-law principle.

2. The parties acknowledge and agree that any controversies and disputes arising out of this License shall be decided exclusively by the courts of or having jurisdiction for Heidelberg, Germany, as far as legally permissible.

3. This License is solely for Licensor's and Licensee's benefit. It is not for the benefit of any other person or entity.

Questions? For questions on Copyright Clearance Center accounts or website issues please contact springernaturesupport@copyright.com or +1-855-239-3415 (toll free in the US) or +1-978-646-2777. For questions on Springer Nature licensing please visit https://www.springernature.com/gp/partners/rights-permissions-third-party-distribution

Other Conditions:

Version 1.4 - Dec 2022

Questions? E-mail us at customercare@copyright.com.

Figure 6.4B

Order Date
24-Jul-2023
Order License ID
1378899-1
ISSN
1540-8140
Type of Use
Republish in a thesis/dissertation
Publisher
ROCKEFELLER UNIVERSITY PRESS
Portion
Image/photo/illustration

LICENSED CONTENT

Publication Title
The journal of cell biology
Article Title
Spatiotemporal dynamics of GEF-H1 activation controlled by microtubule- and Src-mediated pathways.
Date
01/01/1962
Language
English
Country
United States of America

Rightsholder
Rockefeller University Press
Publication Type
e-Journal
Start Page
3077
End Page
3097
Issue
9
Volume
218
URL
http://www.jcb.org/

REQUEST DETAILS

Portion Type
Image/photo/illustration
Number of Images / Photos / Illustrations
1
Format (select all that apply)
Print, Electronic
Who Will Republish the Content?
Academic institution
Duration of Use
Life of current edition
Lifetime Unit Quantity
Up to 499
Rights Requested
Main product
Distribution
United States
Translation
Original language of publication
Copies for the Disabled?
No
Minor Editing Privileges?
No
Incidental Promotional Use?
No
Currency
USD

NEW WORK DETAILS

Title
COMBINED ATOMIC FORCE MICROSCOPY AND LIGHT SHEET MICROSCOPY CHARACTERIZE THE MECHANOBIOLOGY OF PHAGOCYTOSIS
Instructor Name
Richard Superfine
Institution Name
University of North Carolina at Chapel Hill
Expected Presentation Date
2023-07-24

ADDITIONAL DETAILS

Order Reference Number
Figure 6.4B
The Requesting Person/Organization to Appear on the License
Megan Kern

REQUESTED CONTENT DETAILS

Title, Description or Numeric Reference of the Portion(s)
1
Editor of Portion(s)
Azoitei, Mihai L.; Noh, Jungsik; Marston, Daniel J.; Roudot, Philippe; Marshall, Christopher B.; Daugird, Timothy A.; Lisanza, Sidney L.; Sandí, María-José; Ikura, Mitsu; Sondek, John; Rottapel, Robert; Hahn, Klaus M.; Danuser, Gaudenz
Volume / Edition
218
Page or Page Range of Portion
3077-3097
Title of the Article/Chapter the Portion Is From
Spatiotemporal dynamics of GEF-H1 activation controlled by microtubule- and Src-mediated pathways.
Author of Portion(s)
Azoitei, Mihai L.; Noh, Jungsik; Marston, Daniel J.; Roudot, Philippe; Marshall, Christopher B.; Daugird, Timothy A.; Lisanza, Sidney L.; Sandí, María-José; Ikura, Mitsu; Sondek, John; Rottapel, Robert; Hahn, Klaus M.; Danuser, Gaudenz
Issue, if Republishing an Article From a Serial
9
Publication Date of Portion
2019-09-02
Marketplace Permissions General Terms and Conditions

The following terms and conditions ("General Terms"), together with any applicable Publisher Terms and Conditions, govern User's use of Works pursuant to the Licenses granted by Copyright Clearance Center, Inc. ("CCC") on behalf of the applicable Rightsholders of such Works through CCC's applicable Marketplace transactional licensing services (each, a "Service").

- 1)**Definitions.**For purposes of these General Terms, the following definitions apply:

  "License" is the licensed use the User obtains via the Marketplace platform in a particular licensing transaction, as set forth in the Order Confirmation.

  "Order Confirmation" is the confirmation CCC provides to the User at the conclusion of each Marketplace transaction. "Order Confirmation Terms" are additional terms set forth on specific Order Confirmations not set forth in the General Terms that can include terms applicable to a particular CCC transactional licensing service and/or any Rightsholder-specific terms.

  "Rightsholder(s)" are the holders of copyright rights in the Works for which a User obtains licenses via the Marketplace platform, which are displayed on specific Order Confirmations.

  "Terms" means the terms and conditions set forth in these General Terms and any additional Order Confirmation Terms collectively.

  "User" or "you" is the person or entity making the use granted under the relevant License. Where the person accepting the Terms on behalf of a User is a freelancer or other third party who the User authorized to accept the General Terms on the User's behalf, such person shall be deemed jointly a User for purposes of such Terms.

  "Work(s)" are the copyright protected works described in relevant Order Confirmations.

- 2)**Description of Service.**CCC's Marketplace enables Users to obtain Licenses to use one or more Works in accordance with all relevant Terms. CCC grants Licenses as an agent on behalf of the copyright rightsholder identified in the relevant Order Confirmation.
- 3)**Applicability of Terms.**The Terms govern User's use of Works in connection with the relevant License. In the event of any conflict between General Terms and Order Confirmation Terms, the latter shall govern. User acknowledges that Rightsholders have complete discretion whether to grant any permission, and whether to place any limitations on any grant, and that CCC has no right to supersede or to modify any such discretionary act by a Rightsholder.
- 4)**Representations; Acceptance.**By using the Service, User represents and warrants that User has been duly authorized by the User to accept, and hereby does accept, all Terms.
- 5)**Scope of License; Limitations and Obligations.**All Works and all rights therein, including copyright rights, remain the sole and exclusive property of the Rightsholder. The License

provides only those rights expressly set forth in the terms and conveys no other rights in any Works

- 6)**General Payment Terms.**User may pay at time of checkout by credit card or choose to be invoiced. If the User chooses to be invoiced, the User shall: (i) remit payments in the manner identified on specific invoices, (ii) unless otherwise specifically stated in an Order Confirmation or separate written agreement, Users shall remit payments upon receipt of the relevant invoice from CCC, either by delivery or notification of availability of the invoice via the Marketplace platform, and (iii) if the User does not pay the invoice within 30 days of receipt, the User may incur a service charge of 1.5% per month or the maximum rate allowed by applicable law, whichever is less. While User may exercise the rights in the License immediately upon receiving the Order Confirmation, the License is automatically revoked and is null and void, as if it had never been issued, if CCC does not receive complete payment on a timely basis.
- 7)**General Limits on Use.**Unless otherwise provided in the Order Confirmation, any grant of rights to User (i) involves only the rights set forth in the Terms and does not include subsequent or additional uses, (ii) is non-exclusive and non-transferable, and (iii) is subject to any and all limitations and restrictions (such as, but not limited to, limitations on duration of use or circulation) included in the Terms. Upon completion of the licensed use as set forth in the Order Confirmation, User shall either secure a new permission for further use of the Work(s) or immediately cease any new use of the Work(s) and shall render inaccessible (such as by deleting or by removing or severing links or other locators) any further copies of the Work. User may only make alterations to the Work if and as expressly set forth in the Order Confirmation. No Work may be used in any way that is unlawful, including without limitation if such use would violate applicable sanctions laws or regulations, would be defamatory, violate the rights of third parties (including such third parties' rights of copyright, privacy, publicity, or other tangible or intangible property), or is otherwise illegal, sexually explicit, or obscene. In addition, User may not conjoin a Work with any other material that may result in damage to the reputation of the Rightsholder. Any unlawful use will render any licenses hereunder null and void. User agrees to inform CCC if it becomes aware of any infringement of any rights in a Work and to cooperate with any reasonable request of CCC or the Rightsholder in connection therewith.
- 8)**Third Party Materials.**In the event that the material for which a License is sought includes third party materials (such as photographs, illustrations, graphs, inserts and similar materials) that are identified in such material as having been used by permission (or a similar indicator), User is responsible for identifying, and seeking separate licenses (under this Service, if available, or otherwise) for any of such third party materials; without a separate license, User may not use such third party materials via the License.
- 9)**Copyright Notice.**Use of proper copyright notice for a Work is required as a condition of any License granted under the Service. Unless otherwise provided in the Order Confirmation, a proper copyright notice will read substantially as follows: "Used with permission of [Rightsholder's name], from [Work's title, author, volume, edition number and year of copyright]; permission conveyed through Copyright Clearance Center, Inc." Such notice must be provided in a reasonably legible font size and must be placed either

on a cover page or in another location that any person, upon gaining access to the material which is the subject of a permission, shall see, or in the case of republication Licenses, immediately adjacent to the Work as used (for example, as part of a by-line or footnote) or in the place where substantially all other credits or notices for the new work containing the republished Work are located. Failure to include the required notice results in loss to the Rightsholder and CCC, and the User shall be liable to pay liquidated damages for each such failure equal to twice the use fee specified in the Order Confirmation, in addition to the use fee itself and any other fees and charges specified.

- 10)**Indemnity.**User hereby indemnifies and agrees to defend the Rightsholder and CCC, and their respective employees and directors, against all claims, liability, damages, costs, and expenses, including legal fees and expenses, arising out of any use of a Work beyond the scope of the rights granted herein and in the Order Confirmation, or any use of a Work which has been altered in any unauthorized way by User, including claims of defamation or infringement of rights of copyright, publicity, privacy, or other tangible or intangible property.
- 11)**Limitation of Liability.**UNDER NO CIRCUMSTANCES WILL CCC OR THE RIGHTSHOLDER BE LIABLE FOR ANY DIRECT, INDIRECT, CONSEQUENTIAL, OR INCIDENTAL DAMAGES (INCLUDING WITHOUT LIMITATION DAMAGES FOR LOSS OF BUSINESS PROFITS OR INFORMATION, OR FOR BUSINESS INTERRUPTION) ARISING OUT OF THE USE OR INABILITY TO USE A WORK, EVEN IF ONE OR BOTH OF THEM HAS BEEN ADVISED OF THE POSSIBILITY OF SUCH DAMAGES. In any event, the total liability of the Rightsholder and CCC (including their respective employees and directors) shall not exceed the total amount actually paid by User for the relevant License. User assumes full liability for the actions and omissions of its principals, employees, agents, affiliates, successors, and assigns.
- 12)**Limited Warranties.**THE WORK(S) AND RIGHT(S) ARE PROVIDED "AS IS." CCC HAS THE RIGHT TO GRANT TO USER THE RIGHTS GRANTED IN THE ORDER CONFIRMATION DOCUMENT. CCC AND THE RIGHTSHOLDER DISCLAIM ALL OTHER WARRANTIES RELATING TO THE WORK(S) AND RIGHT(S), EITHER EXPRESS OR IMPLIED, INCLUDING WITHOUT LIMITATION IMPLIED WARRANTIES OF MERCHANTABILITY OR FITNESS FOR A PARTICULAR PURPOSE. ADDITIONAL RIGHTS MAY BE REQUIRED TO USE ILLUSTRATIONS, GRAPHS, PHOTOGRAPHS, ABSTRACTS, INSERTS, OR OTHER PORTIONS OF THE WORK (AS OPPOSED TO THE ENTIRE WORK) IN A MANNER CONTEMPLATED BY USER; USER UNDERSTANDS AND AGREES THAT NEITHER CCC NOR THE RIGHTSHOLDER MAY HAVE SUCH ADDITIONAL RIGHTS TO GRANT.
- 13)**Effect of Breach.**Any failure by User to pay any amount when due, or any use by User of a Work beyond the scope of the License set forth in the Order Confirmation and/or the Terms, shall be a material breach of such License. Any breach not cured within 10 days of written notice thereof shall result in immediate termination of such License without further notice. Any unauthorized (but licensable) use of a Work that is terminated immediately upon notice thereof may be liquidated by payment of the Rightsholder's ordinary license price therefor; any unauthorized (and unlicensable) use that is not terminated immediately for any reason (including, for example, because materials containing the Work cannot reasonably be recalled) will be subject to all remedies

available at law or in equity, but in no event to a payment of less than three times the Rightsholder's ordinary license price for the most closely analogous licensable use plus Rightsholder's and/or CCC's costs and expenses incurred in collecting such payment.

- 14)**Additional Terms for Specific Products and Services.**If a User is making one of the uses described in this Section 14, the additional terms and conditions apply:
    - a)***Print Uses of Academic Course Content and Materials (photocopies for academic coursepacks or classroom handouts).***For photocopies for academic coursepacks or classroom handouts the following additional terms apply:
        - i) The copies and anthologies created under this License may be made and assembled by faculty members individually or at their request by on-campus bookstores or copy centers, or by off-campus copy shops and other similar entities.
        - ii) No License granted shall in any way: (i) include any right by User to create a substantively non-identical copy of the Work or to edit or in any other way modify the Work (except by means of deleting material immediately preceding or following the entire portion of the Work copied) (ii) permit "publishing ventures" where any particular anthology would be systematically marketed at multiple institutions.
        - iii) Subject to any Publisher Terms (and notwithstanding any apparent contradiction in the Order Confirmation arising from data provided by User), any use authorized under the academic pay-per-use service is limited as follows:
            - A) any License granted shall apply to only one class (bearing a unique identifier as assigned by the institution, and thereby including all sections or other subparts of the class) at one institution;
            - B) use is limited to not more than 25% of the text of a book or of the items in a published collection of essays, poems or articles;
            - C) use is limited to no more than the greater of (a) 25% of the text of an issue of a journal or other periodical or (b) two articles from such an issue;
            - D) no User may sell or distribute any particular anthology, whether photocopied or electronic, at more than one institution of learning;
            - E) in the case of a photocopy permission, no materials may be entered into electronic memory by User except in order to produce an identical copy of a Work before or during the academic term (or analogous period) as to which any particular permission is granted. In the event that User shall choose to retain materials that are the

subject of a photocopy permission in electronic memory for purposes of producing identical copies more than one day after such retention (but still within the scope of any permission granted), User must notify CCC of such fact in the applicable permission request and such retention shall constitute one copy actually sold for purposes of calculating permission fees due; and

- F) any permission granted shall expire at the end of the class. No permission granted shall in any way include any right by User to create a substantively non-identical copy of the Work or to edit or in any other way modify the Work (except by means of deleting material immediately preceding or following the entire portion of the Work copied).

- iv) Books and Records; Right to Audit. As to each permission granted under the academic pay-per-use Service, User shall maintain for at least four full calendar years books and records sufficient for CCC to determine the numbers of copies made by User under such permission. CCC and any representatives it may designate shall have the right to audit such books and records at any time during User's ordinary business hours, upon two days' prior notice. If any such audit shall determine that User shall have underpaid for, or underreported, any photocopies sold or by three percent (3%) or more, then User shall bear all the costs of any such audit; otherwise, CCC shall bear the costs of any such audit. Any amount determined by such audit to have been underpaid by User shall immediately be paid to CCC by User, together with interest thereon at the rate of 10% per annum from the date such amount was originally due. The provisions of this paragraph shall survive the termination of this License for any reason.

- b)***Digital Pay-Per-Uses of Academic Course Content and Materials (e-coursepacks, electronic reserves, learning management systems, academic institution intranets).***For uses in e-coursepacks, posts in electronic reserves, posts in learning management systems, or posts on academic institution intranets, the following additional terms apply:
  - i) The pay-per-uses subject to this Section 14(b) include:

    - A)**Posting e-reserves, course management systems, e-coursepacks for text-based content,**which grants authorizations to import requested material in electronic format, and allows electronic access to this material to members of a designated college or university class, under the direction of an instructor designated by the college or university, accessible only under appropriate electronic controls (e.g., password);

- B)**Posting e-reserves, course management systems, e-coursepacks for material consisting of photographs or other still images not embedded in text,**which grants not only the authorizations described in Section 14(b)(i)(A) above, but also the following authorization: to include the requested material in course materials for use consistent with Section 14(b)(i)(A) above, including any necessary resizing, reformatting or modification of the resolution of such requested material (provided that such modification does not alter the underlying editorial content or meaning of the requested material, and provided that the resulting modified content is used solely within the scope of, and in a manner consistent with, the particular authorization described in the Order Confirmation and the Terms), but not including any other form of manipulation, alteration or editing of the requested material;
- C)**Posting e-reserves, course management systems, e-coursepacks or other academic distribution for audiovisual content,**which grants not only the authorizations described in Section 14(b)(i)(A) above, but also the following authorizations: (i) to include the requested material in course materials for use consistent with Section 14(b)(i)(A) above; (ii) to display and perform the requested material to such members of such class in the physical classroom or remotely by means of streaming media or other video formats; and (iii) to "clip" or reformat the requested material for purposes of time or content management or ease of delivery, provided that such “clipping” or reformatting does not alter the underlying editorial content or meaning of the requested material and that the resulting material is used solely within the scope of, and in a manner consistent with, the particular authorization described in the Order Confirmation and the Terms. Unless expressly set forth in the relevant Order Conformation, the License does not authorize any other form of manipulation, alteration or editing of the requested material.

- ii) Unless expressly set forth in the relevant Order Confirmation, no License granted shall in any way: (i) include any right by User to create a substantively non-identical copy of the Work or to edit or in any other way modify the Work (except by means of deleting material immediately preceding or following the entire portion of the Work copied or, in the case of Works subject to Sections 14(b)(1)(B) or (C) above, as described in such Sections) (ii) permit "publishing ventures" where any particular course materials would be systematically marketed at multiple institutions.

- iii) Subject to any further limitations determined in the Rightsholder Terms (and notwithstanding any apparent contradiction in the Order

Confirmation arising from data provided by User), any use authorized under the electronic course content pay-per-use service is limited as follows:

- A) any License granted shall apply to only one class (bearing a unique identifier as assigned by the institution, and thereby including all sections or other subparts of the class) at one institution;

- B) use is limited to not more than 25% of the text of a book or of the items in a published collection of essays, poems or articles;

- C) use is limited to not more than the greater of (a) 25% of the text of an issue of a journal or other periodical or (b) two articles from such an issue;

- D) no User may sell or distribute any particular materials, whether photocopied or electronic, at more than one institution of learning;

- E) electronic access to material which is the subject of an electronic-use permission must be limited by means of electronic password, student identification or other control permitting access solely to students and instructors in the class;

- F) User must ensure (through use of an electronic cover page or other appropriate means) that any person, upon gaining electronic access to the material, which is the subject of a permission, shall see:

    - a proper copyright notice, identifying the Rightsholder in whose name CCC has granted permission,

    - a statement to the effect that such copy was made pursuant to permission,

    - a statement identifying the class to which the material applies and notifying the reader that the material has been made available electronically solely for use in the class, and

    - a statement to the effect that the material may not be further distributed to any person outside the class, whether by copying or by transmission and whether electronically or in paper form, and User must also ensure that such cover page or other means will print out in the event that the person accessing the material chooses to print out the material or any part thereof.

        - G) any permission granted shall expire at the end of the class and, absent some other form of authorization, User is thereupon required to delete the applicable material from any electronic storage or to block electronic access to the applicable material.

    - iv) Uses of separate portions of a Work, even if they are to be included in the same course material or the same university or college class, require separate permissions under the electronic course content pay-per-use Service. Unless otherwise provided in the Order Confirmation, any grant of rights to User is limited to use completed no later than the end of the academic term (or analogous period) as to which any particular permission is granted.

    - v) Books and Records; Right to Audit. As to each permission granted under the electronic course content Service, User shall maintain for at least four full calendar years books and records sufficient for CCC to determine the numbers of copies made by User under such permission. CCC and any representatives it may designate shall have the right to audit such books and records at any time during User's ordinary business hours, upon two days' prior notice. If any such audit shall determine that User shall have underpaid for, or underreported, any electronic copies used by three percent (3%) or more, then User shall bear all the costs of any such audit; otherwise, CCC shall bear the costs of any such audit. Any amount determined by such audit to have been underpaid by User shall immediately be paid to CCC by User, together with interest thereon at the rate of 10% per annum from the date such amount was originally due. The provisions of this paragraph shall survive the termination of this license for any reason.

- c)***Pay-Per-Use Permissions for Certain Reproductions (Academic photocopies for library reserves and interlibrary loan reporting) (Non-academic internal/external business uses and commercial document delivery).***The License expressly excludes the uses listed in Section (c)(i)-(v) below (which must be subject to separate license from the applicable Rightsholder) for: academic photocopies for library reserves and interlibrary loan reporting; and non-academic internal/external business uses and commercial document delivery.
    - i) electronic storage of any reproduction (whether in plain-text, PDF, or any other format) other than on a transitory basis;

    - ii) the input of Works or reproductions thereof into any computerized database;

    - iii) reproduction of an entire Work (cover-to-cover copying) except where the Work is a single article;

- iv) reproduction for resale to anyone other than a specific customer of User;

- v) republication in any different form. Please obtain authorizations for these uses through other CCC services or directly from the rightsholder.

Any license granted is further limited as set forth in any restrictions included in the Order Confirmation and/or in these Terms.

- d)***Electronic Reproductions in Online Environments (Non-Academic-email, intranet, internet and extranet).***For "electronic reproductions", which generally includes e-mail use (including instant messaging or other electronic transmission to a defined group of recipients) or posting on an intranet, extranet or Intranet site (including any display or performance incidental thereto), the following additional terms apply:
  - i) Unless otherwise set forth in the Order Confirmation, the License is limited to use completed within 30 days for any use on the Internet, 60 days for any use on an intranet or extranet and one year for any other use, all as measured from the "republication date" as identified in the Order Confirmation, if any, and otherwise from the date of the Order Confirmation.

  - ii) User may not make or permit any alterations to the Work, unless expressly set forth in the Order Confirmation (after request by User and approval by Rightsholder); provided, however, that a Work consisting of photographs or other still images not embedded in text may, if necessary, be resized, reformatted or have its resolution modified without additional express permission, and a Work consisting of audiovisual content may, if necessary, be "clipped" or reformatted for purposes of time or content management or ease of delivery (provided that any such resizing, reformatting, resolution modification or “clipping” does not alter the underlying editorial content or meaning of the Work used, and that the resulting material is used solely within the scope of, and in a manner consistent with, the particular License described in the Order Confirmation and the Terms.

- 15)**Miscellaneous.**
  - a) User acknowledges that CCC may, from time to time, make changes or additions to the Service or to the Terms, and that Rightsholder may make changes or additions to the Rightsholder Terms. Such updated Terms will replace the prior terms and conditions in the order workflow and shall be effective as to any subsequent Licenses but shall not apply to Licenses already granted and paid for under a prior set of terms.

- b) Use of User-related information collected through the Service is governed by CCC's privacy policy, available online at www.copyright.com/about/privacy-policy/.

- c) The License is personal to User. Therefore, User may not assign or transfer to any other person (whether a natural person or an organization of any kind) the License or any rights granted thereunder; provided, however, that, where applicable, User may assign such License in its entirety on written notice to CCC in the event of a transfer of all or substantially all of User's rights in any new material which includes the Work(s) licensed under this Service.

- d) No amendment or waiver of any Terms is binding unless set forth in writing and signed by the appropriate parties, including, where applicable, the Rightsholder. The Rightsholder and CCC hereby object to any terms contained in any writing prepared by or on behalf of the User or its principals, employees, agents or affiliates and purporting to govern or otherwise relate to the License described in the Order Confirmation, which terms are in any way inconsistent with any Terms set forth in the Order Confirmation, and/or in CCC's standard operating procedures, whether such writing is prepared prior to, simultaneously with or subsequent to the Order Confirmation, and whether such writing appears on a copy of the Order Confirmation or in a separate instrument.

- e) The License described in the Order Confirmation shall be governed by and construed under the law of the State of New York, USA, without regard to the principles thereof of conflicts of law. Any case, controversy, suit, action, or proceeding arising out of, in connection with, or related to such License shall be brought, at CCC's sole discretion, in any federal or state court located in the County of New York, State of New York, USA, or in any federal or state court whose geographical jurisdiction covers the location of the Rightsholder set forth in the Order Confirmation. The parties expressly submit to the personal jurisdiction and venue of each such federal or state court.

Last updated October 2022

Figure 7.2A-D

SPRINGER NATURE LICENSE
TERMS AND CONDITIONS
Jul 24, 2023

This Agreement between Ms. Megan Kern ("You") and Springer Nature ("Springer Nature")

consists of your license details and the terms and conditions provided by Springer Nature and Copyright Clearance Center.
License Number
5595481483703
License date
Jul 24, 2023
Licensed Content Publisher
Springer Nature
Licensed Content Publication
European Biophysics Journal
Licensed Content Title
Resolving the molecular structure of microtubules under physiological conditions with scanning force microscopy
Licensed Content Author
Iwan A. T. Schaap et al
Licensed Content Date
Feb 5, 2004
Type of Use
Thesis/Dissertation
Requestor type
academic/university or research institute
Format
print and electronic
Portion
figures/tables/illustrations
Number of figures/tables/illustrations
1
Will you be translating?
no
Circulation/distribution
1 - 29
Author of this Springer Nature content
no
Title
Combined Atomic Force Microscopy and Light sheet Microscopy Characterize the Mechanobiology of Phagocytosis
Institution name
University of North Carolina at Chapel Hill
Expected presentation date
Jul 2023
Order reference number
Figure 7.2A-D
Portions
Figure 5A-D

Requestor Location
Ms. Megan Kern
120 E Cameron Ave
Phillips Hall

CHAPEL HILL, NC 27599
United States
Attn: Ms. Megan Kern
Total
0.00 USD
Terms and Conditions
Springer Nature Customer Service Centre GmbH Terms and Conditions
The following terms and conditions ("Terms and Conditions") together with the terms specified in your [RightsLink] constitute the License ("License") between you as Licensee and Springer Nature Customer Service Centre GmbH as Licensor. By clicking 'accept' and completing the transaction for your use of the material ("Licensed Material"), you confirm your acceptance of and obligation to be bound by these Terms and Conditions.

1. **Grant and Scope of License**

    1. The Licensor grants you a personal, non-exclusive, non-transferable, non-sublicensable, revocable, world-wide License to reproduce, distribute, communicate to the public, make available, broadcast, electronically transmit or create derivative works using the Licensed Material for the purpose(s) specified in your RightsLink Licence Details only. Licenses are granted for the specific use requested in the order and for no other use, subject to these Terms and Conditions. You acknowledge and agree that the rights granted to you under this License do not include the right to modify, edit, translate, include in collective works, or create derivative works of the Licensed Material in whole or in part unless expressly stated in your RightsLink Licence Details. You may use the Licensed Material only as permitted under this Agreement and will not reproduce, distribute, display, perform, or otherwise use or exploit any Licensed Material in any way, in whole or in part, except as expressly permitted by this License.

    2. You may only use the Licensed Content in the manner and to the extent permitted by these Terms and Conditions, by your RightsLink Licence Details and by any applicable laws.

    3. A separate license may be required for any additional use of the Licensed Material, e.g. where a license has been purchased for print use only, separate permission must be obtained for electronic re-use. Similarly, a License is only

valid in the language selected and does not apply for editions in other languages unless additional translation rights have been granted separately in the License.

4. Any content within the Licensed Material that is owned by third parties is expressly excluded from the License.

5. Rights for additional reuses such as custom editions, computer/mobile applications, film or TV reuses and/or any other derivative rights requests require additional permission and may be subject to an additional fee. Please apply to journalpermissions@springernature.com or bookpermissions@springernature.com for these rights.

2. **Reservation of Rights**

Licensor reserves all rights not expressly granted to you under this License. You acknowledge and agree that nothing in this License limits or restricts Licensor's rights in or use of the Licensed Material in any way. Neither this License, nor any act, omission, or statement by Licensor or you, conveys any ownership right to you in any Licensed Material, or to any element or portion thereof. As between Licensor and you, Licensor owns and retains all right, title, and interest in and to the Licensed Material subject to the license granted in Section 1.1. Your permission to use the Licensed Material is expressly conditioned on you not impairing Licensor's or the applicable copyright owner's rights in the Licensed Material in any way.

3. **Restrictions on use**

1. Minor editing privileges are allowed for adaptations for stylistic purposes or formatting purposes provided such alterations do not alter the original meaning or intention of the Licensed Material and the new figure(s) are still accurate and representative of the Licensed Material. Any other changes including but not limited to, cropping, adapting, and/or omitting material that affect the meaning, intention or moral rights of the author(s) are strictly prohibited.

2. You must not use any Licensed Material as part of any design or trademark.

3. Licensed Material may be used in Open Access Publications (OAP), but any such reuse must include a clear acknowledgment of this permission visible at the same time as the figures/tables/illustration or abstract and which must indicate that the Licensed Material is not part of the governing OA license but has been reproduced with permission. This may be indicated according to any standard referencing system but must include at a minimum 'Book/Journal title, Author,

Journal Name (if applicable), Volume (if applicable), Publisher, Year, reproduced with permission from SNCSC'.

4. **STM Permission Guidelines**

    1. An alternative scope of license may apply to signatories of the STM Permissions Guidelines ("STM PG") as amended from time to time and made available at https://www.stm-assoc.org/intellectual-property/permissions/permissions-guidelines/.

    2. For content reuse requests that qualify for permission under the STM PG, and which may be updated from time to time, the STM PG supersede the terms and conditions contained in this License.

    3. If a License has been granted under the STM PG, but the STM PG no longer apply at the time of publication, further permission must be sought from the Rightsholder.
    Contact journalpermissions@springernature.com or bookpermissions@springernature.com for these rights.

5. **Duration of License**

    1. Unless otherwise indicated on your License, a License is valid from the date of purchase ("License Date") until the end of the relevant period in the below table:

Reuse in a medical communications project	Reuse up to distribution or time period indicated in License
Reuse in a dissertation/thesis	Lifetime of thesis
Reuse in a journal/magazine	Lifetime of journal/magazine
Reuse in a book/textbook	Lifetime of edition
Reuse on a website	1 year unless otherwise specified in the License
Reuse in a presentation/slide kit/poster	Lifetime of presentation/slide kit/poster. Note: publication whether electronic or in print of presentation/slide kit/poster may require further permission.
Reuse in conference proceedings	Lifetime of conference proceedings
Reuse in an annual report	Lifetime of annual report
Reuse in training/CME materials	Reuse up to distribution or time period indicated in License

Reuse in newsmedia	Lifetime of newsmedia
Reuse in coursepack/classroom materials	Reuse up to distribution and/or time period indicated in license

6.
7. **Acknowledgement**

    1. The Licensor's permission must be acknowledged next to the Licensed Material in print. In electronic form, this acknowledgement must be visible at the same time as the figures/tables/illustrations or abstract and must be hyperlinked to the journal/book's homepage.

    2. Acknowledgement may be provided according to any standard referencing system and at a minimum should include "Author, Article/Book Title, Journal name/Book imprint, volume, page number, year, Springer Nature".

8. **Reuse in a dissertation or thesis**

    1. Where 'reuse in a dissertation/thesis' has been selected, the following terms apply: Print rights of the Version of Record are provided for; electronic rights for use only on institutional repository as defined by the Sherpa guideline (www.sherpa.ac.uk/romeo/) and only up to what is required by the awarding institution.

    2. For theses published under an ISBN or ISSN, separate permission is required. Please contact journalpermissions@springernature.com or bookpermissions@springernature.com for these rights.

    3. Authors must properly cite the published manuscript in their thesis according to current citation standards and include the following acknowledgement: '*Reproduced with permission from Springer Nature*'.

9. **License Fee**

    You must pay the fee set forth in the License Agreement (the "License Fees"). All amounts payable by you under this License are exclusive of any sales, use, withholding,

value added or similar taxes, government fees or levies or other assessments. Collection and/or remittance of such taxes to the relevant tax authority shall be the responsibility of the party who has the legal obligation to do so.

10. **Warranty**

1. The Licensor warrants that it has, to the best of its knowledge, the rights to license reuse of the Licensed Material. **You are solely responsible for ensuring that the material you wish to license is original to the Licensor and does not carry the copyright of another entity or third party (as credited in the published version).** If the credit line on any part of the Licensed Material indicates that it was reprinted or adapted with permission from another source, then you should seek additional permission from that source to reuse the material.

2. EXCEPT FOR THE EXPRESS WARRANTY STATED HEREIN AND TO THE EXTENT PERMITTED BY APPLICABLE LAW, LICENSOR PROVIDES THE LICENSED MATERIAL "AS IS" AND MAKES NO OTHER REPRESENTATION OR WARRANTY. LICENSOR EXPRESSLY DISCLAIMS ANY LIABILITY FOR ANY CLAIM ARISING FROM OR OUT OF THE CONTENT, INCLUDING BUT NOT LIMITED TO ANY ERRORS, INACCURACIES, OMISSIONS, OR DEFECTS CONTAINED THEREIN, AND ANY IMPLIED OR EXPRESS WARRANTY AS TO MERCHANTABILITY OR FITNESS FOR A PARTICULAR PURPOSE. IN NO EVENT SHALL LICENSOR BE LIABLE TO YOU OR ANY OTHER PARTY OR ANY OTHER PERSON OR FOR ANY SPECIAL, CONSEQUENTIAL, INCIDENTAL, INDIRECT, PUNITIVE, OR EXEMPLARY DAMAGES, HOWEVER CAUSED, ARISING OUT OF OR IN CONNECTION WITH THE DOWNLOADING, VIEWING OR USE OF THE LICENSED MATERIAL REGARDLESS OF THE FORM OF ACTION, WHETHER FOR BREACH OF CONTRACT, BREACH OF WARRANTY, TORT, NEGLIGENCE, INFRINGEMENT OR OTHERWISE (INCLUDING, WITHOUT LIMITATION, DAMAGES BASED ON LOSS OF PROFITS, DATA, FILES, USE, BUSINESS OPPORTUNITY OR CLAIMS OF THIRD PARTIES), AND WHETHER OR NOT THE PARTY HAS BEEN ADVISED OF THE POSSIBILITY OF SUCH DAMAGES. THIS LIMITATION APPLIES NOTWITHSTANDING ANY FAILURE OF ESSENTIAL PURPOSE OF ANY LIMITED REMEDY PROVIDED HEREIN.

11. **Termination and Cancellation**

1. The License and all rights granted hereunder will continue until the end of the applicable period shown in Clause 5.1 above. Thereafter, this license will be terminated and all rights granted hereunder will cease.

2. Licensor reserves the right to terminate the License in the event that payment is not received in full or if you breach the terms of this License.

12. **General**

1. The License and the rights and obligations of the parties hereto shall be construed, interpreted and determined in accordance with the laws of the Federal Republic of Germany without reference to the stipulations of the CISG (United Nations Convention on Contracts for the International Sale of Goods) or to Germany´s choice-of-law principle.

2. The parties acknowledge and agree that any controversies and disputes arising out of this License shall be decided exclusively by the courts of or having jurisdiction for Heidelberg, Germany, as far as legally permissible.

3. This License is solely for Licensor's and Licensee's benefit. It is not for the benefit of any other person or entity.

Questions? For questions on Copyright Clearance Center accounts or website issues please contact springernaturesupport@copyright.com or +1-855-239-3415 (toll free in the US) or +1-978-646-2777. For questions on Springer Nature licensing please visit https://www.springernature.com/gp/partners/rights-permissions-third-party-distribution

Other Conditions:

Version 1.4 - Dec 2022

Questions? E-mail us at customercare@copyright.com.

Figure 2, 3.1A-C, 3.2B-E, 5.1B, 5.1C, 5.1D, 5.1E, 5.1F, 7.1, 7.4, 7.7, 7.8 & Table 7.1

Figure 7.2E-F, & 7.3

End Page	R1292
Type of Use	reuse in a thesis/dissertation
Portion	figures/tables/illustrations
Number of figures/tables/illustrations	2
Format	electronic
Are you the author of this Elsevier article?	No
Will you be translating?	No
Title	Combined Atomic Force Microscopy and Light sheet Microscopy Characterize the Mechanobiology of Phagocytosis
Institution name	University of North Carolina at Chapel Hill
Expected presentation date	Jul 2023
Order reference number	7
Portions	Figure 1 and Figure 2.
Requestor Location	Ms. Megan Kern 120 E Cameron Ave Phillips Hall CHAPEL HILL, NC 27599 United States Attn: Ms. Megan Kern
Publisher Tax ID	98-0397604
Billing Type	Invoice
Billing Address	Ms. Megan Kern 120 E Cameron Ave Phillips Hall CHAPEL HILL, NC 27599 United States Attn: Ms. Megan Kern
Total	**0.00 USD**
Terms and Conditions	

INTRODUCTION

1. The publisher for this copyrighted material is Elsevier. By clicking "accept" in connection with completing this licensing transaction, you agree that the following terms and conditions apply to this transaction (along with the Billing and Payment terms and conditions established by Copyright Clearance Center, Inc. ("CCC"), at the time that you opened your RightsLink account and that are available at any time at https://myaccount.copyright.com).

GENERAL TERMS

2. Elsevier hereby grants you permission to reproduce the aforementioned material subject to the terms and conditions indicated.

3. Acknowledgement: If any part of the material to be used (for example, figures) has appeared in our publication with credit or acknowledgement to another source, permission must also be sought from that source. If such permission is not obtained then that material may not be included in your publication/copies. Suitable acknowledgement to the source must be made, either as a footnote or in a reference list at the end of your publication, as follows:

"Reprinted from Publication title, Vol /edition number, Author(s), Title of article / title of chapter, Pages No., Copyright (Year), with permission from Elsevier [OR APPLICABLE SOCIETY COPYRIGHT OWNER]." Also Lancet special credit - "Reprinted from The Lancet, Vol. number, Author(s), Title of article, Pages No., Copyright (Year), with permission from Elsevier."

4. Reproduction of this material is confined to the purpose and/or media for which permission is hereby given. The material may not be reproduced or used in any other way, including use in combination with an artificial intelligence tool (including to train an algorithm, test, process, analyse, generate output and/or develop any form of artificial intelligence tool), or to create any derivative work and/or service (including resulting from the use of artificial intelligence tools).

5. Altering/Modifying Material: Not Permitted. However figures and illustrations may be altered/adapted minimally to serve your work. Any other abbreviations, additions, deletions and/or any other alterations shall be made only with prior written authorization of Elsevier Ltd. (Please contact Elsevier's permissions helpdesk here). No modifications can be made to any Lancet figures/tables and they must be reproduced in full.

6. If the permission fee for the requested use of our material is waived in this instance, please be advised that your future requests for Elsevier materials may attract a fee.

7. Reservation of Rights: Publisher reserves all rights not specifically granted in the combination of (i) the license details provided by you and accepted in the course of this licensing transaction, (ii) these terms and conditions and (iii) CCC's Billing and Payment terms and conditions.

8. License Contingent Upon Payment: While you may exercise the rights licensed immediately upon issuance of the license at the end of the licensing process for the transaction, provided that you have disclosed complete and accurate details of your proposed use, no license is finally effective unless and until full payment is received from you (either by publisher or by CCC) as provided in CCC's Billing and Payment terms and conditions. If full payment is not received on a timely basis, then any license preliminarily

granted shall be deemed automatically revoked and shall be void as if never granted. Further, in the event that you breach any of these terms and conditions or any of CCC's Billing and Payment terms and conditions, the license is automatically revoked and shall be void as if never granted. Use of materials as described in a revoked license, as well as any use of the materials beyond the scope of an unrevoked license, may constitute copyright infringement and publisher reserves the right to take any and all action to protect its copyright in the materials.

9. Warranties: Publisher makes no representations or warranties with respect to the licensed material.

10. Indemnity: You hereby indemnify and agree to hold harmless publisher and CCC, and their respective officers, directors, employees and agents, from and against any and all claims arising out of your use of the licensed material other than as specifically authorized pursuant to this license.

11. No Transfer of License: This license is personal to you and may not be sublicensed, assigned, or transferred by you to any other person without publisher's written permission.

12. No Amendment Except in Writing: This license may not be amended except in a writing signed by both parties (or, in the case of publisher, by CCC on publisher's behalf).

13. Objection to Contrary Terms: Publisher hereby objects to any terms contained in any purchase order, acknowledgment, check endorsement or other writing prepared by you, which terms are inconsistent with these terms and conditions or CCC's Billing and Payment terms and conditions. These terms and conditions, together with CCC's Billing and Payment terms and conditions (which are incorporated herein), comprise the entire agreement between you and publisher (and CCC) concerning this licensing transaction. In the event of any conflict between your obligations established by these terms and conditions and those established by CCC's Billing and Payment terms and conditions, these terms and conditions shall control.

14. Revocation: Elsevier or Copyright Clearance Center may deny the permissions described in this License at their sole discretion, for any reason or no reason, with a full refund payable to you. Notice of such denial will be made using the contact information provided by you. Failure to receive such notice will not alter or invalidate the denial. In no event will Elsevier or Copyright Clearance Center be responsible or liable for any costs, expenses or damage incurred by you as a result of a denial of your permission request, other than a refund of the amount(s) paid by you to Elsevier and/or Copyright Clearance Center for denied permissions.

LIMITED LICENSE

The following terms and conditions apply only to specific license types:

15. **Translation**: This permission is granted for non-exclusive world **English** rights only unless your license was granted for translation rights. If you licensed translation rights you may only translate this content into the languages you requested. A professional translator must perform all translations and reproduce the content word for word preserving the integrity of the article.

16. **Posting licensed content on any Website**: The following terms and conditions apply as follows: Licensing material from an Elsevier journal: All content posted to the web site must maintain the copyright information line on the bottom of each image; A hyper-text must be included to the Homepage of the journal from which you are licensing at http://www.sciencedirect.com/science/journal/xxxxx or the Elsevier homepage for books at http://www.elsevier.com; Central Storage: This license does not include permission for a scanned version of the material to be stored in a central repository such as that provided by Heron/XanEdu.
Licensing material from an Elsevier book: A hyper-text link must be included to the Elsevier homepage at http://www.elsevier.com . All content posted to the web site must maintain the copyright information line on the bottom of each image.

Posting licensed content on Electronic reserve: In addition to the above the following clauses are applicable: The web site must be password-protected and made available only to bona fide students registered on a relevant course. This permission is granted for 1 year only. You may obtain a new license for future website posting.
17. **For journal authors:** the following clauses are applicable in addition to the above:
Preprints:
A preprint is an author's own write-up of research results and analysis, it has not been peer-reviewed, nor has it had any other value added to it by a publisher (such as formatting, copyright, technical enhancement etc.).
Authors can share their preprints anywhere at any time. Preprints should not be added to or enhanced in any way in order to appear more like, or to substitute for, the final versions of articles however authors can update their preprints on arXiv or RePEc with their Accepted Author Manuscript (see below).
If accepted for publication, we encourage authors to link from the preprint to their formal publication via its DOI. Millions of researchers have access to the formal publications on ScienceDirect, and so links will help users to find, access, cite and use the best available version. Please note that Cell Press, The Lancet and some society-owned have different preprint policies. Information on these policies is available on the journal homepage.
Accepted Author Manuscripts: An accepted author manuscript is the manuscript of an article that has been accepted for publication and which typically includes author-incorporated changes suggested during submission, peer review and editor-author communications.
Authors can share their accepted author manuscript:

- immediately
    - via their non-commercial person homepage or blog
    - by updating a preprint in arXiv or RePEc with the accepted manuscript
    - via their research institute or institutional repository for internal institutional uses or as part of an invitation-only research collaboration work-group

    - directly by providing copies to their students or to research collaborators for their personal use
    - for private scholarly sharing as part of an invitation-only work group on commercial sites with which Elsevier has an agreement
- After the embargo period
    - via non-commercial hosting platforms such as their institutional repository
    - via commercial sites with which Elsevier has an agreement

In all cases accepted manuscripts should:

- link to the formal publication via its DOI
- bear a CC-BY-NC-ND license - this is easy to do
- if aggregated with other manuscripts, for example in a repository or other site, be shared in alignment with our hosting policy not be added to or enhanced in any way to appear more like, or to substitute for, the published journal article.

Published journal article (JPA): A published journal article (PJA) is the definitive final record of published research that appears or will appear in the journal and embodies all value-adding publishing activities including peer review co-ordination, copy-editing, formatting, (if relevant) pagination and online enrichment.
Policies for sharing publishing journal articles differ for subscription and gold open access articles:
Subscription Articles: If you are an author, please share a link to your article rather than the full-text. Millions of researchers have access to the formal publications on ScienceDirect, and so links will help your users to find, access, cite, and use the best available version.
Theses and dissertations which contain embedded PJAs as part of the formal submission can be posted publicly by the awarding institution with DOI links back to the formal publications on ScienceDirect.
If you are affiliated with a library that subscribes to ScienceDirect you have additional private sharing rights for others' research accessed under that agreement. This includes use for classroom teaching and internal training at the institution (including use in course packs and courseware programs), and inclusion of the article for grant funding purposes.
Gold Open Access Articles: May be shared according to the author-selected end-user license and should contain a CrossMark logo, the end user license, and a DOI link to the formal publication on ScienceDirect.
Please refer to Elsevier's posting policy for further information.
18. **For book authors** the following clauses are applicable in addition to the above: Authors are permitted to place a brief summary of their work online only. You are not allowed to download and post the published electronic version of your chapter, nor may you scan the printed edition to create an electronic version. **Posting to a repository:** Authors are permitted to post a summary of their chapter only in their institution's repository.

19. **Thesis/Dissertation**: If your license is for use in a thesis/dissertation your thesis may be submitted to your institution in either print or electronic form. Should your thesis be published commercially, please reapply for permission. These requirements include permission for the Library and Archives of Canada to supply single copies, on demand, of the complete thesis and include permission for Proquest/UMI to supply single copies, on demand, of the complete thesis. Should your thesis be published commercially, please reapply for permission. Theses and dissertations which contain embedded PJAs as part of the formal submission can be posted publicly by the awarding institution with DOI links back to the formal publications on ScienceDirect.

Elsevier Open Access Terms and Conditions

You can publish open access with Elsevier in hundreds of open access journals or in nearly 2000 established subscription journals that support open access publishing. Permitted third party re-use of these open access articles is defined by the author's choice of Creative Commons user license. See our open access license policy for more information.

Terms & Conditions applicable to all Open Access articles published with Elsevier:

Any reuse of the article must not represent the author as endorsing the adaptation of the article nor should the article be modified in such a way as to damage the author's honour or reputation. If any changes have been made, such changes must be clearly indicated. The author(s) must be appropriately credited and we ask that you include the end user license and a DOI link to the formal publication on ScienceDirect.

If any part of the material to be used (for example, figures) has appeared in our publication with credit or acknowledgement to another source it is the responsibility of the user to ensure their reuse complies with the terms and conditions determined by the rights holder.

Additional Terms & Conditions applicable to each Creative Commons user license:

CC BY: The CC-BY license allows users to copy, to create extracts, abstracts and new works from the Article, to alter and revise the Article and to make commercial use of the Article (including reuse and/or resale of the Article by commercial entities), provided the user gives appropriate credit (with a link to the formal publication through the relevant DOI), provides a link to the license, indicates if changes were made and the licensor is not represented as endorsing the use made of the work. The full details of the license are available at http://creativecommons.org/licenses/by/4.0.

CC BY NC SA: The CC BY-NC-SA license allows users to copy, to create extracts, abstracts and new works from the Article, to alter and revise the Article, provided this is not done for commercial purposes, and that the user gives appropriate credit (with a link to the formal publication through the relevant DOI), provides a link to the license, indicates if changes were made and the licensor is not represented as endorsing the use made of the work. Further, any new works must be made available on the same conditions. The full details of the license are available at http://creativecommons.org/licenses/by-nc-sa/4.0.

CC BY NC ND: The CC BY-NC-ND license allows users to copy and distribute the Article, provided this is not done for commercial purposes and further does not permit distribution of the Article if it is changed or edited in any way, and provided the user gives

REFERENCES

[1] S. A. Freeman and S. Grinstein, "Phagocytosis: Receptors, signal integration, and the cytoskeleton," *Immunological Reviews,* vol. 262, no. 1, pp. 193-215, 2014.

[2] J. D. Dunn, C. Bosmani, C. Barisch, R. Lyudmil, L. H. Lefrançois, E. Cardenal-Muñoz, L.-J. A. Teresa and T. Soldati, "Eat prey, live: Dictyostelium discoideum as a model for cell-autonomous defenses," *Front Immunol,* p. 8, 2018.

[3] J. J. Lim, S. Grinstein and R. Ziv, "Diversity and versatility of phagocytosis: roles in innate immunity, tissue remodeling, and homeostasis.," *Front Cell Infect Microbiol,* p. 7:1–12, 2017.

[4] S. Arandjelovic and K. S. Ravichandran, "Phagocytosis of apoptotic cells in homeostasis.," *Nat Immunol,* p. 16:907–917, 2015.

[5] J. Shklover, F. Levy-Adam and E. Kurant, "Apoptotic cell clearance in development," *Current topics in developmental biology,* pp. 114:297-334, 2015.

[6] J. Westman, S. Grinstein and P. E. Marques, "Phagocytosis of necrotic debris at sites of injury and inflammation," *Front Immunol,* p. 10, 2020.

[7] S. Nagata, "Apoptosis and Clearance of Apoptotic Cells," *Annual Review of Immunology,* vol. 36, pp. 489-517, 2018.

[8] R. N. Mohammed, M. Khosravi, H. S. Rahman, A. Adili, N. Kamali, P. P. Soloshenkov, L. Thangavelu, H. Saeedi, N. Shomali, R. Tamjidifar, A. Isazadeh and R. Aslaminabad, "Anastasis: cell recovery mechanisms and potential role in cancer," *Cell Communication and Signaling,* vol. 20, no. 1, p. Article number 81, 2022.

[9] J. Stricker, T. Falzone and M. L. Gardel, "Mechanics of the F-actin cytoskeleton," *Journal fo Biomechanics,* vol. 43, no. 1, pp. 9-14, 2010.

[10] P. K. Mattila and P. Lappalainen, "Filopodia: molecular architecture and cellular functions," *Nature Reviews Molecular Cell Biology,* vol. 9, pp. 446-454, 2008.

[11] L. E. Young, E. G. Heimsath and H. N. Higgs, "Cell type-dependent mechanisms for formin-mediated assembly of filopodia," *Molecular Biology of the Cell,* vol. 26, no. 25, pp. 4646-4659, 2015.

[12] S. Xu, J. Wang, J.-H. Wang and T. A. Springer, "Distinct recognition of complement iC3b by integrins αXβ2 and αMβ2," *PNAS,* vol. 114, no. 13, p. 3403–3408, 2017.

[13] D. M. Underhill and A. Ozinsky, "Phagocytosis of Microbes: Complexity in Action," *Annual Review of Immunology,* vol. 20, p. 825–852, 2002.

[14] M. Krendel and N. C. Gauthier, "Building the phagocytic cup on an actin scaffold," *Current Opinion in Cell Biology,* vol. 77, p. 102112, 2022.

[15] F. Niedergang and S. Grinstein, "How to build a phagosome: new concepts for an old process," *Current Opinion in Cell Biology,* vol. 50, pp. 57-63, 2018.

[16] S. Mylvaganam, S. A. Freeman and S. Grinstein, "The cytoskeleton in phagocytosis and macropinocytosis," *Current Biology,* vol. 31, pp. R619-R632, 2021.

[17] S. M. Mylvaganam, S. Grinstein and S. A. Freeman, "Picket-fences in the plasma membrane: functions in immune," *Seminars in Immunopathology,* vol. 40, p. 605–615, 2018.

[18] G. Kaplan, "Differences in the mode of phagocytosis with Fc and C3 receptors in macrophages," *Scandinavian Journal of Immunology,* vol. 6, no. 8, pp. 797-807, 1977.

[19] L. Allen and A. Aderem, "Molecular definition of distinct cytoskeletal structures involved in complement- and Fc receptor-mediated phagocytosis in macrophages," *Journal of Experiment Medicine,* vol. 184, no. 2, pp. 627-637, 1996.

[20] A. Steffen, T. E. Stradal and K. Rottner, "Signaling Pathways Controlling Cellular Actin Reorganization," *Handbook of Experimental Pharmocology,* vol. 235, pp. 153-178, 2017.

[21] E. Caron and A. Hall, "Identification of two distinct mechanisms of phagocytosis controlled by different Rho GTPases," *Science,* vol. 282, no. 5394, pp. 1717-21, 1998.

[22] P. Massol, P. Montcourrier, J.-C. Guillemot and P. Chavrier, "Fc receptor-mediated phagocytosis requires CDC42 and Rac1," *EMBO Journal,* vol. 17, no. 21, pp. 6219-6229, 1998.

[23] I. M. Olazabal, E. Caron, R. C. May, K. Schilling, D. A. Knecht and L. M. Machesky, "Rho-kinase and myosin-II control phagocytic cup formation during CR, but not FcgammaR, phagocytosis," *Current Biology,* vol. 12, no. 16, pp. 1413-1418, 2002.

[24] P. C. Patel and R. E. Harrison, "Membrane ruffles capture C3bi-opsonized particles in activated macrophages," *Molecular Biology of the Cell,* vol. 19, no. 11, pp. 4628-4639, 2008.

[25] S. Walbaum, B. Ambrosy, P. Schütz, A. C. Bachg, M. Horsthemke, J. H. W. Leusen, A. Mócsai and P. J. Hanley, "Complement receptor 3 mediates both sinking phagocytosis

and phagocytic cup formation via distinct mechanisms," *Journal of Biological Chemistry,* vol. 296, p. 100256, 2021.

[26] V. Jaumouillé, A. X. Cartagena-Rivera and C. M. Waterman, "Coupling of β 2 integrins to actin by a mechanosensitive molecular clutch drives complement receptor-mediated phagocytosis," *Nature Cell Biology,* vol. 21, no. 11, pp. 1357-1369, 2019.

[27] R. C. May, E. Caron, A. Hall and L. M. Machesky, "Involvement of the Arp2/3 complex in phagocytosis mediated by FcgammaR or CR3," *Nature Cell Biology,* vol. 2, no. 4, pp. 246-248, 2000.

[28] J. D. Rotty, H. E. Brighton, S. L, S. B. Asokan, N. Cheng, J. P. Ting and J. E. Bear, "Arp2/3 Complex Is Required for Macrophage Integrin Functions but Is Dispensable for FcR Phagocytosis and In Vivo Motility," *Developmental Cell,* vol. 42, no. 5, pp. 498-513, 2017.

[29] E. Carona, A. J. Self and A. Hall, "The GTPase Rap1 controls functional activation of macrophage integrin αMβ2 by LPS and other inflammatory mediators," *Current Biology,* vol. 10, no. 16, pp. 974-978, 2000.

[30] L. Christina, C. J. Plüss and D. Ricklin, "The Promiscuous Profile of Complement Receptor 3 in Ligand Binding, Immune Modulation, and Pathophysiology," *Frontiers in Immunology,* vol. 12, p. 10.3389/fimmu.2021.662164 , 2021.

[31] S. A. Freeman, J. Goyette, W. Furuya, E. C. Woods, C. R. Bertozzi, W. Bergmeier, B. Hinz, P. A. van der Merwe, R. Das and S. Grinstein, "Freeman SA, Goyette J, Furuya W, Woods EC, Bertozzi CR, Bergmeier Integrins Form an Expanding Diffusional Barrier that Coordinates Phagocytosis," *Cell,* vol. 164, no. 1-2, pp. 128-140, 2016.

[32] T. Mitchison and M. Kirschner, "Cytoskeletal dynamics and nerve growth," *Neuron,* vol. 1, no. 9, pp. 761-772, 1988.

[33] M. L. Gardel, B. Sabass, L. Ji, G. Danuser, U. S. Schwarz and C. M. Waterman, "Traction stress in focal adhesions correlates biphasically with actin retrograde flow speed," *Journal of Cell Biology,* vol. 183, no. 6, p. 999–1005, 2008.

[34] P. Kanchanawong, G. Shtengel, A. Pasapera, E. Ramko, M. Davidson, H. Hess and C. Waterman, "Nanoscale architecture of integrin-based cell adhesions," *Nature,* vol. 468, p. 580–584, 2010.

[35] I. Thievessen, P. M. Thompson, S. Berlemont, K. M. Plevock, S. V. Plotnikov, A. Zemljic-Harpf, R. S. Ross, M. W. Davidson, G. Danuser, S. L. Campbell and C. M. Waterman, "Vinculin–actin interaction couples actin retrograde flow to focal adhesions, but is

dispensable for focal adhesion growth," *Journal of Cell Biology,* vol. 202, no. 1, p. 163–177, 2013.

[36] F. Margadant, L. L. Chew, X. Hu, H. Yu, N. Bate, X. Zhang and M. Sheetz, "Mechanotransduction In Vivo by Repeated Talin Stretch-Relaxation Events Depends upon Vinculin," *PLOS Biology,* vol. 9, no. 12, p. e1001223, 2011.

[37] M. Yao, B. T. Goult, H. Chen, P. Cong, M. P. Sheetz and J. Yan, "Mechanical activation of vinculin binding to talin locks talin in an unfolded conformation," *Scientific Reports,* vol. 4, p. Article 4610, 2014.

[38] B. Klapholz and N. H. Brown, "Talin – the master of integrin adhesions," *Journal of Cell Science,* vol. 130, no. 15, p. 2435–2446, 2017.

[39] T. Isogai, K. M. Dean, P. Roudot, Q. Shao, J. D. Cillay, E. S. Welf, M. K. Driscoll, S. P. Royer, N. Mittal, B.-J. Chang, S. J. Han, R. Fiolka and G. Danuser, "Direct Arp2/3-vinculin binding is essential for cell spreading, but only on compliant substrates and in 3D," *bioRxiv,* p. doi: https://doi.org/10.1101/756718, 2019.

[40] R. Boujemaa-Paterski, B. Martins, M. Eibauer, C. T. Beales, B. Geiger and O. Medalia, "Talin-activated vinculin interacts with branched actin networks to initiate bundles," *eLife,* vol. 9, p. e53990, 2020.

[41] K. A. Beningo and Y.-l. Wang, "Fc-receptor-mediated phagocytosis is regulated by mechanical properties of the target," *Journal of Cell Science,* vol. 115, no. 4, p. 849–856, 2002.

[42] D. Vorselen, R. L. D. Labitigan and J. A. Theriot, "A mechanical perspective on phagocytic cup formation," *Current Opinion in Cell Biology,* vol. 66, p. 112–122, 2020.

[43] A. Bettadapur, H. W. Miller and K. S. Ralston, "Biting Off What Can Be Chewed: Trogocytosis in Health, Infection, and Disease," *Infection and Immunity,* vol. 88, no. 7, 2020.

[44] S. A. Freeman, A. Vega, M. Riedl, R. F. Collins, P. P. Ostrowski, E. C. Woods, C. R. Bertozzi, M. I. Tammi, D. S. Lidke, P. Johnson, S. Mayor, K. Jaqaman and S. Grinstein, "Transmembrane Pickets Connect Cyto- and Pericellular Skeletons Forming Barriers to Receptor Engagement," *Cell,* vol. 172, no. 1-2, pp. 305-317, 2018.

[45] S. Tollis, A. E. Dart, G. Tzircotis and R. G. Endres, "The zipper mechanism in phagocytosis: energetic requirements and variability in phagocytic cup shape," *BMC Systemd Biology,* vol. 4, p. 149, 2010.

[46] M. Herant, V. Heinrich and M. Dembo, "Mechanics of neutrophil phagocytosis: experiments and quantitative models," *Journal of Cell Science,* vol. 119, no. 9, pp. 1903-1913, 2006.

[47] J. S. van Zon, G. Tzircotis, E. Caron and M. Howard, "A mechanical bottleneck explains the variation in cup growth during FcgammaR phagocytosis," *Molecular Systems Biology,* vol. 5, p. 298, 2009.

[48] M. Herant, C.-Y. Lee, M. Dembo and V. Heinrich, "Protrusive Push versus Enveloping Embrace: Computational Model of Phagocytosis Predicts Key Regulatory Role of Cytoskeletal Membrane Anchors," *PLOS Computational Biology,* vol. 7, no. 1, p. e1001068, 2011.

[49] S. E. Malawista, Gee, J. B and K. G. Bensch, " Cytochalasin B reversibly inhibits phagocytosis: functional, metabolic, and ultrastructural effects in human blood leukocytes and rabbit alveolar macrophages.," *Yale Journal of Biological Medicine,* vol. 44, pp. 286-300, 1971.

[50] A. T. Davis, R. Estensen and P. G. Quie, "Cytochalasin B Inhibition of human polymorphonuclear leukocyte phagocytosis," *Proceedings of the Society for Experimental Biology,* vol. 137, p. 161–164, 1971.

[51] M. Herant, V. Heinrich and M. Dembo, "Mechanics of neutrophil phagocytosis: behavior of the cortical tension," *Journal of Cell Science,* vol. 118, no. 9, p. 1789–1797, 2005.

[52] C. C. Scott, W. Dobson, R. J. Botelho, N. Coady-Osberg, P. Chavrier, D. A. Knecht, C. Heath, P. Stahl and S. Grinstein, "Phosphatidylinositol-4,5-bisphosphate hydrolysis directs actin remodeling during phagocytosis," *Journal of Cell Biology,* vol. 169, pp. 139-149, 2005.

[53] V. Heinrich, "Controlled One-on-One Encounters between Immune Cells and Microbes," *Biophysical Perspective,* vol. 109, pp. 469-476, 2015.

[54] M. Irmscher, A. M. de Jong, H. Kress and M. W. J. Prins, "A method for time-resolved measurements of the mechanics of phagocytic cups," *Journal of the Royal Society Interface,* vol. 10, p. 20121048, 2013.

[55] K. Beicker, E. T. O'Brien, M. R. Falvo, Superfine and R, "Vertical Light Sheet Enhanced Side-View Imaging for AFM Cell Mechanics Studies," *Sci Rep,* vol. 8, p. 1504, 2018.

[56] E. Nelsen, C. M. Hobson, M. E. Kern, J. P. Hsiao, E. T. O'Brien III, T. Watanabe, B. M. Condon, M. Boyce, S. Grinstein, K. M. Hahn, M. R. Falvo and R. Superfine, "Combined

Atomic Force Microscope and Volumetric Light Sheet System for Correlative Force and Fluorescence Mechanobiology Studies," *Scientific Reports,* vol. 10, no. 1, p. 8133, 2020.

[57] P. Nalbant, Y. C. Chang, J. Birkenfeld, Z. F. Chang and G. M. Bokoch, "Guanine nucleotide exchange factor-H1 regulates cell migration via localized activation of RhoA at the leading edge," *Mol Biol Cell,* vol. 20, p. 4070–4082, 2009.

[58] B. Liu, C. M. Hobson, F. M. Pimenta, E. F. Nelsen, J. Hsiao, E. T. O'Brien, M. R. Falvo, K. M. Hahn and R. Superfine, "VIEW-MOD: a versatile illumination engine with a modular optical design for fluorescence microscopy," *Optics Express,* vol. 27, no. 14, pp. 19950-19972, 2019.

[59] C. M. Hobson, E. T. O'Brien 3rd, M. R. Falvo and R. Superfine, "Combined Selective Plane Illumination Microscopy and FRAP Maps Intranuclear Diffusion of NLS-GFP," *Biophys J,* vol. 119, no. 3, pp. 514-524, 2020.

[60] F. Geissmann, M. G. Manz, S. Jung, M. H. Sieweke and M. L. K. Merad, "Development of monocytes, macrophages, and dendritic cells," *Science,* vol. 327, p. 656–61, 2010.

[61] I. Levental, P. Georges and P. Janmey, "Soft biological materials and their impact on cell function," *Soft Matter,* vol. 3, no. 3, p. 299–306, 2007.

[62] R. Sridharan, B. Cavanagh, A. R. Cameron, D. J. Kelly and F. J. O'Brien, "Material stiffness influences the polarization state, function and migration mode of macrophages," *Acta Biomater,* vol. 89, p. 47–59, 2019.

[63] B. Dutta, R. Goswami and S. O. Rahaman, "TRPV4 plays a role in matrix stiffness-induced macrophage polarization," *Front Immunol,* vol. 11, p. 570195, 2020.

[64] S. Baratchi, M. T. K. Zaldivia, M. Wallert, J. Loseff-Silver, S. Al-Aryahi and e. al., "Transcatheter aortic valve implantation represents an anti-inflammatory therapy via reduction of shear stress-induced, Piezo-1-mediated monocyte activation," *Circulation,* vol. 142, p. 1092–1105, 2020.

[65] V. A. Morikis, E. Masadeh and S. I. Simon, "Tensile force transmitted through LFA-1 bonds mechanoregulate neutrophil inflammatory response," *J Leukoc Biol ,* vol. 108, p. 1815–1828, 2020.

[66] W. Sun, S. Wang, J. Zhang, K. Arias, B. P. Griffith and Z. J. Wu, "Neutrophil injury and function alterations induced by high mechanical shear stress with short exposure time," *Artif Organs,* vol. 45, p. 577–586, 2021.

[67] R. G. Scheraga, S. Abraham, L. M. Grove, B. D. Southern, J. F. Crish, A. Perelas, C. McDonald, K. Asosingh, J. D. Hasday and M. A. Olman, "TRPV4 Protects the Lung from Bacterial Pneumonia via MAPK Molecular Pathway Switching," *J Immunol,* vol. 204, no. 5, p. 1310–1321, 2020.

[68] D. Vorselen, S. R. Barger, Y. Wang, W. Cai and J. A. Theriot, "Phagocytic 'teeth' and myosin-II 'jaw' power target constriction during phagocytosis," *eife,* vol. 10, p. 68627, 2021.

[69] J. A. Swanson, M. T. Johnson, K. Beningo, P. Post, M. Mooseker and N. Araki, "A contractile activity that closes phagosomes in macrophages," *Journal of Cell Science,* vol. 112, no. 3, pp. 307-16, 1999.

[70] J. Möller, T. Lühmann, M. Chabria, H. Hall and V. Vogel, "Macrophages lift off surface-bound bacteria using a filopodium-lamellipodium hook-and-shovel mechanism," *Sci Rep,* vol. 3, no. 2884, 2013.

[71] H. De Belly, S. Yan, H. Borja da Rocha, S. Ichbiah, J. P. Town, P. J. Zager, D. C. Estrada, K. Meyer, H. Turlier, C. Bustamante and O. D. Weiner, "Cell protrusions and contractions generate longrange membrane tension propagation," *Cell,* vol. 186, p. 1–13, 2023.

[72] Z. Shi, Z. T. Graber, T. Baumgart, H. A. Stone and A. E. Cohen, "Cell Membranes Resist Flow," *Cell,* vol. 175, p. 1769–1779, 2018.

[73] C. G. Perez, N. R. Dudzinski, M. Rouches, A. Landajuela, B. Machta, D. Zenisek and E. Karatekin, "Rapid propagation of membrane tension at retinal bipolar neuron presynaptic terminals," *Sci. Adv,* vol. 8, p. eabl4411, 2022.

[74] Y. Ikeda, K. Kawai, A. Ikawa, K. Kawamoto, Y. Egami and N. Araki, "Rac1 switching at the right time and location is essential for Fcgamma receptor-mediated phagosome formation," *Journal of Cell Science,* vol. 130, no. 15, pp. 2530-2540, 2017.

[75] N. Araki, T. Hatae, A. Furukawa and J. A. Swanson, "Phosphoinositide-3-kinase-independent contractile activities associated with Fcgamma-receptor-mediated phagocytosis and macropinocytosis in macrophages," *Journal of Cell Science,* vol. 116, no. 2, pp. 247-57, 2003.

[76] R. K. Sadhu, S. R. Barger, S. Penič, A. Iglič, M. Krendel, N. C. Gauthier and N. S. Gov, "A theoretical model of efficient phagocytosis driven by curved membrane proteins and active cytoskeleton forces," *Soft Matter,* vol. 19, pp. 31-43, 2023.

[77] D. M. Richards and R. G. Endres, "The mechanism of phagocytosis: two stages of engulfment.," *Biophysical Journal,* vol. 107, no. 7, pp. 1542-53, 2014.

[78] C. Guilluy, V. Swaminathan, R. Garcia-Mata, E. T. O'Brien, R. Superfine and K. Burridge, "The Rho GEFs LARG and GEF-H1 regulate the mechanical response to force on integrins," *Nat Cell Biol,* vol. 13, no. 6, pp. 722-727, 2011.

[79] J. E. Sader, J. W. M. Chon and P. Mulvaney, "Calibration of rectangular atomic force microscope cantilevers," *Review of Scientific Instrument,* vol. 70, no. 10, pp. 3967-3969, 1999.

[80] M. J. Higgins, R. Proksch, J. E. Sader, M. Polcik, S. Mc Endoo, J. P. Cleveland and S. P. Jarvis, "Noninvasive determination of optical lever sensitivity in atomic force microscopy," *Review of Scientific Instruments,* vol. 77, no. 1, pp. 1-5, 2005.

[81] D. Vorselen, Y. Wang, M. M. de Jesus, P. K. Shah, M. J. Footer, M. Huse and W. J. A. Cai, "Microparticle traction force microscopy reveals subcellular force exertion patterns in immune cell–target interactions," *Nature Communications,* vol. 11, p. 20, 2020.

[82] S. R. Barger, N. S. Reilly, M. S. Shutova, Q. Li, P. Maiuri, J. M. Heddleston, M. S. Mooseker, R. A. Flavell, T. Svitkina, P. W. Oakes, M. Krendel and N. C. Gauthier, "Membrane-cytoskeletal crosstalk mediated by myosin-I regulates adhesion turnover during phagocytosis," *Nature Communications,* vol. 10, no. 1, p. 1249, 2019.

[83] J. C. Herron, S. Hu, T. Watanabe, A. T. Nogueira, B. Liu, M. E. Kern, J. Aaron, A. Taylor, M. Pablo, T.-L. Chew, T. C. Elston and K. M. Hahn, "Actin nano-architecture of phagocytic podosomes," *Nature Communications,* vol. 13, p. 4363 , 2022.

[84] P. P. Ostrowski, F. S. A, Fairn and S. Grinstein, "Dynamic Podosome-Like Structures in Nascent Phagosomes Are Coordinated by Phosphoinositides," *Developmental Cell,* vol. 50, no. 4, pp. 397-410, 2019.

[85] A. Labernadie, A. Bouissou, P. Delobelle, S. Balor, R. Voituriez, A. Proag, I. Fourquaux, C. Thibault, C. Vieu, R. Poincloux, G. M. Charrière and I. Maridonneau-Parini, "Protrusion force microscopy reveals oscillatory force generation and mechanosensing activity of human macrophage podosomes," *Nature Communications,* vol. 5, p. 5343, 2014.

[86] K. van den Dries, L. Nahidiazar, J. A. Slotman, M. B. M. Meddens, E. Pandzic, B. Joosten, M. Ansems, J. Schouwstra, A. Meijer, R. Steen, M. Wijers, J. Fransen, A. B. Houtsmuller, P. W. Wiseman, K. Jalink and A. Cambi, "Modular actin nano-architecture enables podosome protrusion and mechanosensing," *Nature Communications,* vol. 10, p. 1–16, 2019.

[87] M. Tertrais, C. Bigot, E. Martin, R. Poincloux, A. Labrousse and I. Maridonneau-Parini, "Phagocytosis is coupled to the formation of phagosome-associated podosomes and a transient disruption of podosomes in human macrophages," *European Journal of Cell Biology,* vol. 100, no. 4, p. 151161, 2021.

[88] K. van den Dries, M. Meddens, d. Keijzer, S. Shekhar, V. Subramaniam, C. G. Figdor and A. Cambi, "Interplay between myosin IIA-mediated contractility and actin network integrity orchestrates podosome composition and oscillations," *Nature Communications,* vol. 4, p. 1412, 2013.

[89] A. B. Jaffe and A. Hall, "Rho GTPases: biochemistry and biology," *Annu Rev Cell Dev Biol,* vol. 21, p. 247–269, 2005.

[90] N. Mosaddeghzadeh and M. R. Ahmadian, "The RHO Family GTPases: Mechanisms of Regulation and Signaling," *Cells,* vol. 10, no. 7, p. 1831, 2021.

[91] J. L. Bos, H. Rehmann and A. Wittinghofer, "GEFs and GAPs: Critical Elements in the Control of Small G Proteins," *Cell,* vol. 129, no. 5, pp. 865-877, 2007.

[92] M. Lammers, S. Meyer, D. Kuhlmann and A. Wittinghofer, "Specificity of interactions between mDia isoforms and Rho proteins," *J Biol Chem,* vol. 283, pp. 35236-35246, 2008.

[93] T. Otomo, C. Otomo, D. R. Tomchick, M. Machius and M. K. Rosen, "Structural basis of Rho GTPase-mediated activation of the formin mDia1," *Mol Cell,* vol. 18, pp. 273-281, 2005.

[94] S. Kurisu and T. Takenawa, "The WASP and WAVE family proteins," *Genome Biol,* vol. 10, p. 226, 2009.

[95] A. M. Lebensohn and M. W. Kirschner, "Activation of the WAVE complex by coincident signals controls actin assembly," *Mol Cell,* vol. 36, pp. 512-524, 2009.

[96] V. Delorme, M. Machacek, C. DerMardirossian, K. L. Anderson, T. Wittmann, D. Hanein, C. Waterman-Storer, G. Danuser and G. M. Bokoch, "Cofilin activity downstream of Pak1 regulates cell protrusion efficiency by organizing lamellipodium and lamella actin networks," *Dev Cell,* vol. 13, pp. 646-662, 2007.

[97] T. Y. Huang, C. DerMardirossian and G. M. Bokoch, " Cofilin phosphatases and regulation of actin dynamics," *Curr Opin Cell Biol,* vol. 18, pp. 26-31, 2006.

[98] P. W. B. Derksen and R. A. H. van de Ven, "Shared mechanisms regulate spatiotemporal RhoA-dependent actomyosin contractility during adhesion and cell division," *Small GTPases,* vol. 11, no. 2, pp. 113-121, 2020.

[99] Y. Mao and S. C. Finnemann, "Regulation of phagocytosis by Rho GTPases," *Small GTPases,* vol. 6, no. 2, pp. 89-99, 2015.

[100] A. B. Hall, M. A. Gakidis, M. Glogauer, J. L. Wilsbacher, S. Gao, W. Swat and J. S. Brugge, "Requirements for Vav guanine nucleotide exchange factors and Rho GTPases in FcgammaR- and complementmediated phagocytosis," *Immunity,* vol. 24, p. 305–316, 2006.

[101] Y. Egami, K. Kawai and N. Araki, "RhoC regulates the actin remodeling required for phagosome formation during FcgammaR-mediated phagocytosis," *J Cell Sci,* vol. 130, p. 4168–4179, 2017.

[102] D. J. Hackam, O. D. Rotstein, A. Schreiber, W. Zhang and S. Grinstein, "Rho is required for the initiation of calcium signaling and phagocytosis by Fcgamma receptors in macrophages," *J Exp Med,* vol. 186, p. 955–966, 1997.

[103] S. Freeman and S. Grinstein, "Phagocytosis: Mechanosensing, Traction Forces, and a Molecular Clutch," *Current Biology,* vol. 30, p. R10–R37, 2020.

[104] O. Pertz, L. Hodgson, R. L. Klemke and K. M. Hahn, "Spatiotemporal dynamics of RhoA activity in migrating cells," *Nature,* vol. 440, pp. 1069-1072, 2006.

[105] M. Machacek, L. Hodgson, C. Welch, H. Elliott, O. Pertz, P. Nalbant, A. Abell, G. L. Johnson, K. M. Hahn and G. Danuser, "Coordination of Rho GTPase activities during cell protrusion," *Nature,* vol. 461, p. 99–103, 2009.

[106] E. Tkachenko, M. Sabouri-Ghomi, O. Pertz, C. Kim, E. Gutierrez, M. Machacek, A. Groisman, G. Danuser and M. H. Ginsberg, "Protein kinase A governs a RhoA-RhoGDI protrusion-retraction pacemaker in migrating cells," *Nat Cell Biol,* vol. 13, p. 660–667, 2011.

[107] M. Krendel, F. T. Zenke and G. M. Bokoch, "Nucleotide exchange factor GEF-H1 mediates cross-talk between microtubules and the actin cytoskeleton," *Nat Cell Biol,* vol. 4, p. 294–301, 2002.

[108] D. Meiri, C. B. Marshall, M. A. Greeve, B. Kim, M. Balan, F. Suarez, C. Bakal, C. Wu, J. Larose, N. Fine and e. al., "Mechanistic insight into the microtubule and actin

cytoskeleton coupling through dynein-dependent RhoGEF inhibition," *Mol Cell,* vol. 45, p. 642–65, 2012.

[109] M. J. Sandí, C. B. Marshall, M. Balan, É. Coyaud, M. Zhou, D. M. Monson, N. Ishiyama, A. A. Chandrakumar, J. La Rose, A. L. Couzens and e. al., "MARK3-mediated phosphorylation of ARHGEF2 couples microtubules to the actin cytoskeleton to establish cell polarity," *Sci Signal,* vol. 10, p. eaan3286, 2017.

[110] S. Seetharaman, B. Vianay, V. Roca, A. J. Farrugia, C. De Pascalis, B. Boëda, F. Dingli, D. Loew, S. Vassilopoulos, A. Bershadsky, M. Théry and S. Etienne-Manneville, "Microtubules tune mechanosensitive cell responses," *Nat Mater,* vol. 21, p. 366–377, 2022.

[111] J. N. Heck, S. M. Ponik, M. G. Garcia-Mendoza, C. A. Pehlke, D. R. Inman, K. W. Eliceiri and P. J. Keely, "Microtubules regulate GEF-H1 in response to extracellular matrix stiffness," *Mol Biol Cell,* vol. 23, no. 13, pp. 2583-92, 2012.

[112] N. Fine, I. D. Dimitriou and R. Rottapel, "Go with the flow: GEF-H1 mediated shear stress mechanotransduction in neutrophils," *Small GTPases,* vol. 11, no. 1, pp. 23-31, 2020.

[113] N. Fine, I. D. Dimitriou, J. Rullo, M. J. Sandí, B. Petri, J. Haitsma, H. Ibrahim, J. La Rose, M. Glogauer, P. Kubes, M. Cybulsky and R. Rottapel, "GEF-H1 is necessary for neutrophil shear stress-induced migration during inflammation," *J Cell Biol,* vol. 15, no. 1, pp. 107-119, 2016.

[114] D. Paul, S. Achouri, Y. Z. Yoon, J. Herre, C. E. Bryant and P. Cicuta, "Phagocytosis dynamics depends on target shape," *Biophys J,* vol. 105, no. 5, pp. 1143-50, 2013.

[115] N. G. Sosale, T. Rouhiparkouhi, A. M. Bradshaw, R. Dimova, R. Lipowsky and D. E. Discher, "Cell rigidity and shape override CD47's "self"-signaling in phagocytosis by hyperactivating myosin-II," *Blood,* vol. 3, no. 542-52, p. 125, 2015.

[116] M. L. Azoitei, J. Noh, D. J. Marston, P. Roudot, C. B. Marshall, T. A. Daugird, S. L. Lisanza, M. J. Sandí, M. Ikura, J. Sondek, R. Rottapel, K. M. Hahn and G. Danuser, "Spatiotemporal dynamics of GEF-H1 activation controlled by microtubule- and Src-mediated pathways," *J Cell Biol,* vol. 218, no. 9, pp. 3077-3097, 2019.

[117] L. Fusco, R. Lefort, K. Smith, F. Benmansour, G. Gonzalez, C. Barillari, B. Rinn, F. Fleuret, P. Fua and O. Pertz, "Computer vision profiling of neurite outgrowth dynamics reveals spatiotemporal modularity of Rho GTPase signaling," *J Cell Biol,* vol. 212, p. 91–111, 2016.

[118] D. T. Kovari, W. Wei, P. Chang, J.-S. Toro, R. F. Beach, D. Chambers, K. Porter, D. Koo and J. E. Curtis, "Frustrated Phagocytic Spreading of J774A-1 Macrophages Ends in Myosin II-Dependent Contraction," *Biophysical Journal,* vol. 111, no. 12, pp. 2698-2710, 2016.

[119] P. Rougerie and D. Cox, "Spatio-temporal mapping of mechanical force generated by macrophages during FcγR-dependent phagocytosis reveals adaptation to target stiffness," *bioRxiv 2020.04.14.041335.*

[120] E. C. O'Shaughnessy, O. J. Stone, P. K. LaFosse, M. L. Azoitei, D. Tsygankov, J. M. Heddleston, W. R. Legant, E. S. Wittchen, K. Burridge, T. C. Elston, E. Betzig, T. L. Chew, D. Adalsteinsson and K. M. Hahn, "Software for lattice light-sheet imaging of FRET biosensors, illustrated with a new Rap1 biosensor," *J Cell Biol,* vol. 218, no. 9, pp. 3153-3160, 2019.

[121] Y. Yoshimura and H. Miki, "Dynamic regulation of GEF-H1 localization at microtubules by Par1b/MARK2," *Biochem Biophys Res Commun,* vol. 408, no. 2, pp. 322-8, 2011.

[122] F. J. Pixley, "Macrophage Migration and Its Regulation by CSF-1," *Int J Cell Biol,* vol. 2012, p. 501962, 2012.

[123] P. Shi, Y. Wang, Y. Huang, C. Zhang, Y. Li, Y. Liu, T. Li, W. Wang, X. Liang and C. Wu, "Arp2/3-branched actin regulates microtubule acetylation levels and affects mitochondrial distribution," *J Cell Sci,* vol. 132, no. 6, p. jcs226506, 2019.

[124] A. Yoshimura, S. Miserey-Lenkei, E. Coudrier and B. Goud, "Branched Actin Maintains Acetylated Microtubule Network in the Early Secretory Pathway," *Cells,* vol. 11, no. 1, p. 15, 2021.

[125] B. E. Steinberg and S. Grinstein, "Analysis of macrophage phagocytosis: quantitative assays of phagosome formation and maturation using high-throughput fluorescence microscopy," *Methods Mol Biol,* vol. 531, pp. 45-56, 2009.

[126] J. Garcia-Anoveros and D. Corey, "The Molecules of Mechanosensation," *Annu Rev Neurosci,* vol. 20, pp. 567-94, 1997.

[127] R. G. Walker, A. T. Willingham and C. S. Zuker, "A Drosophila mechanosensory transduction channel," *Science,* vol. 287, no. 5461, pp. 2229-34, 2000.

[128] R. O'Hagan, M. Chalfie and M. B. Goodman, "The MEC-4 DEG/ENaC channel of Caenorhabditis elegans touch receptor neurons transduces mechanical signals," *Nat Neurosci,* vol. 8, no. 1, pp. 43-50, 2005.

[129] B. Coste, J. Mathur, M. Schmidt, T. J. Earley, S. Ranade, M. J. Petrus, A. E. Dubin and A. Patapoutian, "Piezo1 and Piezo2 are essential components of distinct mechanically activated cation channels," *Science,* vol. 330, no. 6000, pp. 55-60, 2010.

[130] C. Kung, "A possible unifying principle for mechanosensation," *Nature,* vol. 436, p. 647–654, 2005.

[131] A. P. Christensen and D. P. Corey, "TRP channels in mechanosensation: direct or indirect activation?," *Nat Rev Neurosci,* vol. 8, no. 7, pp. 510-21, 2007.

[132] J. Teng, S. Loukin, A. Anishkin and C. Kung, "The Force-From-Lipid (FFL) principle of mechanosensitivity, at large and in elements," *Pflugers Arch,* vol. 467, no. 1, p. 27–37, 2015.

[133] S. Katta, M. Krieg and M. B. Goodman, "Feeling Force: Physical and Physiological Principles Enabling Sensory Mechanotransduction," *Annu Rev Cell Dev Biol,* vol. 31, no. 1, pp. 347-371, 2015.

[134] J. Howard and A. J. Hudspeth, "Mechanical relaxation of the hair bundle mediates adaptation in mechanoelectrical transduction by the bullfrog's saccular hair cell," *Proc Natl Acad Sci U S A,* vol. 84, no. 9, p. 3064–3068, 1987.

[135] P. Jin, D. Bulkley, Y. Guo, W. Zhang, Guo, Zhenhao, W. Huynh, S. Wu, S. Meltzer, T. Cheng, L. Y. Jan, Y.-N. Jan and Y. Cheng, "Electron cryo-microscopy structure of the mechanotransduction channel NOMPC," *Nature,* vol. 547, no. 7661, pp. 118-122, 2017.

[136] X. Liang, J. Madrid, R. Gärtner, J.-M. Verbavatz, C. Schiklenk, M. Wilsch-Bräuninger, A. Bogdanova, F. Stenger, A. Voigt and J. Howard, "A NOMPC-dependent membrane-microtubule connector is a candidate for the gating spring in fly mechanoreceptors," *Curr Biol,* vol. 23, no. 9, pp. 755-63, 2013.

[137] M. B. Goodman, E. S. Haswell and V. Vásquez, "Mechanosensitive membrane proteins: Usual and unusual suspects in mediating mechanotransduction," *J Gen Physiol,* vol. 155, no. 3, p. e202213248, 2023.

[138] M. Prager-Khoutorsky, A. Khoutorsky and C. W. Bourque, "Unique interweaved microtubule scaffold mediates osmosensory transduction via physical interaction with TRPV1," *Neuron,* vol. 83, no. 4, pp. 866-78, 2014.

[139] Z. Yan, W. Zhang, Y. He, D. Gorczyca, Y. Xiang, L. E. Cheng, S. Meltzer, L. Y. Jan and Y. N. Jan, "Drosophila NOMPC is a mechanotransduction channel subunit for gentle-touch sensation," *Nature,* vol. 493, no. 7431, pp. 221-5, 2013.

[140] L. E. Cheng, W. Song, L. L. Looger, L. Y. Jan and Y. N. Jan, "The role of the TRP channel NompC in Drosophila larval and adult locomotion," *Neuron,* vol. 67, no. 3, pp. 373-80, 2010.

[141] W. Zhang, L. E. Cheng, M. Kittelmann, J. Li, M. Petkovic, T. Cheng, P. Jin, Z. Guo, M. C. Göpfert, L. Y. Jan and Y. N. Jan, "Ankyrin Repeats Convey Force to Gate the NOMPC Mechanotransduction Channel," *Cell,* vol. 162, no. 6, pp. 1391-403, 2015.

[142] Y. Wang, Y. Guo, G. Li, C. Liu, L. Wang, A. Zhang, Z. Yan and C. Song, "The push-to-open mechanism of the tethered mechanosensitive ion channel NompC," *Elife,* vol. 10, p. e58388, 2021.

[143] J. Howard and S. Bechstedt, "Hypothesis: a helix of ankyrin repeats of the NOMPC-TRP ion channel is the gating spring of mechanoreceptors," *Curr Biol,* vol. 14, no. 6, pp. R224-6, 2004.

[144] P. Minguez, L. Parca, F. Diella, D. R. Mende, R. Kumar, M. Helmer-Citterich, A. C. Gavin, V. van Noort and P. Bork, "Deciphering a global network of functionally associated post-translational modifications," *Mol Syst Biol,* vol. 8, p. 599, 2012.

[145] D. G. Christensen, X. Xie, N. Basisty, J. Byrnes, S. McSweeney, B. Schilling and A. J. Wolfe, "Post-translational Protein Acetylation: An Elegant Mechanism for Bacteria to Dynamically Regulate Metabolic Functions," *Front Microbiol,* vol. 10, 2019.

[146] A. K. Coleman, H. C. Joca, G. Shi, Lederer, W. Jonathan and C. W. Ward, "Tubulin acetylation increases cytoskeletal stiffness to regulate mechanotransduction in striated muscle," *J Gen Physiol,* vol. 153, no. 7, p. e202012743, 2021.

[147] M. Chalfie and M. Au, "Genetic control of differentiation of the Caenorhabditis elegans touch receptor neurons," *Science,* vol. 243, no. 4894 Pt 1, p. 1027–1033, 1989.

[148] J. S. Akella, D. Wloga, J. Kim, N. G. Starostina, S. Lyons-Abbott, N. S. Morrissette, S. T. Dougan, E. T. Kipreos and J. Gaertig, "MEC-17 is an alpha-tubulin acetyltransferase," *Nature,* vol. 467, no. 7312, pp. 218-22, 2010.

[149] N. Kalebic, C. Martinez, E. Perlas, P. Hublitz, D. Bilbao-Cortes, K. Fiedorczuk, A. Andolfo and P. A. Heppenstall, "Tubulin acetyltransferase αTAT1 destabilizes microtubules independently of its acetylation activity," *Mol Cell Biol,* vol. 33, no. 6, pp. 1114-23, 2013a.

[150] G.-W. Kim, L. Li, M. Gorbani, L. You and X.-J. Yang, "Mice Lacking α-Tubulin Acetyltransferase 1 Are Viable but Display α-Tubulin Acetylation Deficiency and Dentate Gyrus Distortion*," *J Biol Chem.,* vol. 288, no. 28, p. 20334–20350, 2013.

[151] S. J. Morley, Y. Qi, L. Iovino, L. Andolfi, D. Guo and e. al., "Acetylated tubulin is essential for touch sensation in mice," *Elife,* vol. 5, p. e20813, 2016.

[152] C. Janke and G. Montagnac, "Causes and Consequences of Microtubule Acetylation," *Current Biology,* vol. 27, p. R1287–R1292, 2017.

[153] T. Shida, J. G. Cueva, Z. Xu, M. B. Goodman and M. V. Nachury, "The major alpha-tubulin K40 acetyltransferase alphaTAT1 promotes rapid ciliogenesis and efficient mechanosensation," *Proc Natl Acad Sci U S A,* vol. 107, no. 50, pp. 21517-22, 2010.

[154] I. A. T. Schaap, P. J. de Pablo and C. F. Schmidt, "Resolving the molecular structure of microtubules under physiological conditions with scanning force microscopy," *Eur Biophys J,* vol. 33, p. 462–467, 2004.

[155] C. Coombes, A. Yamamoto, M. McClellan, T. A. Reid, M. Plooster, G. W. Luxton, J. Alper, J. Howard and M. K. Gardner, "Mechanism of microtubule lumen entry for the α-tubulin acetyltransferase enzyme αTAT1," *Proc Natl Acad Sci U S A,* vol. 113, no. 46, pp. E7176-E7184, 2016.

[156] L. Schaedel, K. John, J. Gaillard, M. V. Nachury, L. Blanchoin and M. Théry, "Microtubules self-repair in response to mechanical stress," *Nature Mater,* vol. 14, p. 1156–1163, 2015.

[157] D. Portran, L. Schaedel, Z. Xu, M. Théry and M. V. Nachury, "Tubulin acetylation protects long-lived microtubules against mechanical ageing," *Nat Cell Biol,* vol. 19, no. 4, pp. 391-398, 2017.

[158] Z. Xu, L. Schaedel, D. Portran, A. Aguilar, J. Gaillard, M. P. Marinkovich, M. Thery and M. V. Nachury, "Microtubules acquire resistance from mechanical breakage through intralumenal acetylation," *Science,* vol. 356, no. 6335, pp. 328-332, 2017.

[159] C. Yan, F. Wang, Y. Peng, C. R. Williams, B. Jenkins and e. al., "Microtubule Acetylation Is Required for Mechanosensation in Drosophila," *Cell Reports,* vol. 25, p. 1051–1065, 2018.

[160] S. L. Rogers and G. C. Rogers, "Culture of Drosophila S2 cells and their use for RNAi-mediated loss-of-function studies and immunofluorescence microscopy," *Nat Protoc,* vol. 3, no. 4, pp. 606-11, 2008.

[161] J. Cribb, L. Osborne, K. Beicker, M. Psioda, J. Chen, E. T. O'Brien, R. M. Taylor II, L. Vicci, J. P.-L. Hsiao, C. Shao, M. Falvo, J. G. Ibrahim, K. C. Wood, G. C. Blobe and R. Superfine, "An Automated High-throughput Array Microscope for Cancer Cell Mechanics.," *Sci Rep,* vol. 6, p. 27371, 2016.

[162] F. E. Grubbs, "Sample Criteria for Testing Outlying Observations," *Annals of Mathematical Statistics,* vol. 21, no. 1, pp. 27-58, 1950.

[163] V. Swaminathan and C. Waterman, "The molecular clutch model for mechanotransduction evolves," *Nature Cell Biology,* vol. 18, p. 459–461, 2016.

[164] V. Jaumouillé and C. M. Waterman, "Physical Constraints and Forces Involved in Phagocytosis," *Frontiers in Immunology,* vol. 11, p. 1097, 2020.